A Role for the Tail of the Striatum in the Adaptive Control of Innate Escape Behaviour

By: Stephen Lenzi

PhD supervisor: Professor Troy Margrie

A thesis submitted for the degree of
Doctor of Philosophy

Sainsbury Wellcome Centre for Neural Circuits and Behaviour,
University College London

I, Stephen Lenzi, hereby confirm that the work presented in this thesis is my own. Where information has been derived from other sources, I confirm that this has been indicated in the thesis.

Signed: 

Stephen Lenzi, 22nd of January 2021

Abstract

Laboratory mice show robust escape responses to overhead, high-contrast visual looming stimuli. However, it is sometimes evolutionarily advantageous to suppress instinctive behaviours such as escape, for example when through experience, a specific stimulus is realised to be non-threatening. Dopaminergic neurons in the Substantia Nigra pars Lateralis (SNL) which project to the Tail of the Striatum (TS) are part of a candidate pathway for mediating such adaptative behaviours since they are thought to signal threat prediction error. Also, the SNL and the TS are densely interconnected with several key structures that mediate escape behaviour and our preliminary lesion experiments show that they are necessary for escape.

Here I investigated whether the SNL-TS circuit could mediate the learned control of escape behaviour using a behavioural protocol that results in the learned suppression of innate escape (LSIE) to visual stimuli that were previously threatening. LSIE lasted for over two weeks and did not reduce the probability of escape to threatening auditory stimuli. Photometry experiments in the TS showed reliable, large calcium signals in dopaminergic inputs in response to looming stimuli that correlated with threat level and escape probability. Such TS dopamine signals were reduced during and following LSIE. Similarly, both D1- and A2a-receptor-expressing neurons in the TS showed reduced responses following LSIE indicating that these dopaminergic responses to looming stimuli undergo experience-dependent modulation. Dopaminergic TS signals could therefore be involved in the modulation of escape behaviour that may be adjusted according to prior experience and threat prediction.

Impact Statement

Hard-wired innate behaviour is a potentially powerful tool for systems neuroscience since it is extremely robust and believed to rely on relatively simple brain circuitry. For example, visually guided defensive behaviours such as escape can be readily elicited in a highly controlled manner in the laboratory, and this has elucidated circuit mechanisms down to the synaptic level. Throughout life however, learning how to adapt or control innate drive forms the basis of much of our overall adult behavioural repertoire. While the ethological benefits of this form of learning have long been appreciated, we nevertheless still lack a mammalian experimental model system for studying this kind of adaptive control.

In this thesis I have studied the flexibility of innate escape behaviour in laboratory mice. I established a novel paradigm for inducing learned suppression of innate escape to overhead looming visual stimuli. I show that mice rapidly and robustly learn to completely suppress their innate escape response and that this can be induced simply in a controlled laboratory setting in less than 20 minutes. By controlling the lifetime stimulus history of each mouse, I could also determine what aspects of experience influence the modulation of innate escape. To my knowledge this is the first such paradigm for systematically studying the flexibility of an innate behaviour in a mammalian system.

While some detail is known about the neural mechanisms of innate escape, the neural basis of its modulation has not been studied. My anatomical, physiological and behavioural experiments in both control and lesioned mice, together with the new behavioural protocol, reveal that parts of the Basal Ganglia, a system that is known for its role in action selection, is intimately involved in the regulation of innate escape behaviour. These results add to growing literature suggesting there are multiple dopamine systems that are important for the selection of different kinds of behaviour.

The data from this thesis provide a working model by which the Basal Ganglia might interact with the known escape circuitry to influence innate behaviour. This provides a starting point for dissecting the thalamo- or cortico-striatal plasticity mechanisms that may underlie an innately-based yet intelligent catalogue of learned behaviours.

Table of Contents

Acknowledgements

First and foremost, I would like to thank Troy Margrie for his guidance throughout this project. I have learned a lot from his invaluable input and advice along the way and I am a better scientist for it. I am grateful for having had the opportunity to complete my thesis under his supervision.

Every member of the Margrie Lab. has influenced this work in some way, whether through feedback in lab meetings, or informal discussions at the pub. However, I would like to thank several people whose influence was particularly important.

Lee Cossell helped to get this project off the ground and has been a continuing source of helpful advice and insight.

Molly Strom produced many of the plasmids and viruses used in this thesis and helped me devise experimental approaches for anatomical tracing. Additionally, Molly established and maintained the transgenic lines used in this study.

I would also like to thank Chryssanthi Tsitoura and Adam Tyson who provided helpful advice and feedback on thesis figures and chapters and Charly Rousseau, who helped me to further my programming skills that have proven fundamental to this work.

I would also like to thank my secondary supervisor Tiago Branco for his insightful input and would like to thank Marcus Stephenson-Jones and his Lab. for engaging and fruitful discussions, and for their regular input to this work and ongoing collaboration. I would also like to specifically thank Laura Schwarz and Francesca Greenstreet who each contributed some histology to this work.

I would like to thank Ben Grainger for his assistance in running the behavioural experiments in Figure 4.6.

Many thanks to the NRF for their excellent animal husbandry services and to the SWC FabLabs for their help building or modifying behavioural set-ups at short notice.

Several institutions have also made the work possible. I am grateful to The Sainsbury Wellcome Centre for Neural Circuits and Behaviour for backing this work, and for aiming to deliver an open and ambitious scientific community. I would also like to thank the Wellcome Trust and Gatsby foundation for their generous funding support.

Finally, I am extremely grateful to my family and friends and to Laura for their support throughout, and to Constance Holman for proof reading.

Abbreviations

2D – two dimensional

3D – three dimensional

6-OHDA – 6-Hydroxydopamine

D1 – dopamine receptor D_1

A2a – adenosine A_{2A} receptor

GABA – Gamma aminobutyric acid

GFAP – glial fibrillary acidic protein

IR – infrared

LED – light emitting diode

LP – Lateral Posterior Nucleus of the Thalamus

LSIE – learned suppression of innate escape

NIDAQ – National instruments data acquisition

NMDA – N-Methyl-D-Aspartic acid

PAG – Periaqueductal Grey

PBS – phosphate buffered saline

PFA – paraformaldehyde

SC – Superior Colliculus

SCs – superficial layers of the Superior Colliculus

SCd – deep layers of the Superior Colliculus

SNL – Substantia Nigra pars Lateralis

SNr – Substantia Nigra reticulata

TH – Tyrosine Hydroxylase

TS – Tail of the Striatum

Definitions

Acclimatisation period: a period following introduction into the arena before any looming stimuli are presented.

Contrast-response curve: a psychometric curve showing the probability of mice escaping from looming stimuli at different contrast levels.

Escape latency: the time from stimulus onset until return to shelter is initiated.

Learned control: the contextual and learned modification of innate behaviour.

Looming spot: an expanding circular black spot presented overhead.

Looming stimulus: 5 consecutive looming spots with an inter-loom interval of 0.4 seconds.

LSIE protocol: a protocol for inducing the learned suppression of the innate escape response (Figure 2.3).

Naïve mouse: a mouse with no history of previous exposure to looming stimuli.

Post-test: a standard test given after the LSIE protocol.

Pre-test: a standard test given before the LSIE protocol.

Standard contrast: the contrast of looming stimuli used for testing escape responses. Consists of a background luminance of 8 cd/m^2 together with a spot luminance of 0.09 cd/m^2).

Standard test: a test to evaluate behavioural responses to looming stimuli of the trials structure shown in (Figure 2.2B) using looming stimuli at standard contrast.

Test trial: a looming stimulus triggered by mouse entry to the threat zone.

Threat zone: defined as a 20 cm x 20 cm region at the far end of the arena (Figure 2.1A and B). Entry to this threat zone leads to the presentation of a looming stimulus.

General Introduction

Some challenges in life are common to the majority of members of a species, for example, the need to evade a pursuant predator; to hunt prey or forage; to fight off competitors; or to mate and raise infants. These challenges pose a common problem in that they require the selection and enaction of appropriate behaviours without prior experience. Thus, learning must occur in the absence of negative outcomes and the cost of failure is high: poor decisions or outcomes in any of these tasks will lead to a reduced likelihood of reproductive success and the passing on of genes.

An elegant solution for enacting behaviours without experience has arisen through evolution: many organisms inherit a predisposition for engaging appropriate and stereotyped behavioural sequences in response to biologically relevant sensory features (Tinbergen, 1989). Such innate behaviours provide a rapid and direct route to action that does not require prior experience, enabling an organism to escape a predator without previous exposure to one (Sargeant & Eberhardt, 1975) or enabling a newly hatched chick to eat for the first time (Tinbergen & Perdeck, 2008).

While necessary for survival, innate behaviours are often unlikely to be the best course of action – after all, the majority of useful information for guiding behaviour is acquired later in life. Some environments contain consistent features that allow broad, heuristic-based behavioral planning. However, most events are richly contextual and provide opportunities for learning and optimisation. A mouse will need to evade a predator at some point in its life but the best strategy for doing so depends on a diverse set of factors including terrain, motivational state, likelihood of being detected, likelihood of reaching safety and previous experience. This richness and variability of available information that can guide decisions necessitates flexibility and the continual adjustment of behavioural responses depending on circumstance, experience and internal state. Innate behaviours are useful for increasing the likelihood of

appropriate actions being selected. In contrast, *learned control* – the contextual and learned modification of innate behaviours, is necessary to allow for these additional and flexible sources of information to be accounted for when it presents an advantage for the organism. Decision making should be optimally balanced in some way, between innate behaviours that prepare an organism to act without experience and learned control that enables an organism to make informed decisions. If a behaviour is too hard-wired an organism cannot benefit from new information acquired through experience, nor take into account internal factors such as hunger, which might drive them to adopt necessary alternate strategies for acquiring food in desperate times. On the other hand, an over-reliance on flexible strategies risks failure to engage innate behaviour when it is appropriate, which can be costly, if not fatal. How this balance is met between innateness and flexibility and how this is implemented in the brain remain, for the most part, unknown. The broad aim of this thesis is to better understand **the extent of learned control of innate behaviour** and also **how learned control is implemented at the circuit level using mouse innate escape behaviour as a model system.**

I will first review what is known about innate behaviours with a specific focus on innate escape behaviour in rodents, which has recently become a promising field for addressing questions relating to innate decision making and the factors that influence it. I will review what is known about the neural mechanisms that underlie the innate decision to escape. I will then discuss flexibility of this behaviour and the mechanisms that might implement learned control of the innate escape response. I will argue that there are several possible routes through which flexibility could be driven – principally those that are intrinsic to the midbrain circuits that execute the innate behaviour, and those that act extrinsically through top-down systems that are classically involved in action selection, e.g. the Basal Ganglia. I will finish the literature review by summarising how a striatal circuit involving the Substantia Nigra pars Lateralis (SNL) and its projection target in the Tail of the Striatum (TS) might interact with the known escape circuitry to modulate escape decisions.

Chapter 1: Literature Review

1.1 Escape behaviour as a model system

The study of the learned control of innate behaviour requires comprehensive knowledge and control of an organism's environment, firstly to know which aspects of behaviour are innate and which have been learned later in life, and secondly to manipulate the surroundings to understand how this influences the expression of that behaviour. This challenge is formidable in natural settings where stimuli that influence or trigger specific kinds of behaviour can be infrequent, unpredictable and multimodal. It is also challenging to acquire complete datasets of an organism from birth to death or to repeat trials and get reliable population datasets. This has driven many in the field to establish relevant behavioural models of innate behaviours in the laboratory that yield robust responses over many trials while also allowing invasive recordings of neuronal activity.

For a long time, it was thought that the only innately expressed visual behaviours in mice were simple and purely reflexive, such as the eyeblink reflex and the optokinetic reflex. However, it has recently been shown that laboratory mice will exhibit complex visually-guided innate responses to dark expanding circles presented overhead, referred to as *looming spots* (De Franceschi et al., 2016; Evans et al., 2018; Vale et al., 2017; Yilmaz & Meister, 2013), which approximate approaching objects on a collision course such as potential predators (De Franceschi et al., 2016; Yilmaz & Meister, 2013). Under appropriate conditions, looming spots evoke strong and highly stereotyped escape behaviour in laboratory mice that have never previously been exposed to one. This stereotyped behaviour consists of rapid re-orientation to face the direction of shelter, running to the shelter and then hiding, freezing and tail rattling. These responses are also highly stimulus specific: high contrast looming spots presented overhead can yield probabilities of escape upwards of 90 percent of trials (Evans et al., 2018; Vale et al., 2017) whereas white looming spots, inverse looming spots, looming

spots displayed from below or the side and flashing dark spots of a fixed size do not elicit escape (Yilmaz & Meister, 2013; Z. Zhou et al., 2019). Loom-evoked defensive behaviours are also flexible to some degree: when there is no shelter to run to or it is too far away, mice will freeze to remain undetected instead of escaping to a safe place (Vale et al., 2017). Additionally, mice also show escape responses to stimuli in other sensory modalities: auditory ultrasound sweeps (Vale et al., 2018), loud noises, and real predators (Blanchard et al., 1998) can all trigger escape to shelter.

Loom-evoked escape is an appealing model for studying how sensory information guides behaviour. This is because it is thought to involve a well-defined sensorimotor computation that drives a flexible (Vale et al., 2017), visually guided (De Franceschi et al., 2016) and goal directed behaviour that must occur rapidly, and therefore over a limited number of synaptic connections (Peek & Card, 2016). These features potentially allow the complete observation of a behaviour from sensory transduction to motor output. This makes the study of a variety of cognitive processes that may be involved in the *learned control* of innate behaviour tractable, given that there are a limited set of structures that might be influenced by modulatory mechanisms to drive adaptation. Given this assumption that the neural plasticity underlying learned control is likely to occur somewhere in a compact escape circuitry I will review what is currently known about the neural correlates of escape with a view to identifying candidate structures that might modulate escape decisions.

1.2 The neural basis of escape

1.2.1 The Superior Colliculus

After the retina, the first stage of visual processing of an overhead looming spot is likely to be the Superior Colliculus (SC). The SC is a 7 layered structure thought to play a crucial role in driving loom-evoked escape behavior for several reasons. Firstly it receives direct input from the retina, secondly it has

been suggested that it is involved in sensorimotor transformations (Gandhi & Katnani, 2011), and thirdly, it has been known for several decades that stimulation of medial or lateral regions of SC can result in avoidance or approach behavior, respectively (Sahibzada et al., 1986). Visual input first arrives at the retinorecipient superficial layers of the SC, which are retinotopically organised along the rostral-caudal and medial-lateral axes (Figure 1.1) (Drager & Hubel, 1976; Seabrook et al., 2017). The vertical meridian is represented rostrally and the periphery is represented caudally. The upper visual field is represented in the medial SC and the lower visual field in the lateral parts of the SC (Figure 1.1) (Drager & Hubel, 1975, 1976).

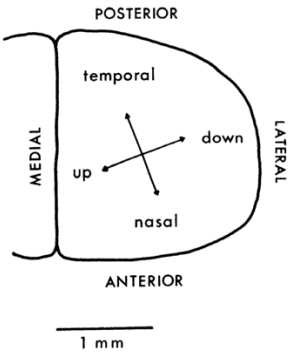

Figure 1.1: *retinotopic map of SC showing medial-lateral and anterior-posterior organization* (Drager & Hubel, 1975, 1976)*. Medial SC represents the upper visual field while lateral parts represent the lower visual field. Posterior SC represents the temporal visual field while anterior SC represents the nasal visual field.*

The superficial SC contains at least 4 neuronal subclasses each with distinct receptive field properties and/or downstream projections targets (Figure 1.2) (Gale & Murphy, 2018a). Widefield neurons express Ntsr1-GN209 and are named for their wide dendritic arbors. They respond to small stimuli anywhere within their large receptive field, are thought to be well-suited for stimulus detection (Hoy et al., 2019) and predominantly project to the Lateral Posterior Nucleus of the Thalamus. Narrow field neurons express Grp-KH288 and are named for their narrow dendritic arbors. They have small receptive fields that are direction-selective and thought to be well suited to detecting changes in

stimulus location (Hoy et al., 2019). Narrow field neurons project to the intermediate SC and Parabigeminal Nucleus. Stellate cells express Rorb, have small receptive fields and project to the Lateral Geniculate Nucleus and Parabigeminal Nucleus. The superficial SC also contains a PV expressing population, which is heterogeneous and contains both glutamatergic and GABAergic subpopulations (Villalobos, Basso 2018) that project to the intermediate SC, Parabigeminal Nucleus, Lateral Geniculate Nucleus and Anterior Pretectal Nucleus (Figure 1.2A and B).

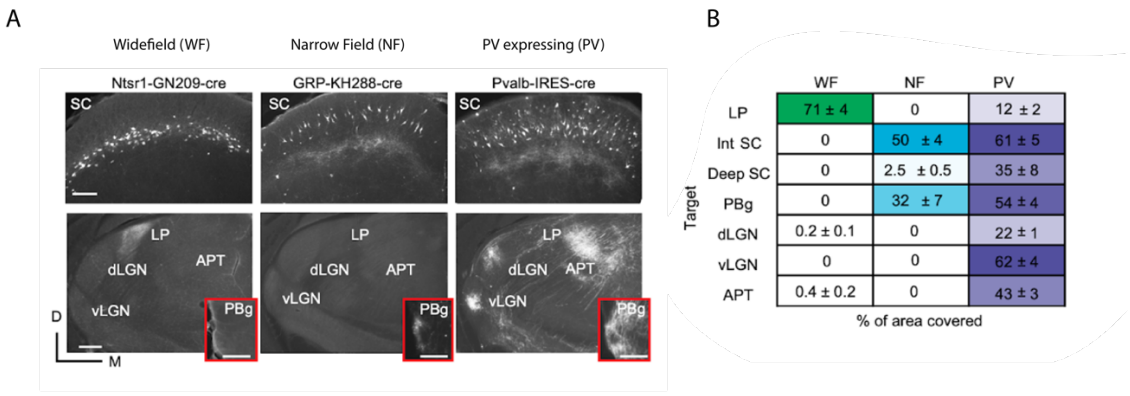

Figure 1.2: the different cell types of the superficial SC project to different targets. *Adapted from* (Gale & Murphy, 2018a; Hoy et al., 2019) *illustrating the different classes of neurons that have been identified in the superficial SC together with their downstream targets. A) a coronal cross section showing mCherry expression following injection of* AAV8-hSyn-DIO-hM4Di-mCherry in *three Cre lines to target distinct populations of genetically targetable neuron populations in the superficial SC (top) with their projection targets shown in the panels below (bottom). B) quantification of axonal density in each of the target regions listed for each Cre line as a percentage of the area of each structure covered +/- s.e.m.*

Nearly all direct downstream target structures of superficial SC neurons have been implicated in either escape or freezing behaviour in response to looming spots and some of these targets are densely interconnected with one another. This has led to conflicting results concerning the neuronal pathways that are required for innate escape, as results of intervention experiments could be

ascribed to activity of multiple regions and cell populations. I will therefore review what is known, with the aim of clarifying which structures are essential for escape or freezing behaviour, and which structures are likely to take a modulatory role, or no role at all. I will focus on a pathway from the superficial SC to the dorsal Periaqueductal Grey (PAG) via the deeper layers of the SC, which I will argue forms the main route of information flow in response to a looming spot. I will also review what is known about alternate pathways from superficial SC to Parabigeminal Nucleus, and from superficial SC to the Central Amygdala via the Ventral Tegmental Area, as these have also been proposed to mediate escape. Finally, I will discuss a pathway from superficial SC to lateral Amygdala via the Lateral Posterior Nucleus of the Thalamus that has been proposed to be a driver of freezing in response to looming spots. Importantly, projections from the SC to the Dorsolateral Geniculate Nucleus, Ventrolateral Geniculate Nucleus and Anterior Pretectal Nucleus are not well characterised and so I will not discuss them here.

1.2.2 The deeper layers of SC

The deep layers of SC are a major target of the superficial SC. Whereas the superficial layers of SC respond almost exclusively to visual stimuli, many neurons in the deep layers of SC respond to multiple sensory modalities such as auditory and somatosensory stimuli (Wallace et al., 1998). The deep SC receives auditory and somatosensory inputs together with non-sensory modulatory inputs from a range of cortical and subcortical structures (May, 2005; Wang & Burkhalter, 2013, Benavidez et al. 2020). In addition to responding to multiple sensory modalities, the deep SC also contains motor-related neurons that are thought to send motor commands to downstream structures including the dorsal PAG. It is thought that they are additionally capable of eliciting movements such as saccades or escape, consistent with the view that the SC may perform sensorimotor transformations along its dorsoventral axis (Gandhi & Katnani, 2011).

While the superficial layers of the SC respond similarly to a variety of stimuli irrespective of their role in driving behaviour (Lee et al., 2020), the deeper layers of the SC show preference for stimuli that directly drive actions, such as high contrast looming spots (Lee et al., 2020) that are known to trigger escape responses. Interestingly, even stimuli that are highly similar to looming spots but do not elicit strong behavioural responses, such as high contrast inverse looming spots do not trigger activity in the deeper layers (Lee et al., 2020). Additionally, the superficial layers of the SC remain responsive over many presentations of such stimuli, while responses in the deep layers rapidly habituate to familiar stimuli and this habituation of responses persists on the time scale of minutes (Lee et al., 2020). Lee and colleagues suggest that the SC sifts visual information such that only behaviourally-relevant information reaches the deep SC (Lee et al., 2020), a view that is consistent with the role of the deep layers in sending motor outputs to downstream structures such as the PAG.

1.2.3 The PAG

The PAG is a region in the midbrain that surrounds the Central Aqueduct and consists of distinct functional territories. Two subregions of the PAG have been repeatedly implicated in the expression of both learned and innate fear responses. Stimulation of the dorsal PAG leads to the expression of defensive avoidance behaviours, whereas stimulation of the ventrolateral PAG results in defensive freezing behaviours (Zhang et al., 1990). Furthermore, lesions of the PAG abolish the expression of defensive behaviours altogether, even in response to real predators (Bandler & Shipley, 1994). Each region of PAG projects to relevant premotor nuclei for engaging appropriate behaviour: the ventrolateral PAG is thought to drive freezing through monosynaptic connections with the Magnocellular Nucleus of the Medulla (Tovote et al., 2016) and the dorsal PAG projects to structures such as the Cuneiform Nucleus that can drive escape-like locomotion (Caggiano et al., 2018) and to the ventrolateral PAG, where it can also suppress the freezing response through direct inputs to inhibitory interneurons (Tovote et al., 2016). The dorsal

PAG is, therefore, a likely a functionally important node in the expression of defensive behaviours.

1.2.4 The deep medial SC to dorsal PAG pathway for computing escape decisions

There is ample evidence suggesting that the dorsal PAG also plays such a role in the expression of loom-evoked escape (Evans et al., 2018). In particular, an important study from Evan and colleagues in Tiago Branco's lab explored the role of the deep medial SC to dorsal PAG connection in loom-evoked escape behaviour (Evans et al., 2018). Evans and colleagues proposed that the decision to escape is computed by the concerted action of deep SC and the dorsal PAG, whereby (1) the SC performs stimulus detection in the upper layers, (2) it computes looming-spot threat-level in the deep layers and (3) the dorsal PAG controls the initiation of escape based on the input it receives. They first showed that the probability of escape in response to looming spots increases gradually with contrast. In line with this behavioural observation, calcium imaging revealed that VGlut+ neurons in deep medial SC increase their activity with looming spot contrast, and that most ramp their activity before escape occurs. Further, they showed that iChloc inactivation of these Vglut+ neurons in the medial SC abolished defensive responses to both looming stimuli and auditory threat stimuli, consistent with a possible role of the medial SC in representing the perceived/potential threat level of the stimulus. Furthermore, Evans and colleagues showed that stimulation of Channelrhodopsin 2 expressing VGlut+ neurons in deep medial SC can drive escape behaviour. Importantly they showed that incremental changes in laser power lead to incremental changes in escape probability.

Calcium imaging also revealed that VGlut+ neurons in the dorsal PAG fire at the onset of escape and scale their firing with escape vigour. Inactivation of the dorsal PAG causes mice to freeze in response to looming stimuli instead of initiating escape. Together these results indicate that the dorsal PAG may

be required for the initiation of escape once a threat has been detected and is consistent with the view that the PAG may implement thresholding and compute and enact the decision to escape.

Evans and colleagues also perform monosynaptic rabies tracing from the dorsal PAG and suggest that the medial SC drives escape through highly convergent projections to the dorsal PAG that they show exist (Figure 1.3).

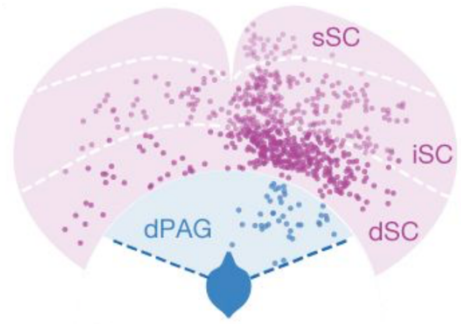

Figure 1.3: SC inputs to dorsal PAG are highly convergent. *Figure taken from* (Evans et al., 2018) *showing the results of rabies tracing from dorsal PAG in which the TVA receptor and rabies glycoprotein (RG) were introduced to the dorsal PAG by injection of an AAV8 helper virus followed by injection of SADB19 rabies virus to reveal monosynaptic inputs (pink dots) onto dorsal PAG starter cells (blue dots). The distribution of dorsal PAG inputs is shown for the different layers of SC – the superficial SC (sSC), the intermediate SC (iSC) and the deep SC (dSC).*

When the dorsal PAG is inactivated, mice respond to looming spots by freezing instead of escaping. This raises the possibility that the level of activity in the same circuit could be sufficient for determining behavioural choice, as previously suggested (Gross & Canteras, 2012), although it has been suggested elsewhere that freezing is mediated through a separate circuit that involves the Lateral Posterior Nucleus of the Thalamus (Shang et al., 2018; Wei et al., 2015). Evans and colleagues proposed a feed-forward mechanism

whereby SC connections to PAG are weak and unreliable but can be overcome through recurrent excitation and short-term facilitation in deep medial SC. Such a mechanism would allow visual stimuli to engage escape behaviours only if they are sufficiently salient. They suggest that neurons in deep medial SC may serve as a thresholded integrator of threat that feeds forward to neurons in the dorsal PAG that represent escape choice and vigour.

1.2.5 Other routes proposed to drive loom-evoked responses

SC – Parabigeminal Nucleus pathway

Although these experiments (Evans et al., 2018) are elegant and convincing in demonstrating the importance of the deep medial SC to dorsal PAG pathway for computing escape decisions, it remains possible that there is more than one pathway for achieving the same behavioural output. Most of the papers that consider alternate pathways begin by looking at downstream targets of the superficial SC. For example, it has been shown that stimulation of PV+ neurons in the superficial SC drives escape (Shang et al., 2015). This population of neurons is heterogeneous and projects to a variety of downstream targets (Figure 1.2A and B). Of these, the Parabigeminal Nucleus has been suggested as a driver of innate escape behaviour because it receives dense innervation from PV+ and NF cells in the superificial SC and sends a direct projection to the Pontine Nucleus that could drive motor output (Shang et al., 2015). Shang and colleagues found that stimulation of PV+ axon terminals in the Parabigeminal Nucleus can drive escape and that long term changes in excitability of the Parabigeminal Nucleus can influence the decision to escape or freeze: tetanus neurotoxin-induced long-term reduction in excitability of the Parabigeminal Nucleus reduces the probability of escape in favour of freezing while an increase in excitability induced through expression of the bacterial depolarisation activated sodium channel, NaChBac, has the opposite effect (Shang et al., 2018). They conclude that the Parabigeminal Nucleus is a crucial downstream target for driving escape.

However, there are some caveats with their approach. There is a fundamental problem with stimulating neurons in the superficial SC because of their diverse projection targets. PV+ neurons in superficial SC form a heterogeneous population that is not completely restricted to the upper layers of SC, and contains both GABAergic and glutamatergic neurons with projection patterns similar to at least two other classes of superficial SC neuron (WF and NF neurons). This makes it difficult to interpret their finding that SC axons in Parabigeminal Nucleus drive escape because other pathways than the ones proposed are likely to have been driven concurrently with their stimulation protocol. Similarly, it is difficult to interpret their finding that increased Parabigeminal Nucleus excitability leads to increased escape probability because the effects of their intervention are likely to be propagated throughout the entire network, including other structures that have been implicated in driving escape. In particular the Parabigeminal Nucleus sends projections to the intermediate SC, may itself influence sensory processing and may indirectly influence alternate pathways of escape (i.e. deep SC to dorsal PAG). While it is not yet entirely clear what role the Parabigeminal Nucleus plays in escape, it has been shown that activity in the Parabigeminal Nucleus scales with retinal position error during saccades in cats (Cui & Malpeli, 2003). It would thus be interesting to know if it performs a similar function in the context of escape e.g. distance to shelter. To answer this question with certainty, it would be essential to test whether Parabigeminal Nucleus activity is sufficient for inducing escape when the dorsal PAG is inactivated or lesioned, thus greatly reducing the possibility for concurrent activation.

SC – Ventral Tegmental Area – Central Amygdala pathway

Zhou and colleagues have suggested another pathway from the SC to the Central Amygdala via the Ventral Tegmental Area that is required for escape (Z. Zhou et al., 2019). They find that stimulation of Ventral Tegmental Area with Channelrhodopsin 2 drives escape behaviour and that they can block this effect through inactivating the Central Amygdala with $GABA_A$ antagonist bicuculine. They also show that bicuculine applied to the Central Amygdala

can prevent behavioural responses to looming spots. It has been shown previously that $GABA_A$ agonist muscimol inactivation of the Central Amygdala reduces escape vigour and results in a modest reduction in escape probability to looming spots, but does not abolish it completely (Evans et al., 2018). However, the study by Zhou is more specifically targeted to the Central Amygdala and uses a larger cohort of mice. The Central Amygdala is well positioned to influence both escape and freezing through projections to the dorsal PAG and ventrolateral PAG respectively. Given that the Central Amygdala is a significant input to dorsal PAG is it likely that this effect is ultimately driven through changes in dorsal PAG activity. Stimulation of the Ventral Tegmental Area will have many off-target effects, especially given the variety of functions that have been attributed to Ventral Tegmental Area dopaminergic and GABAergic neurons such as place aversion (Tan et al., 2012), which makes difficult the interpretation of the result that stimulation can induce escape. Zhou and colleagues also show that inactivation of GABAergic neurons in the Ventral Tegmental Area can prevent escape from looming spots. However, there are several of noteworthy confounds in these experiments. It has been reported that GABAergic neurons in the Ventral Tegmental Area encode head pitch, roll and yaw, and that stimulation of these neurons results in head rotations and disrupt ongoing behaviours such as reward consumption (Hughes et al., 2019). The activity that Zhou and colleagues report in GABAergic Ventral Tegmental Area neurons using calcium imaging precedes escape but could potentially be explained by changes in head angle that are triggered as the mouse turns to face the shelter prior to escape. Ventral Tegmental Area dopaminergic projections to the medial Prefrontal Cortex have also been shown to improve the signal-to-noise ratio of aversive stimuli in the dorsal PAG (Vander Weele et al., 2018), which suggests that while this population of neurons can certainly exert strong influence on escape, its precise nature is unclear.

Divergent pathways for escape and freezing

It has been suggested by several authors that there is a pathway from the SC to the lateral Amygdala via the Lateral Posterior Nucleus of the Thalamus that drives freezing behaviour in response to looming stimuli (Shang et al., 2018; Wei et al., 2015). Both groups show that stimulation of the medial SC in the absence of a shelter can result in freezing responses. They also show stimulation of SC terminals in the Lateral Posterior Nucleus of the Thalamus leads to freezing behaviour. However, a key experiment for concluding that the SC-LP-LA circuit is required for loom evoked freezing, stimulation of medial SC with simultaneous inactivation of Lateral Posterior Nucleus of the Thalamus, was not performed. Wei and colleagues also infuse muscimol in the LA-BLA region and show that they can no longer drive freezing after the intervention. However, it is highly likely from their cannula placements that they also hit Central Amygdala which is known to promote freezing through disinhibition of ventrolateral PAG.

While there is some evidence to support a SC to Lateral Posterior Nucleus of the Thalamus pathway for driving freezing, the studies of Lateral Posterior Nucleus of the Thalamus are far from comprehensive in addressing its role in loom-evoked behaviours in general. The Lateral Posterior Nucleus of the Thalamus stretches over 1.5mm in the anteriorposterior direction, with three functional domains and two separate representations of the upper visual field (Bennett et al., 2019a). It is therefore unclear precisely what role the SC to LP projection plays in innate fear responses.

1.2.6 Summary

In summary, looming visual input first arrives at the superficial SC and can pass through several parallel pathways that are speculated to play different roles in innate fear responses. The projection from the deep layers of the medial SC to the dorsal PAG is required for escape and other structures that have also been shown to strongly modulate escape are upstream of the dorsal

PAG (Central Amygdala, Ventral Tegmental Area, medial Prefrontal Cortex) and may exert influence on the decision to escape by modulating the excitability of the dorsal PAG. The necessity of dorsal PAG in the decision to escape, and also the fact that so many of the structures that seem to modulate escape converge on the dorsal PAG suggests that it may form the final common path– required for escape initiation, but influenced by a variety of modulatory structures that can regulate the threshold for escape.

1.3 The flexibility of innate behaviour

As outlined in the general introduction, innate behaviours are beneficial because they enable action without experience. However, the majority of information that is useful for guiding behaviour can only be acquired later in life through experience. This fact necessitates some degree of flexibility to account for the nuance of the circumstances an organism finds itself in, or to enable an organism to completely suppress such behaviours when it is appropriate to do so. We therefore expect information acquired later in life to influence, compete with, or regulate innate behaviours. Successful modulation of innate behaviour yields the advantages of flexibility, while retaining the advantages of an initial predisposition for behaviours that are highly likely to be adaptive.

There is a wealth of evidence from a variety of species that suggests that innate behaviours are rich, flexible and modified by information acquired later in life. For example, it has been reported that anole lizard flight behaviour differs depending on the level of human presence in their habitats (Cooper et al., 2010), predator avoidance in crabs depends on circadian rhythm (Pereyra et al., 1996), season (Sztarker & Tomsic, 2008), predator abundance or predation risk (Magani et al., 2016), and prior experience (Hemmi & Merkle, 2009; Hemmi & Tomsic, 2012; Tomsic et al., 2009, 2019). In mice, freezing responses evoked by hawk silhouette or black circle stimuli that sweep overhead have been shown to attenuate with repeated exposure in a stimulus-

specific manner (Tafreshiha et al., 2020). Even in drosophila, a wide range of behaviours including foraging, feeding, courtship, aggression and collision avoidance have been shown to undergo modulation due to factors such as hunger (Ache et al., 2019) and current motion state (Su & Wang, 2014). The prevalence of flexibility in behaviours that are crucial for survival across many species suggests that flexibility may be a general feature of innate behaviours. Such flexibility is ethological: decisions that account for the rich variability present in the environment should increase an individual's survival fitness relative to ones that don't.

1.3.1 Responses to looming spots are flexible

Similarly, it has been argued that the perception of looming spots and subsequent decision to escape is flexible and subject to modulation (Evans et al., 2019; Vale et al., 2017). For example, it has been shown that mice incorporate new information to guide their escape actions, either through rapid learning of new shelter locations to escape to (Vale et al., 2017) or by deciding to freeze instead of attempting to escape when there is no shelter or it is too far away. This suggests that action selection in response to overhead looming spots is a cognitively demanding decision-making process that requires continual updating of the value of different actions based on experience and context.

While it is perhaps surprising that such a decision should be cognitively demanding, it is worth noting that escape is an expensive action. Unnecessary escape consumes energy, reduces the time available for other behaviours (e.g. foraging) and increases the chance of being detected by a predator that would otherwise have posed no threat. For a prey organism to succeed it needs to reliably escape when it is appropriate but must also learn about the features of the world that are non-threatening and use this to minimise the cost of false alarm escape responses and guide appropriate behaviour. The advantage of doing so is abundantly clear in the natural world, which is filled with potential threats, the majority of which turn out to be harmless. If an

organism can suppress the innate drive to escape from things that have been identified through experience to be non-threatening, then resources are free to deal with other challenges. Doing so confers a survival advantage from increased access to food or potential mates. This kind of flexibility in the escape decision that facilitates the expression of alternate, advantageous behaviours is not well characterised.

1.4 The neural basis of escape modulation

The neural correlates of the learned control of escape are not well characterised but some predictions can be made based on what is known of escape and its underlying circuitry. Modulation could be implemented in several ways: by changing the threshold for escape initiation in dorsal PAG; the evaluation of threat in deep SC; the saliency of stimuli in superficial SC and, therefore, the likelihood of attending the stimulus; or through changes in the selective gating of specific behaviours. These are not mutually exclusive, and it is plausible that learning to suppress escape involves many redundant mechanisms that are implemented at any of several levels as has been suggested to be the case for zebrafish adaptation to aversive visual stimuli (Randlett et al., 2019).

The findings of (Evans et al., 2018) suggest that modulation of the perception of a stimulus as threatening should occur at the level of the deep SC or upstream of it (superficial SC, intermediate SC, deep SC) in structures that represent the stimulus or its representation as threatening, whereas modulation of the decision to escape and choice of actions following a perceived threat are likely to be implemented at the level of the dorsal PAG or downstream of it (Pedunculopontine Nucleus, Cuneiform Nucleus) in the structures that drive escape motor commands and locomotion. Whatever the mechanism, it is likely that learned control must ultimately result in reduced activity in dorsal PAG where escape is initiated. To date, the majority of modulatory mechanisms that have been put forward appear to do this directly

through modulation of dorsal PAG (Central Amygdala, Zona Incerta, ventromedial Hypothalamus, medial Prefrontal Cortex) i.e. downstream of the putative structures that may represent the perceived threat level of overhead visual stimuli. However, it has been shown recently that changes do occur upstream of this: loom-evoked neuronal responses in the deep SC are suppressed following repeated presentations (Lee et al., 2020). Since we are interested in how mice learn to suppress escape when a stimulus is no longer perceived as threatening, I will pay greater attention to modulatory systems that could influence the superficial SC and deep SC.

1.5 Basal Ganglia control

The decision to escape is cognitively demanding and requires the integrated assessment of competing priorities which could arise from multiple functional systems, both cortical and subcortical. This kind of task is particularly well suited to the Basal Ganglia (McHaffie et al., 2005), which are involved in the selection of actions at the expense of others (Redgrave et al., 1999) by selectively gating appropriate actions and suppressing inappropriate ones (Figure 1.4).

The primary input of the Basal Ganglia, the Striatum, receives a variety of sensorimotor information and influences action selection through inhibition of the substantia nigra pars reticulata (SNr) and Globus Pallidus internal (Figure 1.4A and B), which are the primary outputs of the Basal Ganglia. These structures tonically inhibit many midbrain structures and are therefore well positioned to prevent, modulate or permit actions. When a particular action or set of actions is selected, tonic inhibition of the downstream structures required for enacting those actions is selectively relieved to allow the expression of desired actions (Figure 1.4B) while continuing to suppress other non-selected behaviours.

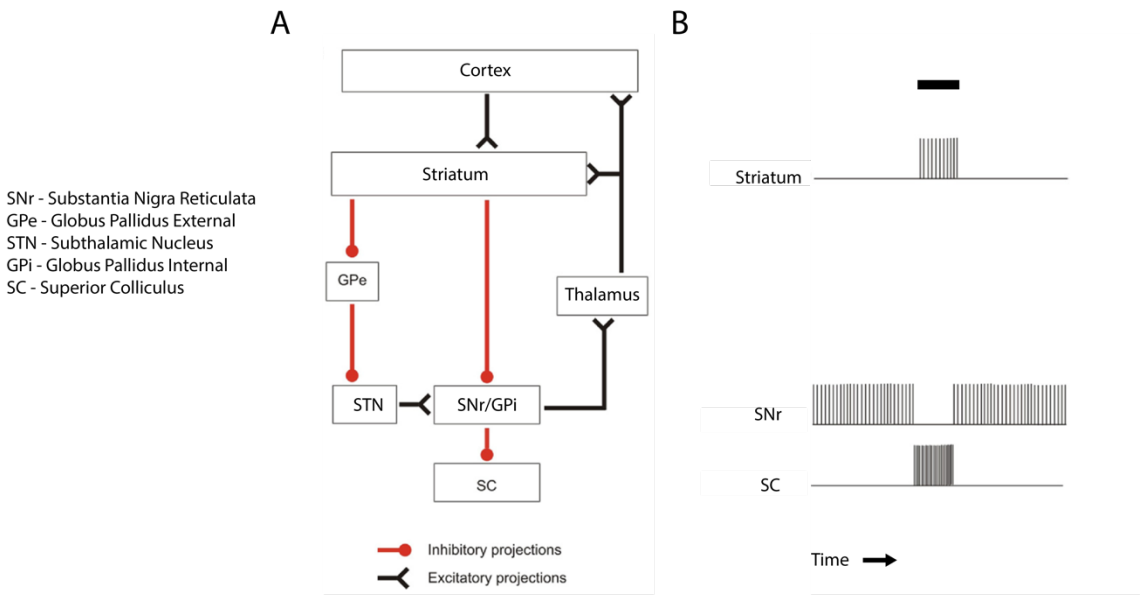

Figure 1.4: The Basal Ganglia gate behaviours by relieving tonic inhibition on downstream sensorimotor structures *adapted from Sommer and Basso 2011. A) a schematic of the Basal Ganglia microcircuitry. B) an example of the discharge profiles of the Striatum, SNr and SC during a saccadic eye movement adapted from traditional models. Vertical lines represent action potentials, thick black bar indicates when a saccade action would be taking place in such a model.*

It has recently been shown that different functional systems may be modulated by distinct populations of dopaminergic neurons that are genetically, anatomically and functionally diverse (Lerner et al., 2015; Matsumoto & Hikosaka, 2009; Watabe-Uchida et al., 2012), raising the possibility that there are dedicated dopaminergic systems for specific kinds of behaviour. In particular it has been proposed that there is a dedicated dopaminergic circuit for processing threat-related information and motivating or reinforcing threat-related avoidance. This circuit consists of dopaminergic neurons in the Substantia Nigra pars Lateralis (SNL) (Figure 1.5 A and B) (Menegas et al., 2017, 2018; Watabe-Uchida & Uchida, 2019) and their major projection target the posterior Tail of the Striatum (TS) (Figure 1.5C).

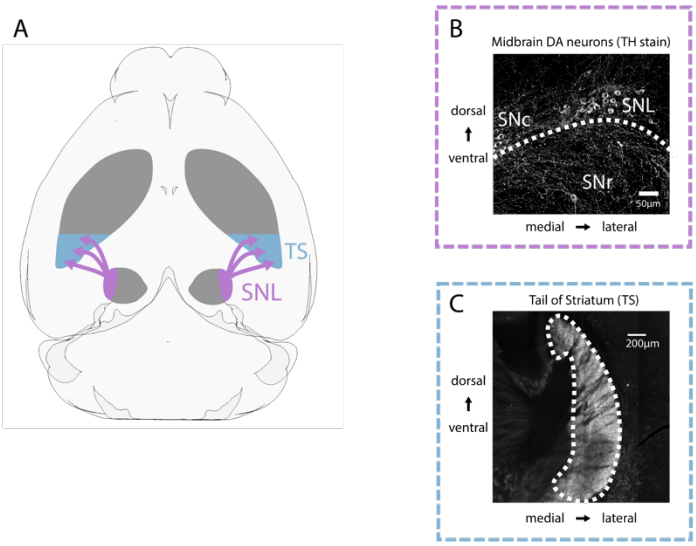

Figure 1.5: the SNL and TS circuit may compute threat prediction error. *A) a whole brain schematic illustrating the approximate location of the SNL-TS circuit, the SNL (purple), sends projections (purple arrows) specifically to the most posterior parts of the Striatum (blue). The Caudoputamen and SNr are shown in grey for reference. B) a coronal section of the SNL and surrounding area stained with a Tyrosine Hydroxylase (white) to reveal dopaminergic neurons. The SNL, SNc and SNr (white dashed line) are all labelled. C) a coronal section of the TS (white dashed line) and surrounding area, stained with Tyrosine Hydroxylase to reveal dopaminergic axons in the region, which predominantly arise from the SNL.*

Interestingly, the SNL-TS circuit exhibits functional and anatomical properties that suggest it may be of particular relevance for the modulation of escape decisions. These will briefly be covered in the next section.

1.5.1 The functional role of dopaminergic neurons in the SNL

Traditionally, the learning of appropriate actions in response to sensory cues is thought to occur through reinforcement learning, whereby dopamine signals modulate the strength of connections that drive rewarded actions thus increasing the likelihood of them being selected again in the future. However,

dopaminergic neurons in the SNL don't respond to reward per se (Figure 1.6A).

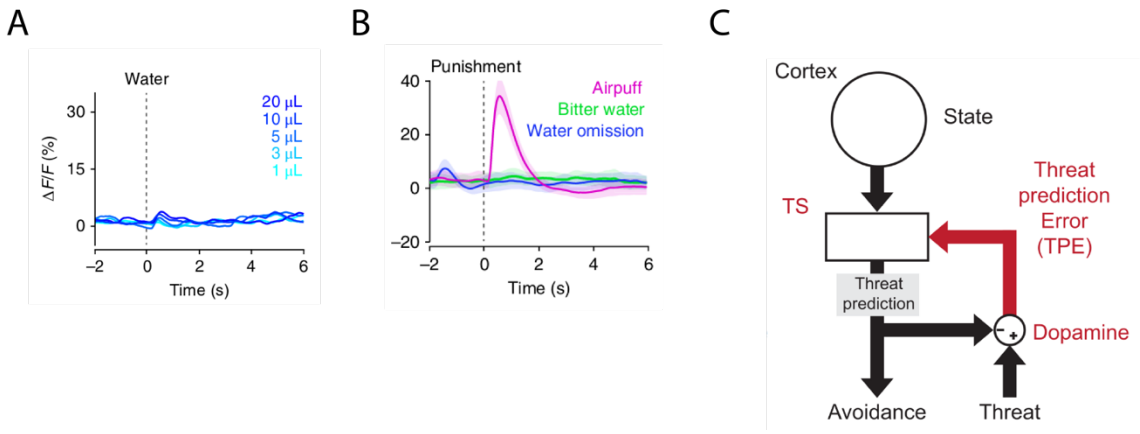

Figure 1.6: the SNL-TS circuit may compute threat prediction error. *A and B) fiber photometry recordings of the SNL, figure adapted from Menegas 2018. The authors express GCaMP6f in the SNL using a dat-Cre mouse line and record from dopaminergic SNL axons in the TS. A) typical responses of SNL neurons to water rewards of a range of volumes and B) typical responses of SNL neurons to a range of aversive stimuli. C) a schematic taken from* (Watabe-Uchida & Uchida, 2019)*, to illustrate the possible role of the SNL-TS circuit in computing threat prediction errors for driving avoidance behaviour.*

Instead, dopaminergic neurons in the SNL preferentially respond to novelty and intensity of stimuli, particularly if those stimuli are external and/or aversive such as air puffs (Menegas et al., 2017, 2018; Watabe-Uchida & Uchida, 2019) (Figure 1.6B). Additionally, it has been shown that SNL signals attenuate with repeated stimulus presentations and this attenuation correlates with avoidance behaviour: in freely moving mice, SNL neurons are responsive during retreat from novel objects, but not familiar ones, and these neurons are not active during approach (Menegas et al., 2018). This activity seems to be causally involved in behaviour: selective lesions of dopaminergic neurons using 6-hydroxydopamine (6-OHDA) lead to an increased rate at which behavioural responses attenuate without affecting initial responses. This is

consistent with a growing literature that considers the role of dopaminergic neurons in reporting novelty, or the absolute value of reward: motivational salience. The reported activity of these neurons is also consistent with models of sensory prediction error, whereby unexpected sensory input leads to large transient dopaminergic signals but expected sensory input doesn't. This has led to the idea of SNL dopamine as a signal that represents threat prediction error (Figure 1.6C), a signal that can reinforce threat-related responses of the TS that, in turn, can gate avoidance responses when they are appropriate or suppress them when they are not. However, while this idea is compelling it remains untested in ethological scenarios or under conditions in which the presumed threat level can be carefully controlled such as innate escape from looming stimuli.

Interestingly, the SNL receives a significant proportion of its input from brain regions that have been shown to be involved in loom-evoked escape (Watabe-Uchida et al., 2012), either crucially, such as the SC and PAG (Evans et al., 2018), or in a modulatory capacity, such as the Central Amygdala, Basolateral Amygdala (Evans et al., 2018; Zheng Zhou et al., 2019) and Zona Incerta (Chou et al., 2018). Together with the distinctive functional properties of the SNL, this suggests that the SNL may also be involved in loom-evoked escape decisions.

1.5.2 The TS is functionally and anatomically distinct from other parts of Striatum

The TS is also functionally and anatomically distinct from neighbouring parts of the Striatum. The TS has been shown to constitute a fourth functional striatal domain based on its distinct inputs from cortex and Thalamus when compared with the other striatal domains (Griggs et al., 2017; Hunnicutt et al., 2016; Jiang & Kim, 2018). In particular, the TS receives dense innervation from regions that receive much of their input from the SC: from the Lateral Posterior Nucleus of the Thalamus, which receives input from widefield neurons of the superficial SC (Gale & Murphy, 2018b) and projects to the TS; from the POm and VPM

of the Thalamus that receive their input from the intermediate and deep SC (McHaffie et al., 2005); and from the cortical Postrhinal Area (2011 Allen Mouse Brain Connectivity Atlas. Available from: https://connectivity.brain-map.org/projection), a region that receives substantial indirect input from the SC (Beltramo & Scanziani, 2019) via the Lateral Posterior Nucleus of the Thalamus. Additionally the TS receives cortical input from visual, auditory, ectorhinal and temporal areas, as well as input from Central Amygdala and Basolateral Amygdala (Hunnicutt et al., 2016). This anatomical distinction may also reflect function and indeed it has recently been shown that optogenetic stimulation of neurons in the superficial SC that drive escape (PV, NTSR1 and CAMKII expressing neurons) leads to a selective increase in activity in the posterior parts of the Striatum, including the Tail of the Striatum (Sans-Dublanc et al., 2020a).

To summarise, although there are many possible routes through which escape could be modulated, it is likely that flexibility in the perception of a particular stimulus as threatening and the subsequent decision to escape from looming stimuli occurs upstream of the dorsal PAG in the superficial SC or deep SC. Modulation of the decision to escape must account for experience and context, which implicates the cortex and Basal Ganglia as possible mediators of such learned control. Given the extensive literature on the role of the Basal Ganglia in action selection, its ability to sample both cortical and subcortical sensory streams, and evidence suggesting there is a dedicated dopaminergic system for evaluating threat, it is possible that the Basal Ganglia plays an as yet unknown role in the modulation of escape. In the following chapters I will address the question of **how innate drives and modulatory processes are balanced to guide behaviour.** More specifically, I will consider **the extent to which prior experience shapes the activity of circuits that drive instinctive behaviours, to modulate or potentially override them under conditions in which they may no longer be advantageous**. In doing so I will specifically consider the role of a Basal Ganglia circuit that has been implicated in threat-based learning, the SNL-TS circuit.

Chapter 2: Materials and methods

2.1 Mice

All procedures were performed in accordance with the UK Home Office regulations Animal (Scientific Procedures) Act 1986 and the Animal Welfare and Ethical Review Body (AWERB). Procedures were carried out using the following mouse lines: Adora2a-Cre (A2a-Cre, MMRRC 036158), C57BL/6J (C57, Jax 000664), Drd1a-Cre (D1-Cre, MMRRC 029178), DAT-tTA (DAT-tTA, Jax, 027178). Mice from the following crosses were also used: D1-Cre/A2a-Cre. Lines were maintained by back crossing with C57BL/6J. Genotypes were determined by PCR using ear biopsies. For purely behavioural experiments, male wild type mice (C57BL/6, Charles River) arrived and were housed in cages of 5 at 6-8 weeks of age and were separated into single housing for at least 2 days prior to testing. For all other experiments, mice were separated into single housing after surgery and kept under these conditions until behavioural testing (2-4 weeks for viral expression, 5 days for NMDA lesions, 2 weeks for 6-OHDA lesions).

2.2 Histology

2.2.1 Perfusion

Mice were anaesthetised with Euthatal (100 – 150μl, 1:3 Euthatal:saline mix) perfused transcardially with 10-20ml of phosphate buffered saline (100mM PBS) followed by 10ml of PFA (4% in PBS) brains were extracted, and fixed overnight in PFA before being transferred to PBS.

2.2.2 Confirmation of lesion sites

For histological confirmation of lesion sites, brains were sliced at 50μm (Leica SM2010 R Sliding Microtome). All steps were carried out in solution in well plates: 1-3 hours in blocking solution (1 % BSA, 0.3% Triton-X and 0.02% sodium azide); incubation with primary antibodies (NeuN Rb and GFAP ChK,

1:1000 for NMDA lesions, TH Rb for 6-OHDA lesions), and incubated overnight on a shaker. Slices were then washed twice in blocking solution. Slices were then incubated for 1-3 hours in secondary antibodies (Goat anti-chicken 488 and and Donkey anti-rabbit 594 for NMDA lesions, Goat anti-Rb 647 for TH) and mounted on slides.

2.2.3 Tracing, cell detection and visualization

For tracing experiments, on the day of imaging brains were removed from PBS, mounted (5% agar), and then glued to a microscope slide and transferred to a serial section (Mayerich et al., 2008) two-photon (Ragan et al., 2012) microscope. The microscope was controlled using (ScanImage v5.6, Vidrio Technologies, USA) with BakingTray, a custom software wrapper for setting imaging parameters (https://github.com/SainsburyWellcomeCentre/BakingTray, https://doi.org/10.5281/zenodo.3631609). The agar block was submerged in 50mM PBS and the brain was imaged using a 780nm LASER (MaiTai eHP DS) for simultaneous GFP and mCherry excitation. Dichroic mirrors and bandpass filters were used to separate red, green and blue (background channel) signals, detected using three PMT channels (Hamamatsu R10699 multialkali with Femto DHCPA 100 amplifiers). The brain was imaged at 1.2μm x 1.2μm x 5μm (XYZ) resolution, with 10 images taken per 50μm slice, to acquire 3d whole-brain datasets for cell counting. Images were assembled following acquisition using StitchIt (https://github.com/SainsburyWellcomeCentre/StitchIt, https://zenodo.org/badge/latestdoi/57851444).

2.3 Viruses

Experiment	Virus	From
SNL input tracing	AAV1-tet-G-TVA-N2cG	SWC
SNL input tracing	EnvA CVS-N2c-G-mCherry	SWC
SC input tracing	EnvA CVS-N2c-G-mCherry	SWC
D1 input tracing	AAV8-EF1a-Flex-GT	SWC, Addgene (26198)
D1 input tracing	AAV1-hSyn-Flex-H2B-EGFP-P2A-N2cG	SWC, Addgene (126469)
SNL photometry	AAV5 tre-GCaMP6f	Vector Builder
D1/D2 TS photometry	AAV1-Syn-Flex-GCaMP6f-WPRE-SV40	Addgene (100833-AAV1)

Table 2.1: list of viral constructs used.

Structure	**AP**	**ML**	**DV**
SNL	-3.40	+/- 2.15	-3.70
TS	-1.82	+/- 3.41	-3.35
medial SC	-0.4 rel. lambda	+/- 0.4	-1.8

Table 2.2: list of injection coordinates used. *Coordinates are in millimetres relative to bregma unless otherwise stated.*

2.4 Drugs

N-Methyl-D-Aspartic acid (NMDA) was obtained from Tocris and mixed 1mg/100μl in cortex buffer (NaCl 125mM, KCl 5mM, Glucose*H20 10mM, Hepes 10mM, MgSO4*7H20 2mM and CaCl2*2H20 2mM, at pH 7.4). HB1889 6-Hydroxydopamine (6-OHDA) hydrobromide was obtained from HELLOBIO and dissolved in saline solution containing 0.2% ascorbic acid (Sigma Aldrich). Drugs were mixed immediately prior to surgery and kept in the dark on ice to avoid decomposition. After ~3 hours solutions were discarded and made fresh. Paragyline and desipramine pre-treatment solution consisted of 28.5mg desipramine (Sigma-Aldrich, D3900-1G) and 6.2mg paragyline (Sigma-Aldrich, P8013-500MG) in 10ml of water and NaOH to pH 7.4. Mice were injected intraperitoneally with 10mg/kg just before surgery.

2.5 Surgical procedures

2.5.1 Stereotaxic injections and fiber implantation

Male mice between 5-12 weeks of age were anaesthetised in an isofluorane induction chamber (3-4% isofluorane, 1L/min) before being transferred to a nose cone (2% isofluorane, 1L/min) where the scalp was shaved. Surgical procedures were performed under anaesthesia using isofluorane (1.5-2%, 1L/min). Protective gel was applied to the eyes (Puralube Vet Ointment), analgesia was given subcutaneously (Metacam 25μl/10g) and the temperature was maintained at 36 degrees Celsius using a heating pad and temperature probe. The mouse was then secured on a stereotaxic frame (Angle Two, Leica Biosystems). After incision or a small skin resection, the skull was leveled such that the difference along the dorsoventral (DV) axis between bregma and lambda was 0μm and the DV difference between two points (AP: -1.5mm, ML +/- 2.3mm) was also 0μm. Small (~0.5-1mm) craniotomies were made in the skull using a dental drill (Osada Electric, Japan) and, if necessary, the skull was re-leveled to account for any displacement following drilling. Viral vectors or neurotoxic substances were administered using glass pulled pipettes (3.5" Drummond #3-000-203-G/X) with tips clipped to a diameter of ~20μm. Injections were performed at an average rate of 0.33nl/s (5nl per injection cycle, 1nl/s and 10s wait) using a motorised injector (Nanoject 3, Drummond) and 5-10 minutes were given before retracting the glass pipette to reduce excessive spreading of the injected volume. Following injection, craniotomies were filled with silicone elastomer (Kwik-Cast, WPI). If no implant was inserted, then the scalp was closed using sutures (Vicryl Rapide).

For photometry experiments, implantation of fiber optic cannulae (200μm or 400μm diameter core, Doric Lenses) was performed during the same surgical session as viral injection at least 5 minutes following viral injection. The dura was removed, the skull was roughened, and implants were inserted.

Implants were attached to the skull using UV cure dental cement (RelyX Unicem 2 Automix) reinforced with dental cement (Super-Bond). Following surgery, the mouse was returned to its home-cage to recover on a heat pad and was closely monitored to ensure good recovery. All injections and fiber placements were confirmed post-hoc histologically.

2.5.2 Lesions

NMDA induced excitotoxic lesions: Bilateral lesions of the TS were attained by injection of 150nl of NMDA (3nl per injection cycle, 1nl/s, 10s wait) into the TS of each hemisphere. The mouse was allowed to recover over a period of at least 5 days before testing.

6-OHDA: We followed a protocol previously demonstrated to selectively reduce dopaminergic projections to the site of injection (Menegas et al., 2018; Thiele et al., 2012). 250nl of 6-OHDA was injected bilaterally into the TS of each hemisphere. In a subset of experiments a second injection was also carried out, 300μm further anterior than the first. A pre-treatment solution of paragyline and desipramine was also given to prevent 6-OHDA uptake in noradrenergic neurons.

2.5.3 Photometry

For SNL recordings we injected 200-450nl of tre-GCaMP6f in the SNL of heterozygous DAT-tTA mice. A fibre cannula (Doric Lenses 0.57NA, 400μm diameter) was then implanted in the TS. For TS recordings, we injected 30-150nl of flex-GCaMP6f into Drd1-cre or A2a-cre mice. Fibers were placed 50-80μm above the site of injection.

2.5.4 Tracing

To label monosynaptic inputs to particular brain regions, we followed an approach that utilizes a modified rabies virus that lacks the glycoprotein gene required for multi-synaptic spread (Wickersham et al., 2007). Tracing

experiments consisted of two separate surgeries, the first to transfect the population of neurons to be traced with helper AAVs that reintroduce this missing glycoprotein gene along with a gene for the TVA receptor required for rabies to gain entry to cells. 3-7 days later a second surgery was performed in which rabies virus was injected to the target structure. 20-30nl of each virus was injected. At least 10 days were given for expression of rabies before sacrifice.

2.6 Behavioural testing

Each mouse was transferred in their home cage to the experimental room and given at least 5 minutes to acclimatise to the room under low light conditions. After this time, mice were transferred to the behavioural arena using a cardboard mouse house, allowing the mouse to freely climb on the house before transferring them to the behavioural arena and moving the computer monitor into place. The sound deadening box was then closed and the behavioural protocol initiated (see section 2.9, Behavioural protocols, below). For photometry experiments, prior to behaviour, mice were briefly anaesthetised (< 2 mins, 3.5% isofluorane, 1L/min) and transferred to the set-up where an optic fiber was attached to each implant. Mice were then transferred to their open home cage and given 5-10 minutes to acclimatise to the fiber attachment before being transferred to the behavioural arena for testing.

2.7 Experimental set-up

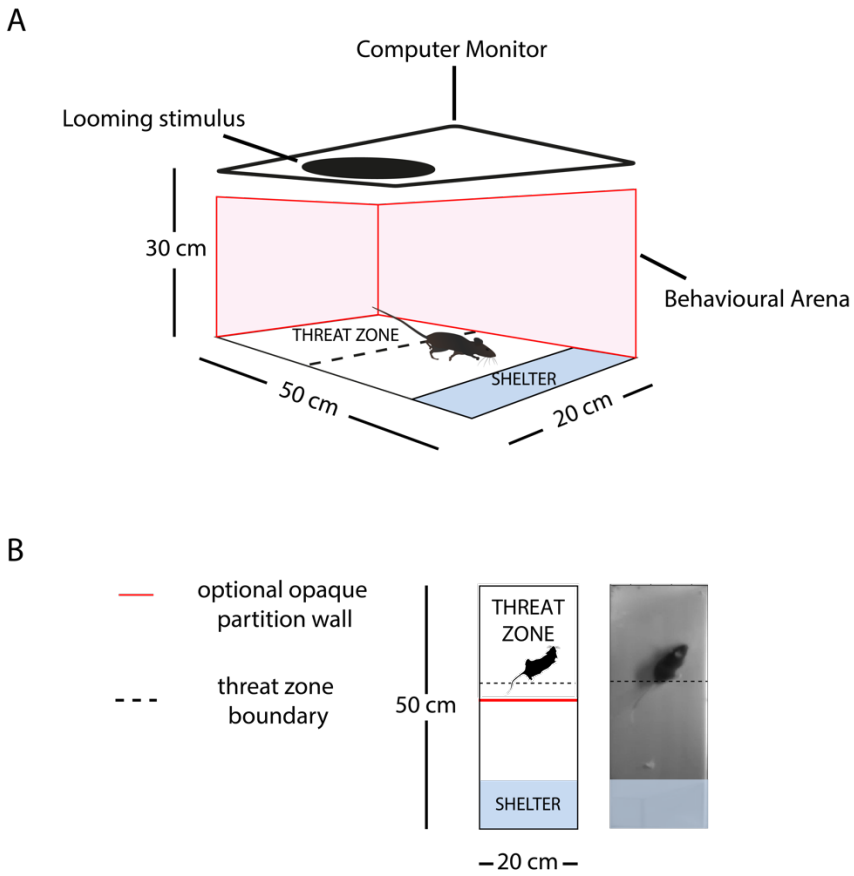

Figure 2.1: the behavioural set-up. *A) 3D schematic of the set-up used for behavioural experiments consisting of a 50cm x 20cm x 30cm Perspex box, with a shelter at one end projecting 10cm from the wall (blue shaded area), and a computer monitor 30cm above the floor for presentation of visual stimuli. The threat zone, a region that, if entered triggers the onset of visual stimuli, is indicated by the dashed line and is 20cm from the opposite end of the arena to the shelter. B) Aerial view of the arena (left) with an example frame following preprocessing (right).*

The behavioural arena (Figure 2.1A and B) was adapted from one previously shown to elicit escape with high probability (Evans et al., 2018): a 50 cm x 20 cm x 28 cm (L x W x H) red Perspex arena with a white opaque floor. At one end, the arena included a red Perspex shelter, which was either round (10cm diameter) or rectangular (10cm x 20cm x 10cm). An optional red Perspex

partition could be inserted to block the corridor 28 cm from the far end of the arena for use in the LSIE protocol. A computer monitor (Dell E2210F Black (WSXGA+) 22" TN) was positioned 30 cm above the floor, parallel with the floor and was used for displaying visual stimuli. The set-up was contained within a custom-built sound deadening box (LS Fabrications) with the following outer dimensions: 120cm (W) x 90cm (inc. door, D) x 100cm (H) with a 6cm thick wall.

2.8 Sensory Stimuli

2.8.1 Looming stimulus

Each *looming stimulus* consisted of 5 consecutive looming spots presented with an inter loom interval of 0.4 seconds (Figure 2.2A). Each of the 5 looming spots consisted of an expanding circular black spot (Vale et al., 2017) presented on the computer monitor with background of constant luminance (8 cd/m^2 as measured at the floor of the arena). The looming spot subtended a visual angle of 3 - 50 degrees over 0.2 seconds (220 deg / sec) and remained at maximum radius for 0.25 seconds. Where contrast was manipulated it was done by either modifying the spot luminance while keeping the background luminance constant, or by modifying the background luminance while keeping the spot luminance constant (see section 2.9, Behavioural protocols).

2.8.2 Auditory stimulus

Auditory threat stimuli consisted of a 85db pink noise of 3s in duration played with a short ramp to prevent onset and offset artifacts.

2.9 Behavioural protocols

2.9.1 Testing of escape

Unless otherwise stated mice tested were *naïve*, meaning that they had no previous experience of loom-evoked escape. For all protocols testing escape behaviour, mice were first introduced to the arena and allowed 7 minutes

exploration without any looming stimuli. After this *acclimatisation period*, looming stimuli were presented the next time the mouse entered the threat zone. Consecutive presentations had a minimum inter-trial interval of 90s irrespective of whether the mouse entered the threat zone during that period.

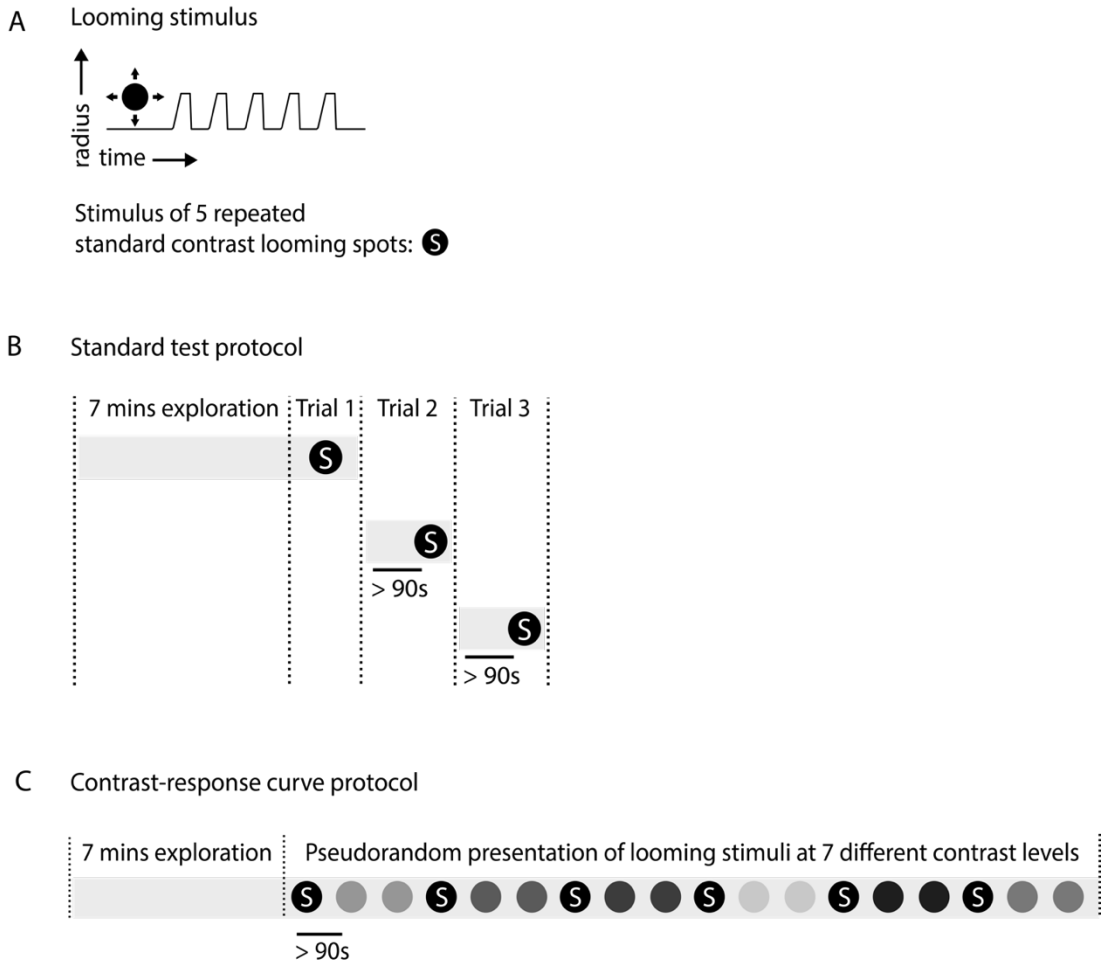

Figure 2.2: protocols for testing behavioural responses to looming stimuli. *A) the looming stimulus, consisting of 5 consecutive looming spots. Black line illustrates how the looming spot radius changes over time. This stimulus of 5 looming spots at standard contrast is denoted as a black circle with an S. B) the protocol for testing escape behaviour consists of 4 sections, the starts and ends of which are indicated by dashed lines. Mice are first given 7 minutes to explore before being presented with a looming stimulus (A) triggered by threat-zone entry provided that no stimulus has occurred in the last 90 seconds. This test consists of 3 trials in total. C) schematic of a different*

protocol, used to test the same mouse multiple times at different contrast levels. Stimuli of 7 different contrast levels (grey and black circles) were pseudorandomly presented, stimuli at standard contrast were presented on the first trial and on every 3rd trial after this, indicated as black circles with an S on them.

2.9.2 Standard test

The *standard test* used for measuring escape behaviour (Figure 2.2B) consisted of a 7-minute exploration period and 3 *test trials* only, separated by at least 90s. In a standard test, looming stimuli are presented at *standard contrast* (background luminance: 8 cd/m^2; spot luminance: 0.09 cd/m^2). Throughout the thesis this symbol represents a looming stimulus at standard contrast: ❶ (Figure 2.2A). This test was used for all naïve mice and also for pre- and post-tests before and after the LSIE protocol (Figure 2.3).

2.9.3 Contrast-response protocol

To generate *contrast-response curves* for individual mice we tested mice with up to 18 stimuli at 7 different contrast levels. In this protocol, the contrast was varied pseudorandomly by changing the luminance of the looming spot (Figure 2.2C). In the first test trial the stimulus was always at standard contrast, and subsequent trials were structured as follows: two trials at low contrasts followed by one trial at standard contrast. To build contrast-response curves for the population, escape probability was calculated for all trials pooled at each contrast.

2.9.4 The learned suppression of innate escape (LSIE) protocol

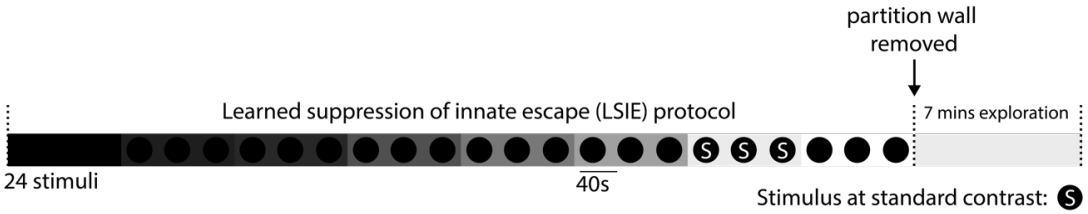

Figure 2.3: the learned suppression of innate escape (LSIE) protocol. *A schematic of the LSIE protocol, consisting of 24 stimuli (black circles) spaced 40s apart presented to a mouse in a restricted arena. Stimulus presentation occurs irrespective of the mouse's position within the restricted arena (Figure 2.1B, with partition in place). Every 3 trials the background luminance is increased. After these stimuli have been presented, the partition wall is removed and mice are given 7 minutes to explore the full arena, before being given test trials or returned to their home cage for later testing.*

For LSIE experiments, mice were placed in the partitioned threat zone of the behavioural arena (Figure 2.1B). Once in the behavioural apparatus, the stimulus monitor was positioned overhead (Figure 2.1A) and the LSIE protocol (Figure 2.3) was presented to the mouse. After this, typically the partition was removed, and mice were allowed 7 minutes to explore the arena before undergoing a standard test. However, for some experiments, following the LSIE protocol, mice were removed from the arena and returned to their home cage to be tested at a later date.

2.10 Data acquisition

2.10.1 Behaviour

Data acquisition was controlled using custom scripts in MATLAB or Python and synchronised using NIDAQ (National Instruments, BNC2090A and PCI-6363). Videos were acquired at 30Hz using an IR sensitive camera (Basler acA640-750um USB 3.0) positioned 70cm away from the arena and 70cm

above the floor of the arena. IR LED strips provided diffuse illumination of the arena. Frames were acquired using a NIDAQ generated synchronization pulse that triggered frame acquisition and was recorded on the NIDAQ along with the rest of the data for post-hoc synchronisation. As the computer monitor used to present visual threat stimuli prevented the camera being positioned directly overhead, videos were first perspective-corrected using a projective transformation applied to raw images using the coordinates of the corners of the arena and the known geometry of the arena (Figure 2.4).

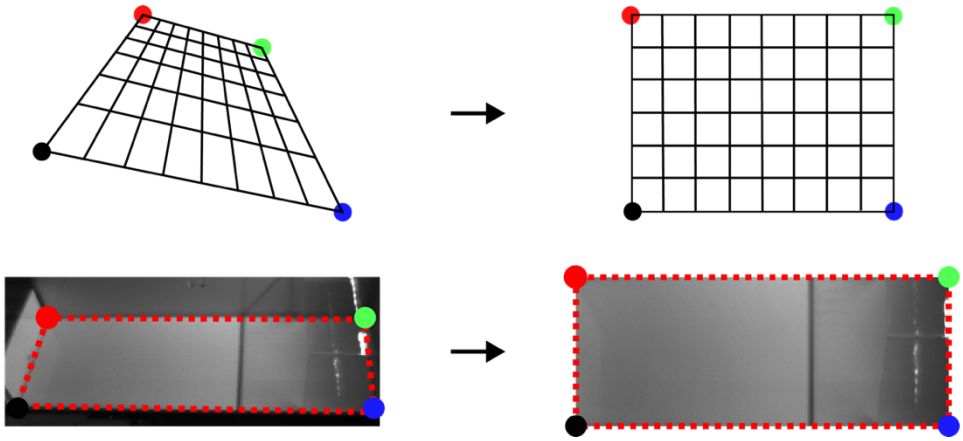

Figure 2.4: transforming videos to standard space. *A pre-processing step applied to all videos to normalise the position of the mouse in the arena correcting for camera angle. Schematic of the preprocessing transformation applied to correct all videos (top row) adapted from https://www.graphicsmill.com/docs/gm5/Transformations.htm, which takes a trapezium and transforms it into a rectangle, together with the result of applying the transformation to a single frame of acquired data (bottom row).*

The position of the mouse was tracked during the experiment and used to trigger the presentation of stimuli when mice entered a “threat zone” defined as a 20 cm x 20 cm region at the far end of the arena (Figure 2.1A and B). Some data were acquired by manually triggering the stimulus upon entry to the threat zone. *Looming stimuli* were presented with Psychtoolbox and real-time stimulus presentation onsets were determined post-hoc using a

photodiode (Thorlabs APD430C) acquired at 10kHz. Auditory stimuli were either played using NIDAQ generated waveform amplified with a Kemo MO32S amplifier or was played using the sound card amplified using a qtx-kad2 amplifier. Sounds were presented using a loudspeaker (8Ohm, 10W) attached to the far end of the monitor, above the threat zone and facing downwards.

2.10.2 Photometry

Data were acquired, demodulated and filtered using custom scripts in Python and a NIDAQ (National Instruments, BNC2090A and PCI-6363). We followed a protocol for acquiring signal and background channels from GCaMP6f-expressing cells by stimulating at calcium sensitive (465nm) and insensitive (405nm) wavelengths that allows ratiometric measurements, bleaching and artifact correction with a single fluorophore (Lerner et al., 2015). LED output power was matched for the two channels and was amplitude modulated with a sine wave (peak amplitude 0.2 μW) at different frequencies for each channel (211Hz and 531 Hz, respectively) to enable source separation after data acquisition. All optical acquisition components had a numeric aperture of at least 0.57, and stimulation components 0.22 (Doric lenses).

2.11 Data analysis

2.11.1 Anatomical tracing: cell detection and transformation to standard space

We detected cells using cellfinder (Tyson et al., 2020). We segmented and registered brains with brainreg (http://doi.org/10.5281/zenodo.3991718 , Niedworok et al., 2016)) using the Allen Mouse Brain Atlas (Wang et al., 2020) and the Enhanced and Unified Common Mouse Brain Atlas (Chon et al., 2019) provided by the BrainGlobe atlas API (F Claudi et al., 2020). Data was visualised using napari (doi:10.5281/zenodo.3555620) and brainrender (F Claudi et al., 2020).

Analysis was performed using cellfinder (version 0.4.7). Cell detection identified candidates as bright regions larger than a sphere 6μm x 6μm x 15μm in size. These candidates were refined to exclude false positives using a custom trained network based on the default ResNet provided as part of cellfinder. This was further trained for 994 epochs, until a final loss of 0.006, using 50 manually classified cells and 89 manually classified non-cells

together with the original training dataset provided with cellfinder to prevent overfitting.

2.11.2 Behavioural tracking

The position in the behavioural arena of each mouse was tracked in 2 dimensions using DeepLabCut2.0 (Nath, Mathis 2019) using a single label of the centre of the body. The training dataset was composed of 911 manually annotated frames selected from 20 videos of open field exploration after video pre-processing steps including transformation to standard space had been applied. This dataset was used to train the default network provided (Resnet_v1_50). Training was allowed to run to completion > 1,000,000 iterations resulting in a final loss of 0.001, a training error of 1.53 pixels, and a testing error of 4.57 pixels. Tracks were filtered using DeepLabCut's built-in median filtering with a window length of 5 frames. 64 videos were suboptimal for automated tracking and were tracked manually.

Positional tracks were converted to cm from pixels using the known dimensions of the arena. All other metrics were derived from the positional track of the mouse along the longest edge of the arena, calculated as follows: speed was the smoothed differential of position; acceleration was the smoothed double differential of position; *escape latency* was defined as the time from stimulus onset to the onset (acceleration and speed thresholds) of the first trajectory back to shelter; time to shelter was defined as the time from stimulus onset to the next shelter entry; time to leave shelter was defined as the time from entry of the shelter to the next time the mouse left the shelter. Escape was defined as a return to shelter within 5 seconds of stimulus onset at a speed of at least 25.5 cm/s.

2.11.3 Photometry signal processing and analysis

Raw photometry recordings were demodulated (see section 2.10.2) and were then normalised by calculating ΔF/F using the 405nm channel as reference by

first fitting this background channel to the signal channel using linear regression before computing the following:

$$\Delta F/F = \frac{465nm\ channel - 405nm\ channel}{405nm\ channel}$$

Signals were baseline corrected using the median of 0.8s of signal immediately preceding the onset of the looming stimulus.

Analysis of photometry data for contrast-response curves

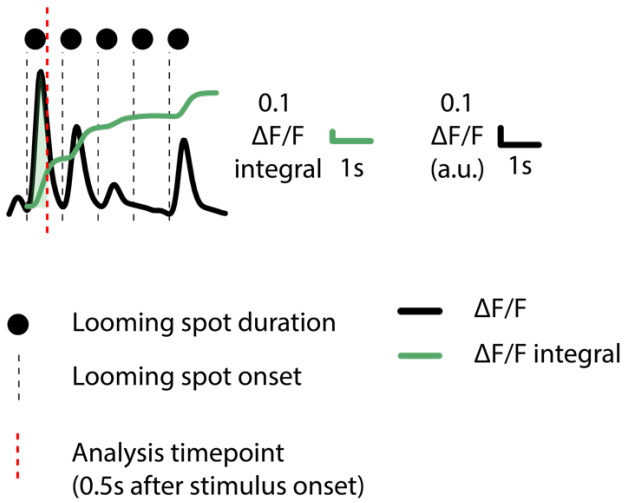

Figure 2.5: estimation of loom-evoked signals at a fixed timepoint. *An example ΔF/F trace (black line) and its corresponding integral (green line) taken from a test trial at standard contrast to illustrate the analysis of loom-evoked Ca^{2+} signals for trials obtained using the contrast-response protocol. The value of the integral trace is taken from the analysis timepoint (red dashed line), 0.5 seconds after the onset of the looming stimulus to only include the signal during the first looming spot.*

To analyse the magnitude of these signals in response to the looming stimuli we computed the integral of the ΔF/F traces from the onset of the stimulus until the end of the window used to classify escape (5s following stimulus onset). Integrals were estimated using the trapezium rule. For analysis of signals acquired during the contrast-response curve protocol (Figure 2.2C) we take

the value of this integral 0.5s after the onset of the 1st looming spot (Figure 2.5).

Analysis of photometry data for standard tests pre- and post- LSIE

In order to analyse loom-evoked activity before and after our LSIE protocol within a given mouse we analyse the ΔF/F integral traces from stimulus onset until the escape latency. The escape latency was determined for each mouse by taking the average escape latency of the three pre-test trials (Figure 2.6A). The integral is therefore taken up until this time point (Figure 2.6B and C) for all trials. Signals were normalised by taking the maximum value at this timepoint for all trials included in the analysis (Figure 2.6D).

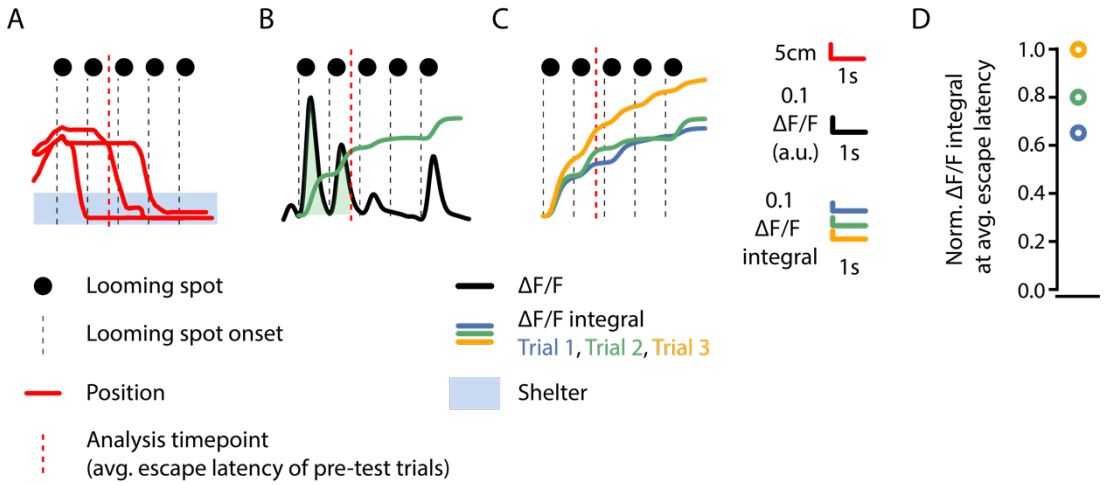

Figure 2.6: estimation of loom-evoked signals using escape latency. *A) position tracks (red, solid line) from three example trials with the average escape latency (red, dashed line). B) a ΔF/F trace (black solid line) from an example trial, the ΔF/F integral (green, solid line) and the analysis timepoint shown (red, dashed line) which is the average escape latency of this mouse. C) the ΔF/F integrals taken from three standard test trials, with the corresponding values at escape latency in D), which are normalised to the largest value at this time point for all trials included in the analysis. A value of 1 indicates that this is the largest signal measured in this way for all trials included in the analysis for a given mouse.*

Chapter 3: The Substantia Nigra pars Lateralis and Tail of Striatum are required for escape.

3.1 Introduction

As outlined in Chapter 1, the innate decision to escape from overhead looming spots is computed within a compact circuit consisting of the medial SC and dorsal PAG. We expect factors that influence escape behaviour, such as prior experience, to lead to changes in activity within this circuitry. Thus we predict that neural systems capable of driving such change in the context of looming stimuli should receive stimulus-related input, and they should also project back to the medial SC and/or dorsal PAG in order to influence the activity there. A sub-circuit of the Basal Ganglia comprised of the SNL and TS is known to receive some input from midbrain structures such as the SC and PAG (Menegas et al., 2015) and the SNL-TS circuit has recently been proposed to compute threat prediction error for the reinforcement of avoidance responses (Watabe-Uchida & Uchida, 2019). Such a prediction would be useful for learning to suppress the escape decision based on prior experience if, for example, a stimulus is observed to be less threatening than initially estimated. Together, this suggests that the SNL-TS circuit is an important candidate pathway that could be involved in the modulation of innate escape responses. In this chapter, we investigate whether the SNL-TS circuit plays such a modulatory role through anatomical studies of the connectivity of the SNL-TS circuit, lesion experiments, and physiological recordings obtained using fiber photometry of SNL axons in the TS. We reason that, in order to modulate escape decisions, candidate structures ought to be:

1) Connected with the escape circuitry;
    a. Receive direct input from medial SC and/or dorsal PAG;
    b. Project to the medial SC and/or dorsal PAG;
2) Required for normal escape behaviour;
3) Responsive to looming stimuli, with responses that closely follow escape metrics such as escape probability and vigour.

We address each of these points in this chapter.

3.2 Results

3.2.1 The SNL-TS circuit receives direct input from the innate escape circuitry

The deep SC and PAG project to the SNL

The SNL has been previously shown to receive inputs from a variety of midbrain structures, but it has not been shown precisely how these inputs are distributed within midbrain structures that are involved in computing or modulating escape decisions. In the SC and PAG, distinct functional roles have been attributed to different subregions (Bandler & Shipley, 1994; Dean et al., 1989; Evans et al., 2018; Hoy et al., 2019; Illing & Graybiel, 1986; Lee et al., 2020; Tovote et al., 2016), and thus it is particularly important to determine how inputs to SNL are distributed across these subregions. To better understand the relationship between the SNL and the escape circuitry, we therefore performed monosynaptic rabies tracing from a subset of dopaminergic neurons in the SNL which project to the TS. To label monosynaptic inputs to these SNL dopaminergic neurons, we used a modified rabies virus that lacks the glycoprotein gene required for multi-synaptic spread (Wickersham et al., 2007) (Figure 3.1A). We first selectively re-introduced this missing gene, and a gene for the TVA receptor required for rabies to gain entry to cells to dopaminergic neurons of the SNL using a helper virus driven by tTA (tre-ΔG-TVA) in a DAT-tTA mouse line. 3-7 days later we performed a second injection to introduce the modified rabies virus into the TS. This approach allowed us to label the monosynaptic inputs of a subset of dopaminergic neurons that project to the TS (Figure 3.1B) following a similar approach to Menegas et al. (2017) (see Methods, Tables 2.1 and 2.2).

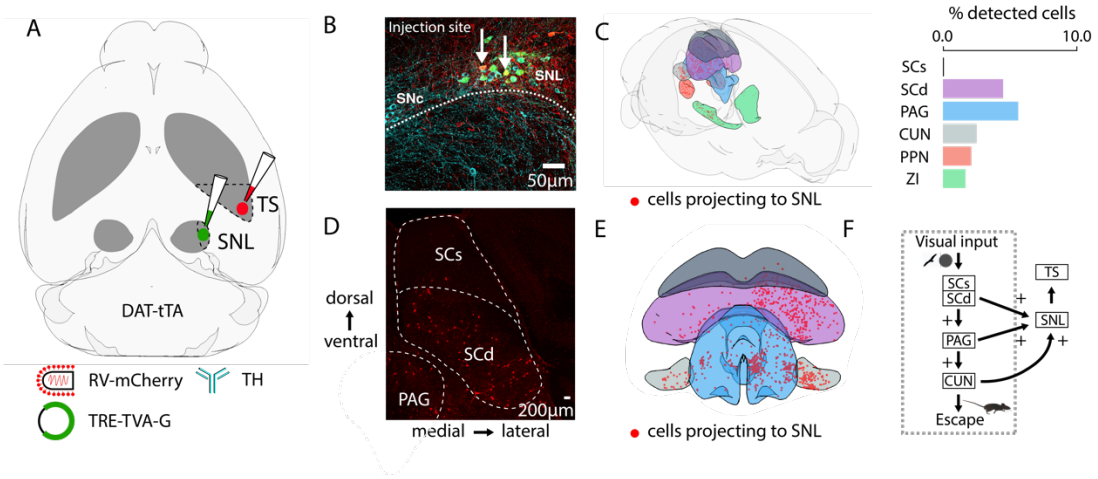

Figure 3.1: SNL inputs arise from structures that have been implicated in escape or modulation of innate fear responses*. A) schematic of the viral injection protocol used, in which a virus that drives the expression of the receptor required for rabies virus entry together with its deleted G-protein (AAV1 TRE-TVA-G) is injected into the SNL, followed several days later with a second injection consisting of ENVA N2C mCherry rabies virus in the TS. B) image of the injection site containing cells that express TVA and G protein (green), cells that are presynaptic to dopaminergic neurons in the SNL (red), and dopaminergic neurons (cyan) identified with a TH stain. White arrows indicate starter cells, labelled by all three markers. C) left, the coordinates of traced cells (red dots) in standard space within a subset of brain structures that have been implicated in innate fear responses or their modulation. Right, the % of the total detected cells that arise from each of the structures shown in B). D) a coronal section of the SC and PAG. E) the coordinates of traced cells (red dots) in standard space within the SC, PAG and Cuneiform Nucleus. F) a simplified circuit schematic showing connectivity from SC and PAG to SNL and TS. + signs indicate known/presumed glutamatergic connections.*

We find a variety of regions previously implicated in escape project to the SNL (Figure 3.1C; Table 3.1, n=1 mouse, 7687 detected cells) including the SC, PAG, Cuneiform Nucleus, Pedunculopontine Nucleus and Zona Incerta (Figure 3.1C, right; Table 3.1). We also find that nearly all neurons in the SC that project to the SNL reside in the deep layers (Figure 3.1D and E, deep

layers: n=355 cells, 4.6% of total cells c.f. superficial layers: n=4 cells, 0.05 % of total detected cells). We thus show that the SNL, which projects to the TS, receives input from the deep layers of the SC, from the dorsal and ventral PAG and from the Cuneiform Nucleus (Figure 3.1F).

Structure	Count	% of total	Cells per mm3
Caudoputamen (CP)	1083	14.09	37.8
Periaqueductal gray (PAG)	431	5.61	98.0
Superior colliculus, motor related (SCm)	355	4.62	59.7
Cuneiform nucleus (CUN)	196	2.55	373.5
Pedunculopontine nucleus (PPN)	163	2.12	174.5
Zona incerta (ZI)	130	1.69	72.0
Superior colliculus, sensory related (SCs)	4	0.05	1.8

Table 3.1: summary of inputs to the SNL showing *brain regions found to contain more than 100 detected*, ordered by total cell number*. The percentage of total cells and the cell count per* volume is also shown for each structure.

3.2.2 Mice escape from overhead high contrast looming spots

In order to assess the relevance of the SNL and TS to escape behaviour, we first reproduced a behavioural set-up for robustly eliciting escape. In this behavioural paradigm, mice with no previous experience of looming spots (*naïve mice*) are introduced into the behavioural arena and given 7 minutes to explore, after which each entry to the threat zone triggers the presentation of a looming stimulus (Figure 3.2A-C; Methods 2.2).

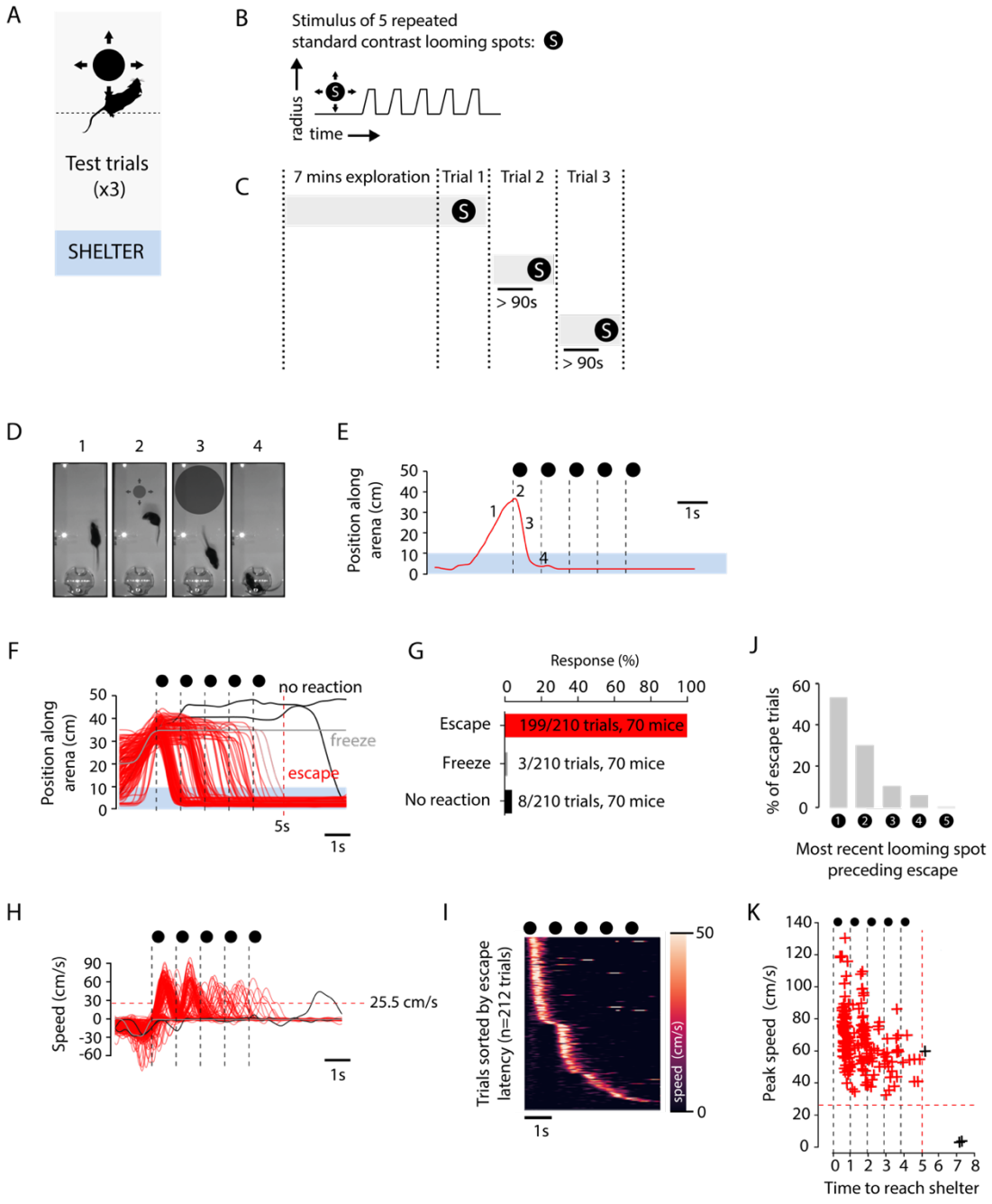

Figure 3.2: mice escape robustly from looming stimuli. *A) schematic of the set-up for testing escape. At one end of the arena there is a shelter (blue). At the opposite end there is a region defined as the threat zone in which looming stimuli are presented (black, dashed line). B) the looming stimulus used for testing escape, consisting of 5 consecutively presented looming spots. S indicates that the stimulus used is at standard contrast. C) the trial structure of the standard test. Dashed lines indicate different phases of the protocol, which consists of a 7-minute exploration phase in which no stimuli*

are presented, followed by three trials that are each triggered upon entry to the threat zone provided no stimulus has been presented in the last 90 seconds. D) images of typical stages in an escape response. Each image has a number above it which indicates the time point that this corresponds to in the corresponding position track (E). 1 is taken as the mouse is approaching the threat zone; 2 the mouse reorienting to face the shelter following detection of the looming stimulus; 3 the mouse while it is running to shelter; and 4 the mouse hiding in the shelter. E) the corresponding position track for this mouse (red line) along the long axis of the behavioural arena. Looming spot onsets (black, dashed lines) and their durations (black circles) are shown. Numbers indicate the corresponding image in (D). F) a representative set of position tracks across the population of mice for behavioural responses classified as escape (red), freeze (grey) or no reaction (black), the cut-off time to reach the shelter for classifying a return to shelter as escape is shown (red, dashed line). G) a bar plot indicating the fraction of behavioural responses observed categorised as escape, freezing or no response for all trials. H) velocity traces for the position tracks shown in (F) with the speed threshold used to classify escape responses plotted (vertical red dashed line). I) a heatmap of velocity traces for all trials, positive values indicate that velocity is in the direction towards shelter. All trials are sorted by escape latency. J) histogram showing the most recent loom preceding escape latency for the population, expressed as a percentage of the total number of trials. K) peak speeds of each trial plotted against the time to reach the shelter. Red dashed lines indicate the thresholds used to define escape. Red crosses indicate trials that were classified as escape, black crosses indicate trials that were classified as freeze or no reaction.

Typically, mice reacted to the stimulus by orienting to the shelter, running to the shelter and hiding in it (Figure 3.2D and E). We find that we can classify escape responses using the position along a single axis of the arena using the positional track and the speed derived from it (Figure 3.2F and H).

Using this protocol we attained a high escape probability to looming spots of standard contrast (Figure 3.2F and G, 94.7%, 199/210 trials from 68/70 mice) similar to that reported previously for a similar stimulus and set-up (Evans et al., 2018). We observed a low probability of no reactions (Figure 3.2F and G, 3.8 %, 8/210 trials from 5/70 mice) and an even lower probability of freezing responses (Figure 3.2F and G, 1.4%, 3/210 trials from 1/70 mice). We found that these escape responses all occurred within 5 seconds of stimulus onset, observing the range of speeds of escape reactions (Figure 3.2H and I) we also find that the peak speed reached in all escape trials exceeded 25.5 cm/s. We therefore chose to classify escape as a return to shelter within 5 seconds of stimulus onset, at a speed of at least 25.5 cm/s in the direction of the shelter (Figure 3.2K, upper left quadrant). Freezing responses were manually classified. 83.6% of escapes were initiated before the third looming spot.

3.2.3 The SNL and TS are required for normal escape behaviour and form a critical part of the escape circuitry that may modulate innate escape

Having established a set-up in which we can robustly elicit escape behaviour and reliably classify escape outcomes, we next assessed whether the SNL-TS pathway could influence escape probability or vigour.

It has been previously shown that escape outcomes are dependent on stimulus contrast (Evans et al., 2018)(Figure 3.3F). If the SNL and TS perform a significant role in the learned modification of escape, then we would expect lesions of either structure to lead to a measurable effect on normal escape behaviour, manifesting as a shift in the contrast-response curve to the left or right. Therefore, we next performed lesions of these structures and tested escape to looming spots with different contrasts (Figure 3.3). We performed lesions in two separate groups of mice: in one group the lesion was targeted to dopaminergic cells in the SNL projecting to TS; and in the other group

lesions were targeted to neurons in the TS (Figure 3.3A-D). We assessed each of these lesions histologically post-hoc. For SNL dopaminergic lesions, we used a tyrosine hydroxylase stain to measure the degeneration of dopaminergic inputs to the TS (Figure 3.3C, top), and compared with non-lesioned parts of Striatum (Figure 3.3C, bottom). For TS lesions we used a NeuN and GFAP co-stain to assess neuronal death following excitotoxic lesion with NMDA (Figure 3.3D).

We tested the contrast sensitivity of mice in both of these groups by pseudo-randomly presenting looming spots of different luminance (Figure 3.3E) to obtain contrast-response curves (Figure 3.3F) for each group. We presented pairs of low contrast stimuli intermingled with high contrast stimuli (Figure 3.3E, see Methods Figure 2.2C) and pooled the escape responses at each contrast tested.

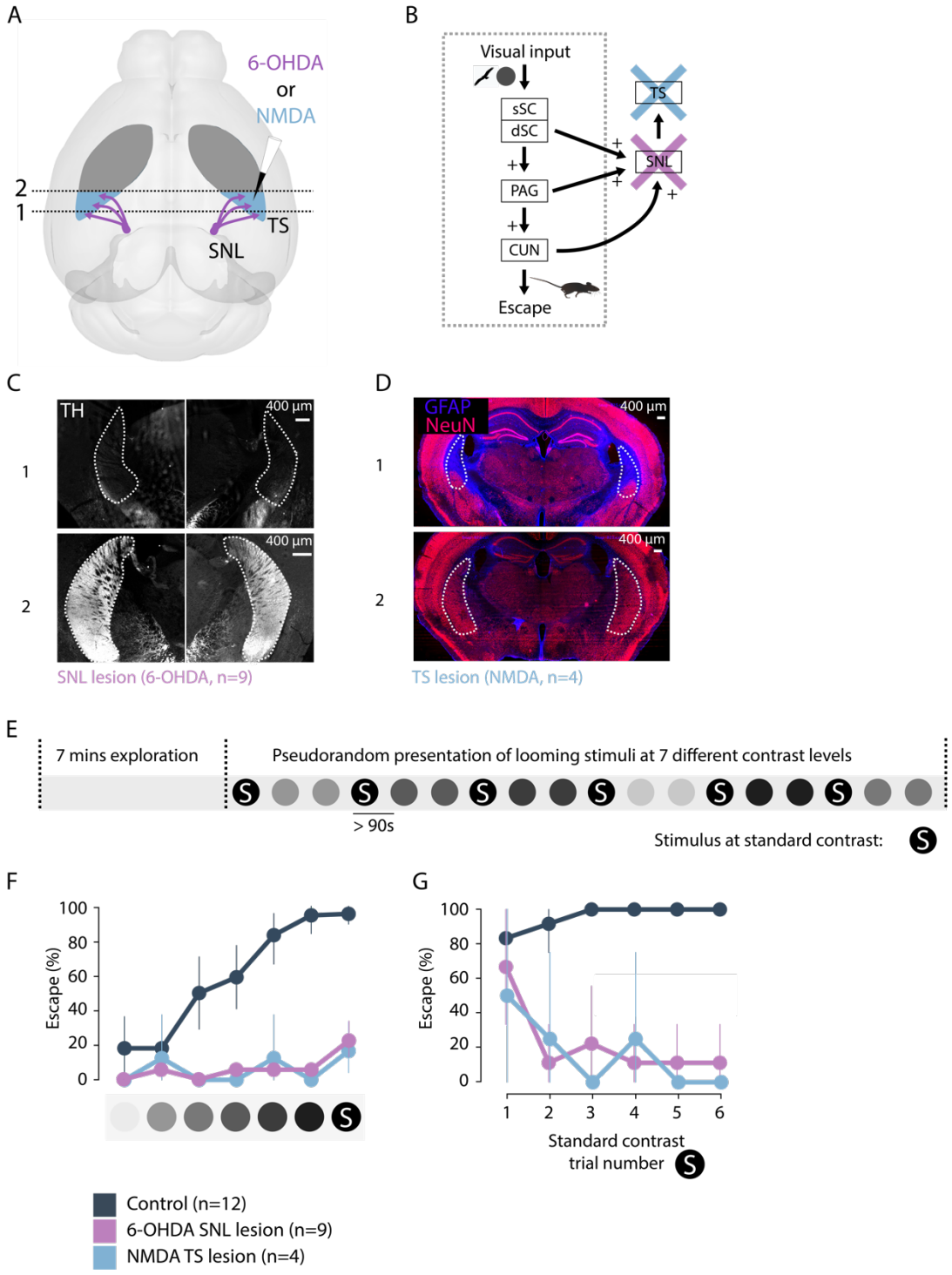

Figure 3.3: lesions of the SNL and TS impair escape. *A) schematic of the injection strategies used in which either 6-OHDA or NMDA was injected into the TS to kill SNL dopaminergic neurons or TS neurons, respectively. B) circuit schematic illustrating each lesion strategy, + signs indicate known/presumed glutamatergic connections. C) and D) example histology for each lesion. C) an image of a TH antibody stain in white and for different sections of the Striatum,*

one inside the lesion and one just outside of it. These numbers correspond approximately to the numbered lines in (A). D) a NeuN antibody stain for neuronal cell bodies in red with a GFAP antibody stain for astrocytes shown in blue. E) the behavioural protocol used to measure contrast-response curves in which stimuli of 7 different contrast levels (grey and black circles) were pseudorandomly presented, with standard contrast stimuli presented on the first trial and on every 3rd trial after this, indicated as black circles with an S. F) contrast-response curves for each group. Trials are pooled at each contrast for all mice tested and curves displayed as the group average. G) responses to standard contrast stimuli from this protocol, for each trial shown in order of presentation. All error bars shown indicate 95% confidence intervals.

Consistent with previously reported results (Evans 2018), escape probability increased incrementally with contrast in control mice (Figure 3.3F). However, we find that escape probability is diminished at all contrasts tested following lesions of the SNL (Figure 3.3F, $p=7.65 \times 10^{-07}$, control vs. 6-OHDA, mixed ANOVA) or the TS (Figure 3.3F, control vs. NMDA, $p=9.5 \times 10^{-05}$, mixed ANOVA). We also find that lesion effect is not significantly different between the two lesion groups (6-OHDA vs. NMDA, p=1.0, mixed ANOVA). Interestingly, while escape is diminished even at standard contrast when pooled, many mice still escape on the first standard contrast trial and we do not observe responses on the first trial to be significantly different between control mice and the 6-OHDA group (11/13 mice escape in the control group vs. 6/9 mice, p=0.609, Fisher's Exact) nor between control mice and the NMDA group (11/13 mice escape in the control group vs. 2/4 mice in the NMDA group, p=0.2189, Fisher's Exact) (Figure 3.3G). Together this suggests that both the SNL and the TS are important parts of the escape circuitry.

3.2.4 The SNL responds to looming spots and these responses correlate with stimulus contrast

If the SNL is involved in the modulation of escape and conveys some form of threat-prediction that can be used to update escape behaviour when stimuli are found to be non-threatening, then we would expect to see neural activity within the SNL in response to looming spots. We would also hypothesise that SNL response magnitude correlate with the intensity of the threat stimulus presented. We therefore selectively recorded from dopaminergic neurons of the SNL using fiber photometry with a fiber positioned over the TS and GCaMP6f expressed selectively in dopaminergic neurons (Figure 3.4A and B) using a DAT-tTA mouse line and TRE-GCaMP6f to restrict expression. We then tested mice using 7 different contrast levels pseudorandomly presented upon entry of the threat zone (Figure 2.2C).

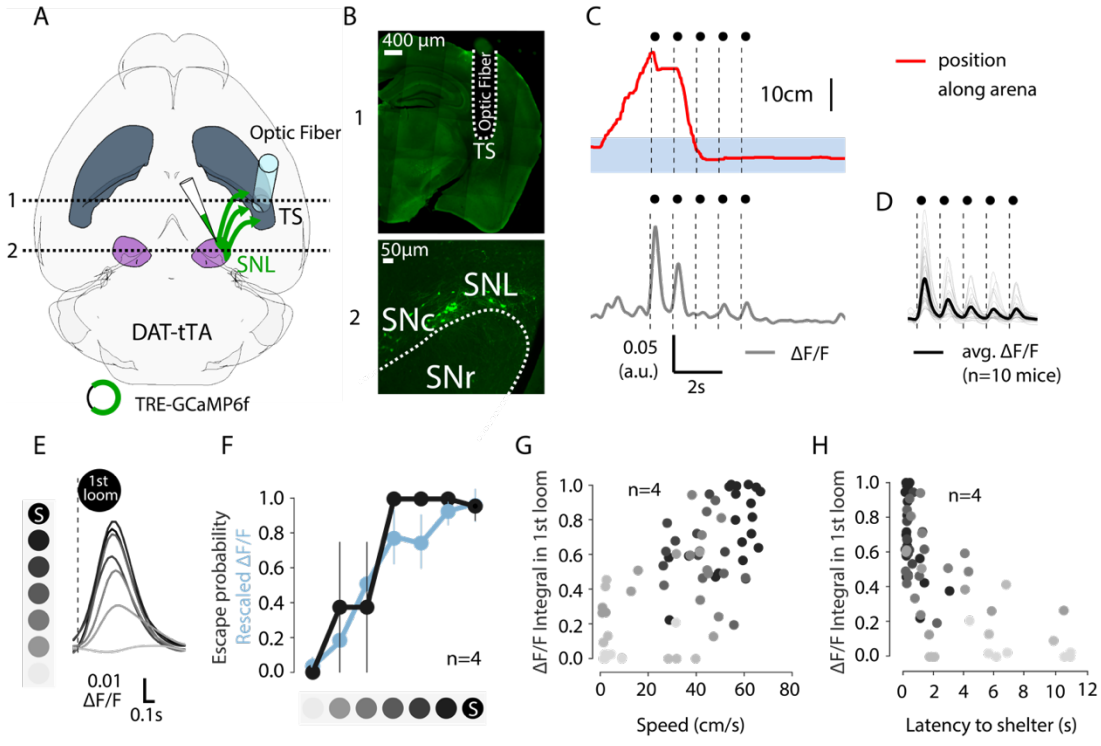

Figure 3.4: the SNL responds to looming spots and the magnitude of responses correlates with stimulus contrast*. A) schematic of the surgical procedure, in which TRE-GCaMP6f was injected into the SNL of a DAT-tTA mouse to selectively express GCaMP6f in dopaminergic neurons, and a fiber*

implanted over the TS to record from SNL axons. B) an example coronal brain slice to indicate a typical fiber placement and infected cells. C) the position track (red, top) from an example escape trial at standard contrast with corresponding ΔF/F trace (grey line, bottom) recorded with fiber photometry. D) ΔF/F traces (grey lines) for all trials and average ΔF/F trace (black line), pooled from all mice and behavioural protocols. E) ΔF/F traces during the first loom for a range of different contrast stimuli (shades of grey). F) the contrast-response curve for these mice (black) with the ΔF/F signal (blue), measured as the integral in the first loom and normalised to the mean response at standard contrast for visualisation. Signal magnitude measured as the ΔF/F integral during the first looming spot is shown as a function of speed (G) and latency to return to shelter (H). All error bars shown indicate 95% confidence intervals.

We find that SNL axons in the TS show large Ca^{2+} transients in response to looming stimuli (Figure 3.4C and D). The peak ΔF/F signal during the first looming spot, was found to be 48.3% larger than the peak ΔF/F signal observed during the second (mean normalised ΔF/F +/- s.e.m: 99.4 +/- 0.5% vs. 51.1 +/- 4.5% , p=0.000009, Wilcoxon signed-rank, n=42 trials, 10 mice), and 70.1% larger than the pooled responses from looms 3-5 (Figure 3.4C and D, 99.4 +/- 0.5% vs. 29.3 +/- 2.1%, $p=6.03 \times 10^{-15}$, Mann-Whitney U test, n=42 trials, 10 mice). We also find that the magnitude of these signals, measured as the integral of the ΔF/F signal during the first loom, correlates with stimulus contrast (Figure 3.4E and F) (ρ*: 0.746 p-value: 5.80 x* 10^{-14}*, Spearman*'s *correlation, n=72 trials, 4 mice*) and therefore also with escape probability and the speed (ρ*: 0.639 p-value: 1.57 x* 10^{-9}*, Spearman*'s *correlation, n=72 trials, 4 mice*) and latency of escape (ρ*: 0.806 p-value: 1.35 x* 10^{-17}*, Spearman*'s *correlation, n=72 trials, 4 mice*) (Figure 3.4F-H). Furthermore, we do not record similar transients in returns to shelter, at speeds exceeding the threshold required for classifying escape, when no stimulus has been presented (Figure 3.5, normalised ΔF/F mean peak during stimulus: 93.2 +/- 2.3 % vs. ΔF/F mean peak without stimulus: 31 +/- 2.8 %, p=0.0034, Mann-Whitney U test).

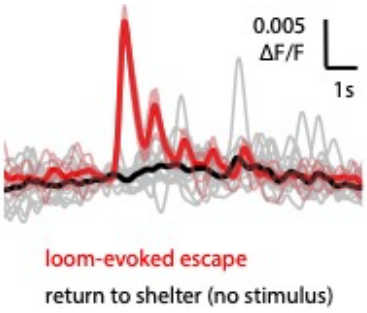

Figure 3.5: SNL is not active during returns to shelter in absence of stimuli. *Example ΔF/F traces taken from a single mouse, for returns to shelter in response to looming stimuli at standard contrast (red lines), and spontaneous returns to shelter at speeds exceeding the threshold required for classification as escape in the absence of any stimuli (grey lines, black line is the average).*

3.2.5 The TS projects to the dorsolateral SNr, which projects to medial SC

We show in Figure 3.3 that lesions of the SNL and TS greatly impair escape and in Figure 3.4 that responses in the SNL correlate with stimulus contrast and escape vigour, raising the possibility that these structures together could regulate escape outcomes. We therefore aimed to better characterise the anatomical output of this circuitry, specifically to understand whether and how activity in this circuit might lead to changes in activity in the structures that execute escape decisions, the deep SC and dorsal PAG (Figure 3.6).

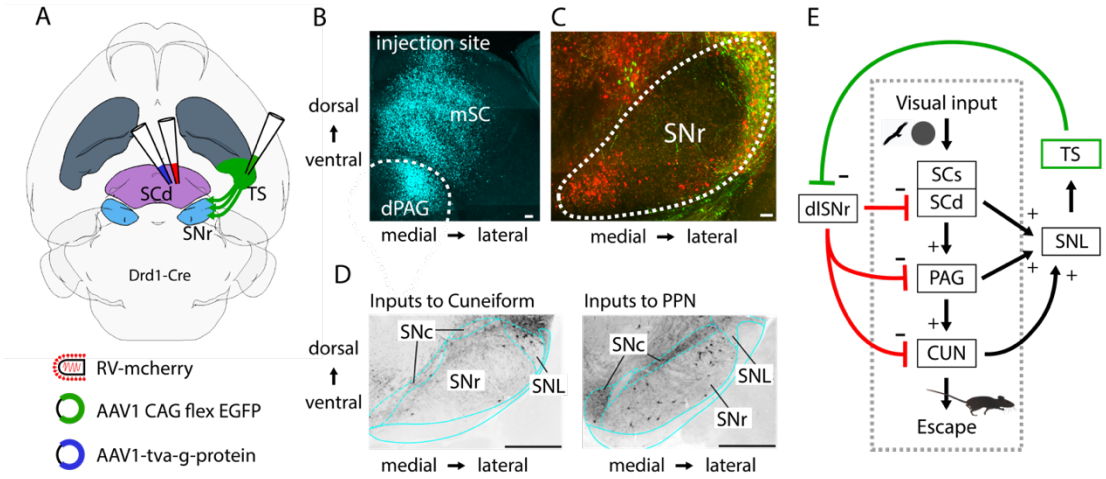

Figure 3.6: the TS is positioned to disinhibit the deep SC, PAG and the Cuneiform Nucleus. *A) a surgical schematic of the injection protocols used to study the output of the TS. An AAV that drives expression of rabies TVA receptor was injected together with its deleted G-protein is injected into the medial SC. Rabies virus was injected several days later to the same region. In the same mouse, an AAV that drives expression of GFP was also injected into the TS of a Drd1-cre mouse to label D1 neurons and reveal the overlap of D1 projections to the SNr and presynaptic inputs to the medial SC. B) nuclei of cells that express the TVA receptor (blue) in the injection site that includes parts of the superficial and deep medial SC and also dorsal PAG. Scale bar indicates 200μm. C) an example coronal cross section of the SNr showing the overlap of cells that are presynaptic to the SC injection site (red) together with axons (green) that arise from the flex GFP injection site in the TS. Scale bar indicates 200μm. D) is taken/adapted from Caggiano 2018 showing the results of monosynaptic rabies tracing to reveal SNr/SNL inputs to glutamatergic neurons in the Cuneiform Nucleus (left) and Pedunculopontine Nucleus (right). Scale bars indicate 500μm. E) a simplified circuit diagram of TS outputs based on B-D. + signs indicate known/presumed glutamatergic connections. – signs indicate inhibitory GABAergic connections.*

To do so we transfected D1-expressing cells in the TS of a Drd1-Cre mouse with AAV1 CAG flex EGFP (Figure 3.6A) and observed the innervation pattern in the SNr. We find that the TS projects specifically to the dorsolateral parts of the SNr but not to medial or ventral parts (Figure 3.6C, n=1 mouse). Furthermore, in the same mouse we also performed rabies tracing from the medial SC and dorsal PAG (Figure 3.6A and B). We co-injected two helper viruses, containing the genes for the TVA receptor and the deleted G-protein and later injected modified rabies virus into the same area. We find cell bodies in the same part of the SNr that the TS projects (Figure 3.6C), suggesting that the TS output selectively reaches the medial SC and dorsal PAG. Furthermore, it has also been shown previously (Caggiano et al., 2018) using rabies tracing that the Cuneiform Nucleus also receives input from a similar region at the border of the SNL and dorsolateral SNr (Figure 3.6 D), which suggests that the output of D1 neurons in the TS, which are inhibitory, are anatomically positioned to control the output of parts of the SNr which project to the medial SC, dorsal PAG and the Cuneiform Nucleus (Figure 3.6E).

3.3 Discussion

3.3.1 The SNL-TS circuit is anatomically and functionally relevant to escape behaviour

In this chapter we aimed to assess whether the SNL and TS could be involved in the modulation of the innate decision to escape from overhead looming spots. We reasoned that in order to modulate escape decisions, candidate structures ought to be:

1) Connected with the escape circuitry;
    a. Receive direct input from medial SC and/or dorsal PAG
    b. Project to the medial SC and/or dorsal PAG
2) Required for normal escape behaviour
3) Responsive to looming stimuli, with responses that closely follow escape metrics such as escape probability and vigour.

We find all three of these conditions are met by the SNL-TS circuit and we identify several features that make this circuit well suited for a role in modulating escape responses. Consistent with previous literature (Menegas et al., 2015), we find the SNL-TS circuit to be suitably connected with the escape circuitry for a possible role in modulating escape decisions: the SNL receives direct inputs from the SC and PAG and the TS is positioned disinhibit the SC and/or PAG, via the SNr. Furthermore, we find that inputs from the SC arise from the deep layers of SC but not the superficial layers. The superficial SC has been reported to respond similarly to a wide range of stimuli whereas neurons in the deep SC are more likely to respond in a highly selective manner to particular stimuli such as high contrast looming spots (Lee et al., 2020). Furthermore, it has been suggested that the deep SC encodes threat stimulus intensity (Evans 2018). It therefore seems plausible that information pertaining to behavioural relevance, threat stimulus intensity, or motor output from escape decisions could be passed from the SC to the SNL to influence dopamine levels in the TS. We also find that the TS is anatomically positioned to disinhibit the deep layers of medial SC: the TS inhibits the dorsolateral parts of the SNr, which in turn inhibit the medial SC, allowing activity in the TS to effectively relieve presumed tonic inhibition on the medial SC.

The SNL-TS circuit receives information from escape-relevant structures and is anatomically positioned to exert inhibitory influence over the medial SC. Together this suggests that the SNL-TS circuit could be specialised in some way for a role in escape behaviour, possibly the modulation of escape decisions based on experience by regulating the threshold for escape in the deep SC based on the history of activity of the inputs to the SNL or TS. Consistent with this, we find that lesions of either SNL or TS result in clear impairments of normal escape behaviour. Mice with lesions of the TS show impaired escape behaviour at all contrasts, suggesting that when the inhibitory output of this circuit is at its theoretical maximum, and when the SNr is not inhibited at all by the TS, then escape does not occur. SNL lesions show a similar result, but interestingly we still observe escape behaviour on a minority

of trials at standard contrast. These post-lesion escape trials almost exclusively occur on the first presentation of a stimulus at standard contrast, which suggests that while the SNL may not be necessary for escape per se, it may be required for the reinforcement of escape. This would be consistent with previously reported findings (Menegas et al., 2018) that show lesions of the SNL lead to more rapid acclimatisation to novel objects and a reduction in avoidance responses. On the other hand, these escapes would also be explained if lesions performed were incomplete and there is residual dopaminergic input following 6-OHDA. However, we also observed some returns to shelter that were classified as escape in the NMDA group, and this could suggest that either these lesions insufficient in a subset of mice or that the SC can sufficiently drive escape on the first encounter with a standard contrast looming stimulus irrespective of the SNL-TS circuit. It is therefore important to follow these lesions with further experiments that can disambiguate these possibilities, e.g. by repeating these lesions with a larger injection volume of NMDA and performing in depth post-hoc quantification of lesions with respect to different subregions within the Striatum.

Dopamine acts as both a short-term modulator of cellular excitability and a modulator of long-term changes in synaptic strength (Surmeier et al., 2011). Our observation that lesioned mice require fewer trials to suppress escape than controls could be explained, therefore, either as a diminished excitability of the TS in the absence of dopamine that effectively increases the threshold for escape or it could reflect a decreased reinforcement through LTP of glutamatergic synapses in the TS that are required to drive/permit escape to occur. If the latter is the case, then neurons that project to the TS should also be required for escape to occur. Our tracing of D1 populations in the TS (see Chapter 5 for data and discussion) identify several posterior thalamic nuclei and lateral cortical visual areas as plausible candidates for this since they receive substantial input from the SC.

3.3.2 What does activity in the SNL represent?

Our photometry recordings of SNL axons in TS reveal large loom-evoked Ca^{2+} transients that correlate with stimulus intensity and therefore correlate with escape probability and vigour, providing further evidence that the SNL may play a role in escape behaviour. Previously it has been suggested that dopaminergic neurons in the SNL may convey threat predictions (Menegas et al., 2018; Watabe-Uchida & Uchida, 2019) because of observations that these neurons respond to a variety of external aversive stimuli such as airpuffs and auditory tones, with no responses to purely aversive stimuli such as reward omission or bitter flavour. However, our data here are inconclusive regarding the nature of the SNL signals and what they precisely convey. The observed relationship between the magnitude of SNL signals and stimulus contrast could be explained as any of the following: a pure report of stimulus salience; a readout of decision confidence; premotor signals relating purely to movement planning; or threat per se. One issue of particular importance is the possibility that the SNL signals premotor activity, given that it receives substantial input from structures that control speed and gait selection such as the Pedunculopontine and Cuneiform nuclei. Both are involved in slow locomotion but the Cuneiform Nucleus has been shown to be specifically able to elicit high speed locomotion such as in escape (Caggiano et al., 2018). Additionally, normalised for structure volume we find that the Cuneiform Nucleus is the largest input to the SNL. However, it is unlikely that the activity we see in the SNL reflects activity in the Cuneiform Nucleus driving high intensity locomotion because latencies between optogenetic stimulation of the Cuneiform Nucleus and the onset of locomotion have been found to be 100-150ms (Caggiano et al., 2018) whereas the activity we observe in the SNL can precede escape by seconds and does not always lead to escape outcomes (see Chapter 5). This argues against the possibility that the SNL signals are purely driven by e.g. the Cuneiform Nucleus.

Furthermore, analysis of SNL signals during returns to shelter in the absence of looming stimuli reveals that the SNL is not active in return to shelter per se (Figure 3.5) and this provides evidence that the signals we observe in the SNL are driven by the threat stimulus rather than the simple motoric consequences of escape to shelter. However, there are a couple of possible caveats with this control. Firstly, even though spontaneous returns to shelter are fast enough to classify as escape they are generally slower than escapes from looming stimuli. Secondly, it has been previously shown that dopaminergic projections to the dorsal Striatum show signals that correlate with movement only if a mouse transitions from stationary to moving and that there is no further signal if a mouse changes direction or increases speed (Howe & Dombeck, 2016). Further experiments and analysis are therefore required to convincingly assess the contribution of premotor planning to the activity observed (see Chapter 5, Figure 5E-G. for an in-depth analysis).

3.3.3 Limitations

In our tracing of D1 axons arising from the TS and projecting to the SNr (Figure 3.6) there is some background expression and axonal uptake of flexGFP, which leads to some green cells in the SNr region that may contribute to the axonal bundle that we see. There was also some minor off target expression in Cortex that is not shown here. However, we do not believe that this affects the interpretability of this result because the off-target expressing structures do not project to the region substantially and because this result is consistent with recent findings of others (Foster, 2020; Magani et al., 2016).

In our SNL lesions we use 6-OHDA to selectively lesion dopaminergic neurons that project to the TS. However, there is some innervation of the TS by the SNc and these neurons will also selectively degenerate following 6-OHDA injection. While the overwhelming effect is likely to be the degeneration of SNL inputs to the TS, this experiment should be followed up with genetically targeted lesion of SNL neurons taking advantage of the markers that are now available (Poulin et al., 2020).

3.4 Summary

Here we show that the SNL-TS circuit is both anatomically and functionally suitable for the modulation of escape responses based on e.g. previous experience. Our results suggest that the SNL-TS circuit could receive information pertaining to behaviourally relevant stimuli from the deep SC as well as motor plans or outcomes from e.g. the Pedunculopontine Nucleus and Cuneiform Nucleus and is connected such that it could potentially gate escape decisions through disinhibition of deep SC via the SNr. We show that the SNL and TS are each required for normal escape behaviour suggesting they are critical, previously unappreciated, parts of the escape circuitry. Additionally, our preliminary finding that mice still escape on early trials but adapt much faster than non-lesioned mice is consistent with ideas put forward by Uchida (Watabe-Uchida & Uchida, 2019) that the SNL can act as a reinforcer of actions based upon threat predictions. Alternatively it would also be consistent with an impaired reinforcement of previously chosen actions (law of exercise (Thorndike, 1911), see full discussion in Chapter 6).

Our photometry recordings of SNL axons in the TS reveal a correlation between threat stimulus intensity and SNL Ca^{2+} activity. As discussed above, this activity could be explained in several ways: in terms of motor invigoration and premotor signals; as a pure report of stimulus intensity; decision confidence; or relating purely to movement planning or threat per se. Nonetheless these data show that the SNL and TS are suitable candidates for a role in the modulation of escape behaviour based on previous experience, whether that experience arises from the sensory quality of the stimulus or from its motor consequences (see Chapter 6 for further discussion). Indeed, some unanswered questions remain: is the SNL signal related to threat or something else? Does activity in the SNL-TS circuit change during learned suppression of escape? If the SNL doesn't drive the TS, then which structures do? These questions will be addressed in Chapters 5 and 6.

Chapter 4: A paradigm for studying the learned suppression of innate escape

4.1 Introduction

While it is evolutionary advantageous for animals to innately escape from threatening stimuli, it is useful to learn to suppress escape when a stimulus is realised to be non-threatening, for example to obtain maximum benefit from alternate behaviours such as exploration or foraging. However, it remains unclear whether this is the case for escape behaviours that can be readily studied in a laboratory setting. The nature and extent of flexibility in the decision to escape from looming spots in mice is not known.

As outlined in Chapter 1, there is evidence from both natural and laboratory settings showing that escape behaviour is flexible. For example, mice dynamically learn the location of new shelter locations (Vale et al., 2017), Jamaican anole lizards that live in the presence of humans initiate escape at shorter distances to potential threat than those that do not (Cooper et al., 2010) and there is evidence that species such as crabs stop responding to simulated threat-stimuli after repeated exposure (Hemmi & Merkle, 2009; Hemmi & Tomsic, 2012; Tomsic et al., 2009, 2019). These examples suggest that loom-evoked escape responses in mice may be similarly flexible and they raise the possibility that the innate escape response might be suppressed as evidence accumulates that a particular stimulus, in this case an overhead high contrast looming spot, does not actually pose a threat. However, relatively little is published relating to the flexibility of the decision of whether or not to escape from a looming spot in mice. An understanding of such flexibility is an important step towards the study of the mechanisms by which a variety of factors (e.g. previous experience) can modulate innate decisions.

Here, we seek to better understand the flexibility of innate escape from looming spots in mice, with particular focus on the role of previous experience

in modulating the decision to escape. Do mice learn to suppress escape responses when, for example, it is learned that a previously threatening stimulus is no longer threatening? Which factors are important? Can we develop a robust assay that rapidly leads to quantifiable suppression of the innate escape response?

In this chapter we aim to develop a behavioural paradigm that will enable us to experimentally interrogate the brain circuits involved in modulating escape. Ideally, such a paradigm should be highly robust, modality-specific, and it should induce behavioural modifications that are long-lasting enough to permit recordings of the circuits and potential physiological changes involved.

4.2 Results

4.2.1 Mice learn to suppress the innate escape response

In Chapter 3 we reproduced a behavioural set-up for robustly eliciting escape responses that can be reliably quantified. We found that we could elicit escape with high probability and with minimal likelihood of observing other behavioural responses such as freezing or non-reactions (Figure 3.2). Here we aimed to develop a high throughput behavioural paradigm that rapidly and robustly leads to the suppression of such innate escape responses.

Although looming spots trigger escape to shelter, they don't pose any risk to life. One might hypothesise, therefore, that repeated exposure of mice to visually threatening stimuli alone facilitates suppression of escape. We therefore first tested a protocol in which we present 120 high contrast looming spots to mice that do not have anywhere safe to hide, thus providing experience that looming stimuli do not lead to negative outcomes (Figure 4.1). In this protocol we restrict mice to a 22 cm x 20 cm region, which includes the threat zone, and with no access to a shelter (Figure 4.1A). We allowed mice to acclimatise to this restricted arena for 10 minutes, before presenting 24

standard contrast stimuli (Figure 4.1B) over a period of 16 minutes with an inter-stimulus interval of 40 seconds.

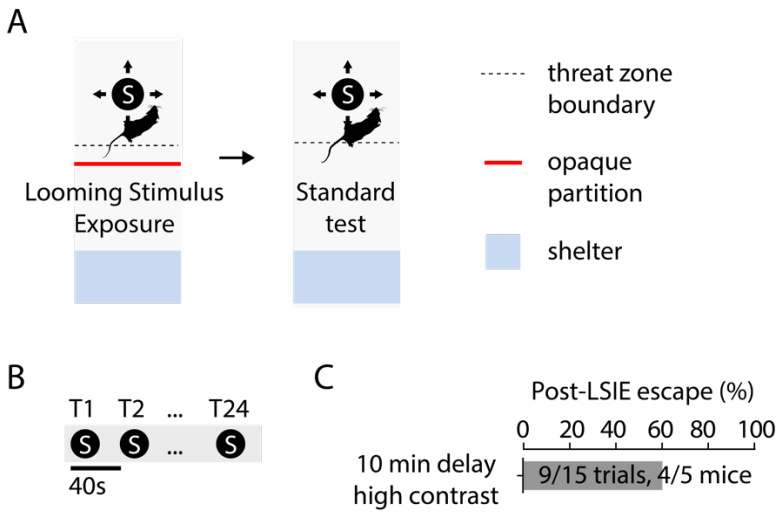

Figure 4.1: exposing mice to high contrast stimuli leads to only a minor change in escape probability. *A) schematic aerial view of the set-up and behavioural protocol used for exposing naïve mice to standard-contrast looming stimuli. The arena is the same as that used to test escape (see Figure 3.2. Mice were restricted to the threat zone using an opaque partition (red line) and given 10 minutes to acclimatise to the arena before initiation of the stimulus protocol. B) trial structure consisting of 24 stimuli in total, each separated by 40s, giving a total presentation time of 16 minutes and 120 looming spots in total. C) the fraction of escape responses observed in the standard test immediately following this protocol in (B).*

Following this protocol, we find that the fraction of escape responses recorded is lower than in naïve mice (Figure 4.1C, 9/15 escape trials following the protocol vs. Figure 3.2G, 199/210 escape trials p=0.0002, Fisher exact test). However, this reduction is modest: the majority of mice still escape to shelter on 60% of trials (Figure 4.1 C).

Given that high contrast looming stimuli evoke innate fear responses such as escape or freezing it is possible that behavioural responses, or associated

changes in internal state that presumably occur in response to visual threat stimuli, might occlude learning to suppress escape. It has been previously shown that the probability that mice escape from overhead looming spots depends on contrast (Evans et al., 2018): low contrast looming stimuli elicit lower probabilities of escape than high contrast stimuli (Figure 3.3F). We therefore next devised a protocol in which mice are exposed to a set of looming stimuli presented in a gradually increasing contrast ramp. We reasoned that incrementally increasing the contrast might provide experience of looming stimuli without evoking any fearful responses, thus facilitating learning. We hypothesised that this might be more robust than simply using high contrast stimuli. We therefore introduced mice to the restricted arena and presented 24 stimuli arranged in a contrast ramp whereby the background luminance of the monitor was increased incrementally every three stimuli while keeping the luminance of the looming spot constant (Figure 4.2A).

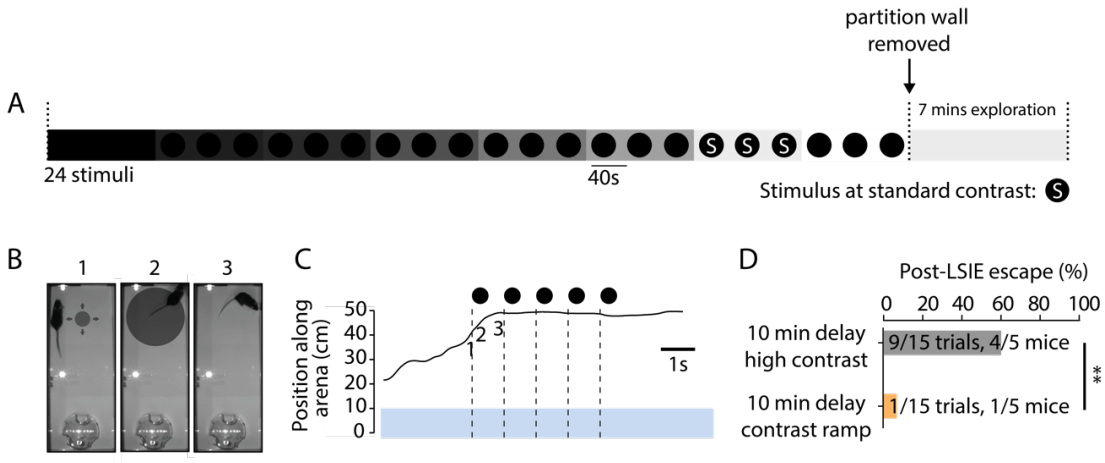

***Figure 4.2: A protocol for the learned suppression of innate escape**. A) schematic of the learned suppression of innate escape (LSIE) protocol. In this protocol mice are restricted to a part of the behavioural arena using an opaque red partition which prevents them from seeing the shelter (same as Figure 4.1A). The background luminance is gradually increased while maintaining the luminance of the looming spot (black). After the LSIE protocol the partition is removed, and escape behaviour is tested using our standard escape test protocol (Figure 2.5A). Every 3 trials the background luminance is increased.*

*After these stimuli have been presented, mice are given 7 minutes to explore the unrestricted arena before either being given test trials or returned to their home cage for testing of escape at a later time. B) images from typical stages in a test trial following LSIE, each image has a number above it which indicates the time point that this corresponds to in the position track in C). 1 the mouse shortly after the onset of the looming spot, 2 the same mouse as it continues to explore during the looming stimulus and 3 the mouse shortly after the first looming spot in our stimulus. C) the position track for this mouse (black line) along the long axis of the behavioural arena. Black circles indicate the duration of each loom within a trial, vertical dashed lines indicate the onsets of these looming spots. D) bar plot indicating the percentage of behavioural responses that were classified as escape in a standard test following this contrast ramped LSIE protocol (yellow bar) compared with the previous protocol of 24 standard contrast stimuli (grey bar). ** denotes a p-value < 0.01.*

We find that, following this protocol mice typically do not react strongly to standard contrast looming stimuli and they do not orient to, or return to, shelter but instead continue to explore the threat zone during and shortly following the presentation of the test stimuli (Figure 4.1B and C). We find this protocol leads to a robust suppression of escape (Figure 4.2D, 1/15 escape trials vs. 199/210, $p<0.0001$, Fisher's exact test) and is significantly more effective than the standard contrast stimuli protocol (Figure 4.2D, 9/15 vs. 1/15 escape, $p=0.0052$, Fisher's exact test).

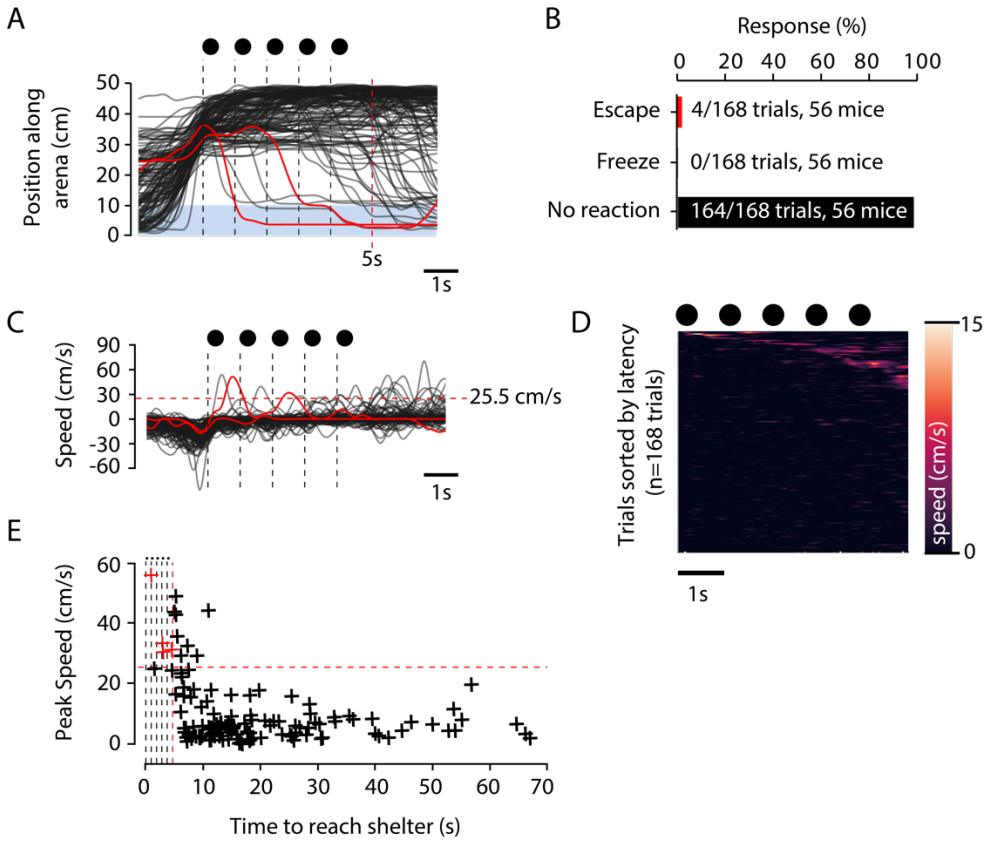

Figure 4.3: the learned suppression of innate escape (LSIE). *A) a representative set of position tracks across the population of mice for behavioural responses classified as escape (red), or no reaction (black). B) a bar plot indicating the fraction of behavioural responses observed for all test trials following LSIE categorised as escape, freezing or no response. C) the velocities for the position tracks shown in A), and speed threshold used for classifying escape (red, dashed line). D) a heatmap of velocity traces for all trials, positive values indicate that velocity is in the direction towards shelter. Trials are sorted by time to reach shelter. E) peak speed of each trial plotted against the time to reach the shelter. Thresholds used to define escape (red dashed lines) are plotted for reference. Red crosses indicate trials that were classified as escape, black crosses indicate trials that were classified as non-escape.*

We also found that the period of 10 minutes allocated for mice to acclimatise to the arena before the protocol starts does not increase the likelihood of mice

suppressing their escape responses to this protocol (Figure 4.3A and B) (1/15 responses with 10 minutes acclimatation compared with 4/168 responses without the 10 minutes, p=0.351 Fisher's exact test). We therefore removed this from the LSIE protocol. This contrast-ramped protocol with no delay leads to robust suppression of innate escape responses in naïve mice that have no previous experience of loom-evoked escape (Figure 4.3A and B, 4/168 trials vs. 199/210 trials (Figure 3.2G), $p < 0.0001$, Fisher exact test), while the probability of observing no response was significantly higher in the post-LSIE test than in naïve mice (164/168 trials vs. 8/210 trials (Figure 3.2G), $p<0.0001$, Fisher's exact test) and we did not observe a change in the probability of observing freezing behaviour (0/168 trials vs. 3/210 trials (Figure 3.2G), p=0.2573, Fisher's exact test). Additionally, in the vast majority of trials, the peak speed reached towards shelter is less than the threshold defined for escape (Figure 4.3C, D and E, also see Chapter 3, Figure 3.2). When we plot the metrics used here to define escape against each other we find that the majority of trials fall outside of the quadrant that defines escape (Figure 4.3 E, upper left quadrant).

4.2.2 The learned suppression of innate escape is long lasting and modality specific

In an ethological setting, once it is learned that a particular stimulus is non-threatening, it is presumably advantageous to remember this information for a long enough period to guide future actions. It is important to understand the permanence of the suppression of escape that we observe in the laboratory, to see whether it exhibits similar properties. We therefore ask whether our protocol leads to the formation of a lasting memory e.g. that the stimulus is non-threatening, or whether it instead leads to a transient and short-lasting desensitisation arising from repeated stimulus exposure.

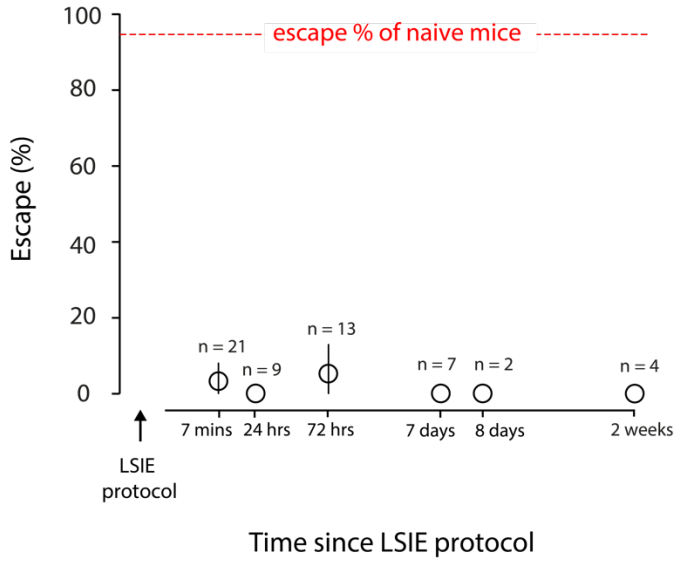

Figure 4.4: the learned suppression of innate escape is long lasting*. The LSIE protocol is indicated by the black arrow. Open circles indicate escape probabilities measured at time points at which escape was tested (3 trials for each mouse pooled). Each mouse was tested at a single time point only (error bars show 95% confidence interval).*

To address this question, we measured the escape probabilities of mice at different times following LSIE. We find that naïve mice that underwent the LSIE protocol but were tested at a later time showed consistently low escape probabilities (Figure 4.4) for up to two weeks. Escape responses were found to be suppressed at all time points tested when compared against the control group of mice tested at 7 mins (2/63 trials, 21 mice, p-values were as follows using Fisher's exact test: 24 hrs, 0/27 trials vs. 2/63 trials, p=1.0; at 72 hrs, 2/39 trials vs. 2/63 trials, p=0.635; at 7 days, 0/21 trials vs. 0/63 trials, p=1.00; at 8 days, 0/6 trials, p=1.00 ; and at 2 weeks, 0/12 trials, p=1.00). This suggests that the LSIE protocol leads to a lasting memory, perhaps that looming stimuli are non-threatening, rather than an acute desensitisation to the stimulus due to recent exposure. This suggests that learned suppression of escape lasts long enough to influence future actions and permit long term recordings of the circuit mechanisms involved.

A secondary but nevertheless important question relates to the generality of suppression on innate escape responses. Does LSIE result in suppression of escape in general or is it specific, at least to visual threats? To test this, we take advantage of the fact that mice are known to escape from threat stimuli in other sensory modalities such as auditory stimuli. We evaluated the responses of naïve mice to aversive auditory stimuli in our behavioural arena, using a loud (85dB) pink noise stimulus that we find elicits escape responses with high probability (Figure 4.5). We then tested whether mice that have learnt to suppress loom-evoked escape responses will still escape from auditory threats or whether the suppression of escape is generalised across threat modalities.

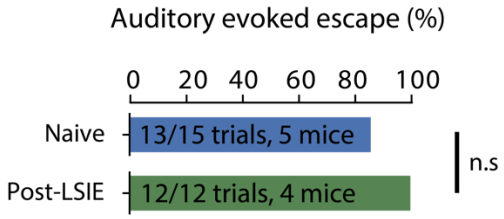

Figure 4.5: the LSIE protocol is modality specific. *Bar plot of the proportion of responses classified as escape in response to a 3s 85dB pink noise stimulus presented from above in naïve mice (blue) and for mice that previously underwent the LSIE protocol (green).*

We find, following LSIE, that these responses are not significantly different from naive control mice (Figure 4.5, 13/15 vs 12/12 p=0.487, Fisher's exact test). This suggests that the LSIE protocol is modality specific and selectively leads to the suppression of visually evoked escape responses while leaving escape responses to auditory stimuli intact.

4.2.3 The LSIE protocol is disrupted by previous experience of loom-evoked escape

Thus far we have only tested animals that were naïve prior to them being exposed to the LSIE protocol. If this established LSIE protocol is relevant to behavioural changes that might occur under ethologically more realistic scenarios, then one might expect the likelihood of suppression of escape to be related to, or dependent on, the history of the animal's exposure to threat and escape behaviour. For example, previous experience of escape to a particular stimulus might occlude suppression of escape responses and one might expect recent experience to have a greater impact than experience a long time in the past. To test this idea, we measured the extent of LSIE induced escape suppression in mice that have previously encountered and escaped from high contrast looming stimuli in the past. To do this we put mice through our standard test (Figure 4.6 A, left) either 0.2 hours before the LSIE protocol (Figure 4.6A, orange) or the 24 hours before the LSIE protocol (Figure 4.6A, blue) and measured their post-LSIE escape responses (Figure 4.6A, right).

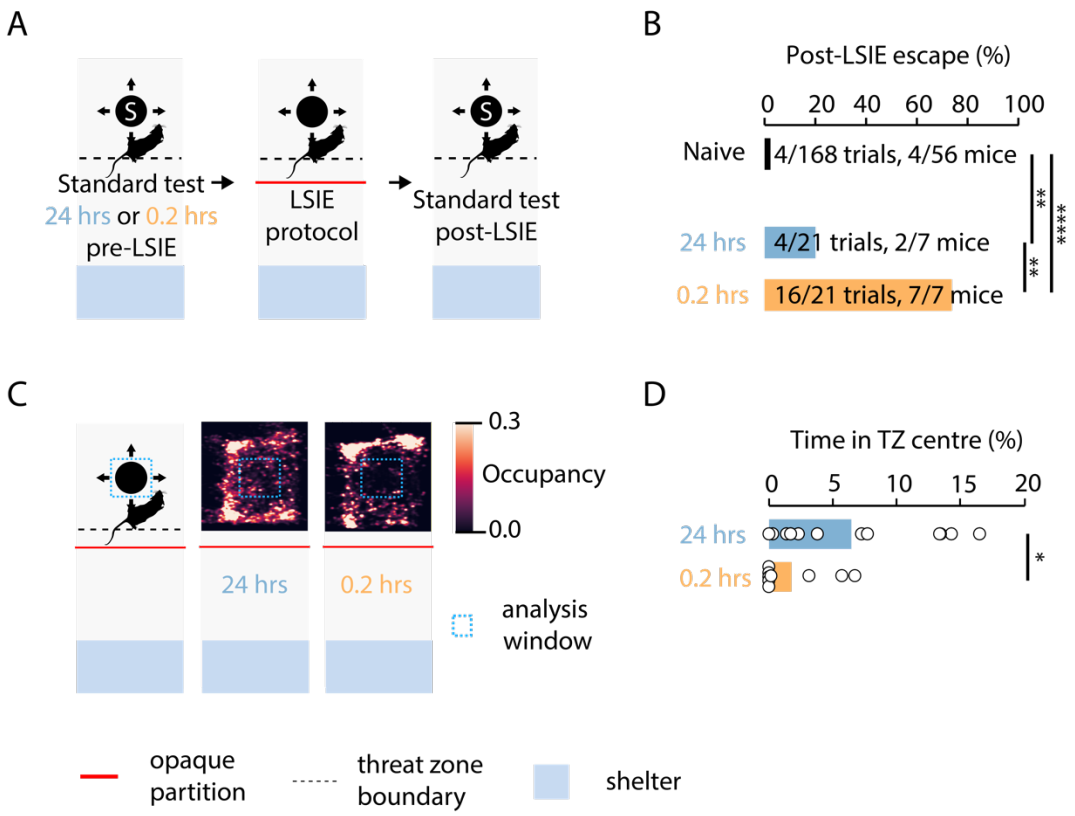

Figure 4.6: the LSIE protocol is disrupted by previous experience of loom-evoked escape. *A) schematic of the behavioural protocol in which mice are previously exposed to high contrast looming stimuli before undergoing the LSIE protocol and then a post-LSIE standard test to measure escape probability. B) a bar plot indicating the percentage of responses classified as escape in a standard test following LSIE for naïve mice (black bar), and for mice that have been exposed to three test trials either 24 hrs (blue) or 0.2 hrs (orange) before LSIE. C) heatmaps of the occupancy of mice in each group overlaid on the restricted arena. D) the % of time each group spends within a central rectangular analysis region of the restricted arena in (C). *, **, and **** denote p-values of <0.05, < 0.01, and <0.0001 respectively.*

We find that mice with previous experience of loom-evoked escape are less likely to suppress responses following the LSIE protocol (pooled 24hrs and 0.2hrs 20/42 escape responses vs. 4/168 responses, p<0.0001) and the extent of this effect depends on how recent this previous experience is to the LSIE protocol (Figure 4.4B). If previous loom-evoked escape occurs the day

before LSIE, the pre-test leads only to a minor reduction of escape suppression in a subset of mice (Figure 4.4B, 19% escape, 2/7 mice, 4/21 trials vs. 4/168 trials, p=0.006, Fisher exact test), but if it occurs just 0.2 hours beforehand then this experience occludes suppression of escape to a much greater extent, although not completely (Figure 4.6B): all mice escape at least once and the escape probability is high (Figure 4.4B 76% escape, 7/7 mice, 16/21 trials, $p<0.0001$ Fisher exact test). The 0.2 hrs and 24 hrs groups are also significantly different from one another ($p<0.0005$, Fisher exact test). While LSIE is occluded in the 0.2 hrs group, they do show a reduced escape probability when compared with naïve mice (0.2hrs vs. no LSIE: 16/21 vs. 201/211, Figure 3.2G, p=0.0087, Fisher's exact).

Furthermore, we find that this effect correlates with differences observed in the exploratory behaviour of mice during the LSIE protocol (Figure 4.4C and D). Mice that receive the pre-test 0.2 hours before LSIE spend significantly more time away from the centre of the threat zone during the LSIE protocol (Figure 4.4D). The centre of the threat zone for this analysis was defined as a 10x10cm region in the centre of the restricted part of the arena (Illustrated in Figure 4.4C, blue dashed line) (p=0.04, same day 1.2% total time in analysis region, day before 6.1%). Of the seven mice that received pre-test on the same day as LSIE, four spent no time in the analysis region at all.

4.3 Discussion

4.3.1 The Learned Suppression of Innate Escape

In this chapter we sought to understand the conditions required for mice to learn to suppress escape responses and also to develop a behavioural protocol that would allow the systematic and high throughput study of the mechanisms that drive the modulation of innate escape.

We find that innate escape can be completely and reliably suppressed using a short and simple protocol consisting of overhead looming spots of gradually

increasing contrast presented to mice that are restricted to an arena with no access to shelter. Furthermore, we find that this suppression effect is robust: the vast majority of naïve mice that undergo the protocol learn to completely suppress escape. We also find the effect to be long lasting: mice tested up to two weeks after the LSIE protocol still show greatly reduced probability of escape. This suggests that, rather than an acute and short-term habituation to the stimulus, our observations instead reflect a lasting memory, perhaps that the stimulus is non-threatening, and presumably this reflects plastic change occurring somewhere within the escape circuitry or structures that project there. Such characteristics would be important in ethological settings in which changes in behaviour should last long enough to improve outcomes in future encounters with the same stimulus that may be separated by days or even weeks.

Incrementally increasing stimulus salience in the form of contrast ramping may be an important factor in the learned suppression of escape, but it is not necessary for suppression to occur, and, although we do not show this here it is also possible to attain suppression of escape using only standard-contrast stimuli provided there is no acclimatisation period prior to the onset of the suppression protocol. This suggests that the novelty of the environment, or perhaps the unexpectedness of the stimulus may be an important factor that impacts the efficacy by which high-contrast protocols lead to suppression of escape. Additionally, we find that a second contrast ramped protocol in which we vary the luminance of the spot while keeping the background luminance constant also effectively leads to suppression of escape responses.

In developing this protocol, we initially tried several strategies. Simply presenting looming stimuli in the unrestricted test arena was sometimes, but not always, successful and required a variable number of stimuli and a long time to achieve suppression of escape. This might be because that mice that have the option will run to shelter and hide. Mice that have access to shelter therefore spend a significant amount of time hiding where they cannot attain

as much exposure to the stimulus when compared with mice that were restricted to the threat zone. Additionally, it is possible that the action of running away from the stimulus by itself partly reinforces the decision to escape and so access to shelter may be a factor in determining the rate of learning to suppress escape.

Our LSIE protocol leads to a lasting suppression of escape from overhead visual stimuli. One question that naturally follows is whether this suppression is specific to visual threat stimuli or whether it instead generalises across threat modalities. It is advantageous to learn to suppress escape from non-threatening stimuli. However, if the learned suppression of escape transfers to other stimuli or types of threat then this could lead to failures to escape from real threats when they do occur. This would be disadvantageous in evolutionary terms and so we expect escape suppression to be specific in some way to prevent this from happening. Our finding that mice maintain robust escape responses to auditory threats following the LSIE protocol supports the view that the suppression of escape responses that we observe is modality or perhaps even stimulus specific. This is also consistent with physiological observations of others (Lee et al., 2020) that reductions in activity in the deep SC following repeated looming stimuli are stimulus specific, suggesting that something similar may occur during LSIE. The fact that mice still escape from auditory stimuli following LSIE also shows that mice are still able to run to shelter following LSIE: they have not simply learned alternative strategies for dealing with threat stimuli (e.g. freezing), and they have not failed to learn that the shelter is a safe place.

4.3.2 The learned suppression of innate escape protocol is dependent on threat and escape history

We find that previous experience of loom-evoked escape in the form of a pre-test can occlude LSIE: naïve mice rapidly learn to suppress their innate escape response while mice that have escaped from standard contrast looming stimuli

before the LSIE protocol learn this less effectively or fail to learn altogether. This suggests that learning to suppress escape is a dynamic process that incorporates the recent history of threat encounters. Further, we find that the timing of this pre-test is an important determinant of the extent of occlusion. Mice that are given a pre-test immediately prior to the LSIE protocol show little suppression of their escape responses compared to naïve mice however a 24 hour interval from pre-test to LSIE protocol is long enough for this occlusion effect to wear off. This suggests that the memory of previous encounters with visual threat stimuli diminishes within 24 hours of exposure.

One explanation for this is that previous experience of loom-evoked escape only leads to acute changes in behavioural state (i.e. fear), or a heightened state of vigilance, that occludes learning to suppress escape. It has been shown previously (Evans et al., 2018) that mice will spontaneously escape from locations from which they have previously escaped, which suggests that experience of escape leads to a lasting memory and changes in behaviour and/or behavioural state. Indeed we also show here that mice that receive looming stimulus exposure in a pre-test immediately beforehand explore the arena differently during the LSIE protocol (Figure 4.6 C and D) and they spend significantly less time in the centre of the arena compared with those given a pre-test 24 hours before, suggestive of an altered behavioural state and a measure often taken as a proxy for fearfulness. This suggests that changes in behavioural state triggered by loom-evoked escape can last long enough to impact the LSIE protocol.

From an ethological perspective, such a state of heightened vigilance following a threat encounter is advantageous because it may account for factors such as predation risk, that are well known to influence escape behaviour (Hemmi, 2005; Magani et al., 2016). However, such vigilance comes at an energetic cost as well as a cost derived from a reduction in time available for behaviours such as foraging. For example, it has been observed that insectivorous lizards permit closer predator approach when insects are experimentally introduced

into their vicinity and that they leave shelter sooner following a threat encounter if there is a visible food source outside the shelter (Cooper, 2004), suggesting that there is a trade-off between the need to forage and the need to evade predators. We therefore hypothesise that such behavioural changes following threat encounters should be transient to facilitate a return to exploratory behaviours once they are no longer advantageous. Permanent or very long-term sensitisation of escape behaviour is likely to be less advantageous than transient sensitisation simply because the presence of threats is transient: as soon as the threat has gone, or the mouse has entered a new, safer, environment the vigilant state becomes a cost with no benefits.

Additionally, it has been shown that prolonged or chronic fear can adversely impact the long-term wellbeing of an organism in a variety of ways. For example it has been shown that high underlying fearfulness in domestic chicks can lead to impaired developmental growth, reduced food conversion, reduced eggshell quality and poor quality plumage (Bryan Jones & Waddington, 1992). “Forgetting” may therefore provide a means of avoiding “accumulation effects” and may reduce the chronic impact of long-term/maintained fear responses and vigilance states that may be detrimental, overall, to an organism. This may also help to explain why mice forget threatening encounters rapidly but are able to learn to suppress escape responses for a long time: if learned to an appropriate stimulus, the suppression of escape does not carry such costs and so it would be advantageous to remember this information for as long as possible to maximise the available benefits of alternate behaviours.

4.4 Summary

In Chapter 3 we constructed an experimental set-up for eliciting escape with high probability in naïve mice and reproduced findings that show escape probability and vigour varies as a function of stimulus contrast. Here, we used such stimulus and behavioural parameters to develop a protocol that leads to the lasting suppression of innate escape. Escape behaviour is therefore

flexible, and its learned suppression is robust with this protocol in naïve mice. With this protocol we have successfully suppressed escape for up to two weeks while escape responses to threatening auditory stimuli remain intact.

Additionally, we find that prior experience of loom-evoked escape in the form of a pre-test can prevent LSIE: mice that have recently escaped from looming spots are less likely to suppress escape after the protocol than naïve mice. Also, the timing of this experience is a key determinant of the extent of suppression: recent experience (less than 1 hr) has significantly more impact on LSIE than exposures to looming stimuli that occurred more than 24 hours previously. This finding is experimentally highly advantageous for two reasons; firstly, we are able to control the extent of learned suppression by varying the time of the pre-test and secondly, it enables us to compare mice that have had the same overall number of life-time exposures to looms but exhibit very different behavioural responses. In the next chapter we will take advantage of this to compare the circuit function of mice that have learnt to suppress their escape behaviour versus those that have not.

Chapter 5: The SNL and TS in the suppression of innate escape

5.1 Introduction

In Chapter 3, using anatomical tracers, targeted lesions, and photometry recordings, we identified the SNL and TS as structures that could play a role in the modulation of escape. We found that each is required for normal escape behaviour and that Ca^{2+} transients recorded in the SNL correlate with the contrast, and presumably the perceived threat level, of looming stimuli. In Chapter 4 we developed a behavioural paradigm in which progressive experience of low-contrast looming stimuli leads to reliable and lasting suppression of escape in naïve mice and that the efficacy of suppression is dependent on recent prior experience of such stimuli. Here, we combine the recording methods of Chapter 3 with the LSIE paradigm established in Chapter 4 to experimentally interrogate the role of the SNL and TS in modulating escape.

5.2 Results

5.2.1 Signals in the SNL are reduced following suppression of escape

In Chapter 4 we found that mice that have recently (<1 hour) escaped from looming stimuli are less likely to subsequently suppress escape than naïve mice or mice that had received looming stimuli more than 24 hours beforehand. Here, we take advantage of this to compare the SNL-TS circuit function of mice that have learnt to suppress their escape behaviour versus those that have not.

Data from Chapter 3 indicated that SNL signals exhibit loom-evoked response properties that may be useful for modulating escape behaviours: the magnitude of the responses varies with stimulus contrast, and lesions of the SNL lead to deficits in escape behaviour. However, it is also possible that such

responses could signal different types of information such as stimulus salience, decision confidence, threat level or even pre-motor planning. To begin to disambiguate these potential roles we first hypothesised that if loom-evoked signals in the SNL are involved in modulation of escape then these signals should be altered in mice that have learnt to suppress escape behaviour.

We therefore injected AAV5 tre-GCaMP6f into dopaminergic neurons in the SNL and recorded from SNL axons within the TS using fiber photometry (Figure 5.1 A and B) during looming test trials (Figure 5.1C) before (Figure 5.1 D, left column) and after (Figure 5.1 D, right column) the learned suppression of innate escape. Similar to the results of Chapter 3 (Figure 3.4), we observe large Ca^{2+} transients in response to looming stimuli during the pre-LSIE test (Figure 5.D, bottom left). We find that that these signals are attenuated (Figure 5.1 D, bottom right panel) during suppression of escape in mice that receive their pre-test 24 hours prior to the LSIE protocol.

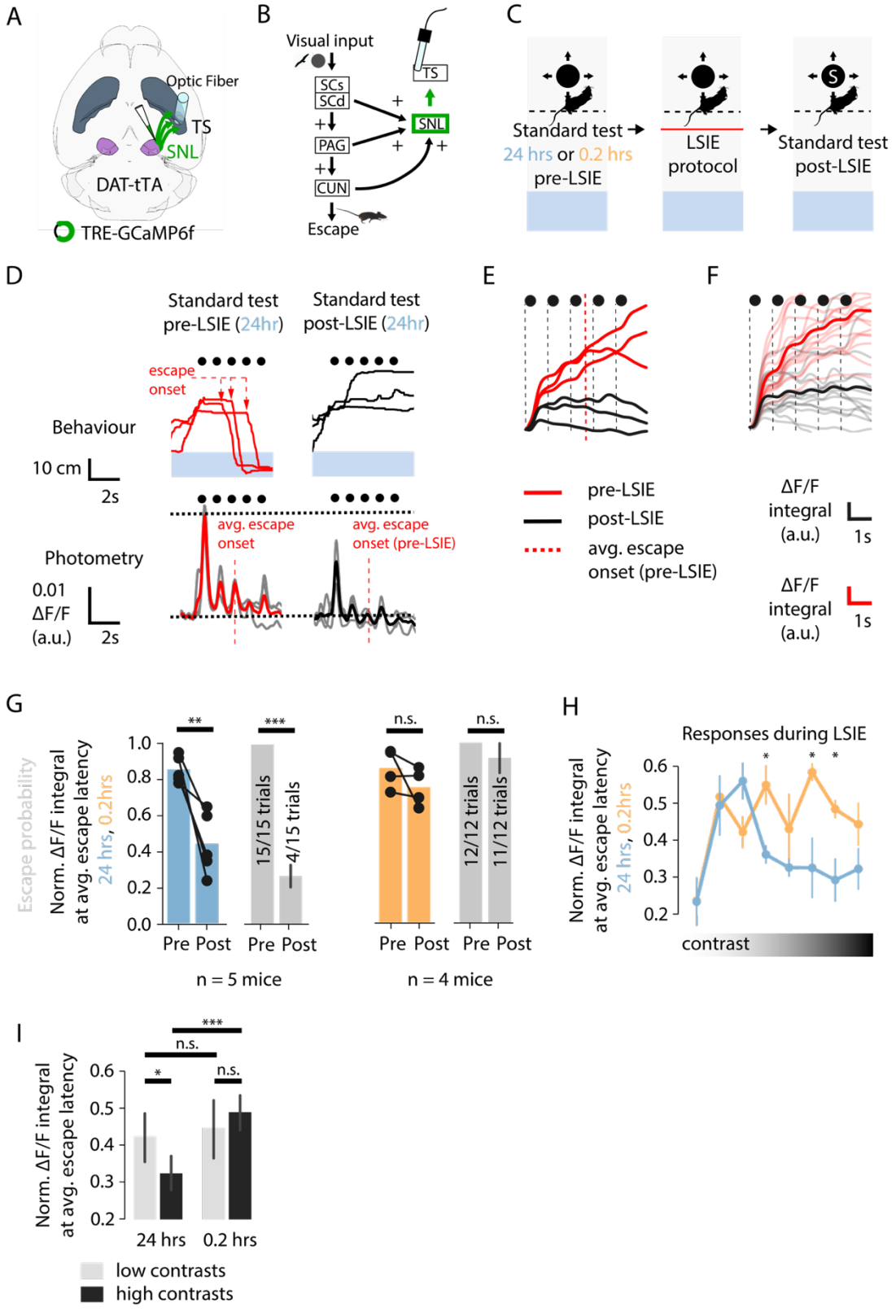

Figure 5.1: SNL signals are reduced following suppression of escape. *A) a surgical schematic. TRE-GCaMP6f was injected into the SNL of a DAT-tTA*

*mouse to express GCaMP6f in dopaminergic neurons in the SNL, and a fiber implanted above the TS to record from SNL axons. B) a simplified circuit diagram of the recording paradigm. C) the behavioural paradigm. Mice receive a pre-test either 24 hrs (blue) or 0.2 hrs before the LSIE protocol and subsequently receive a post-LSIE standard test. D) position tracks (top) from an example mouse that received its pre-test 24 hrs before LSIE together with the corresponding ΔF/F signals measured for these trials (bottom) before (left) and after (right) the LSIE protocol. The baseline and largest peak (black dashed lines) of the average trace from all pre-test trials are shown for reference, together with the escape latencies for the pre-test trials (red, dashed lines). E) ΔF/F integrals for pre-test trials (red) and post-test trials (black) from an example mouse with its average escape latency (red, dashed line) from pre-test trials, used as the analysis timepoint, shown. F) ΔF/F integrals for pre-test trials (red) and post-test trials (black) for the whole population. G) the average normalised ΔF/F integral at the analysis timepoint for the pre-test and post-test showing the extent of signal attenuation in the SNL following the LSIE protocol for mice that receive a pre-test 24hrs (blue) before and 0.2 hrs (orange) before the LSIE protocol. Corresponding escape probabilities for these groups and conditions are also shown (grey bars). Error bars indicate s.e.m. H) the average normalised ΔF/F integral at the analysis timepoint for looming stimuli presented during the LSIE protocol, binned by contrast (pooled from 3 trials per contrast). Error bars indicate 95% confidence intervals. I) the average normalised ΔF/F integral at the analysis timepoint for looming stimuli presented during the LSIE protocol binned into two groups – low contrasts and high contrasts, which correspond to the first half, and second half of the LSIE protocol respectively. Error bars indicate s.e.m. *, **, and *** denote p-values of <0.05, < 0.01, <0.001 respectively.*

In order to quantify these signals, we measure the integral of the ΔF/F trace from the onset of the looming stimulus until the end of the window used to classify escape responses (5 seconds) (Figure 5.1E and F). However, the decision to escape to shelter is usually made much earlier than this (Figure

3.2I and J, 83.6% of escapes are initiated before the 3rd looming spot) and so we restrict our analysis to a window that presumably incorporates the decision window for escape while excluding signal measured long after the escape decision has been made. To achieve this, we take the value of the integral at the average latency of escape, taken to be the average escape latency of the three pre-test trials (Figure 5.1 D and E, and Methods Figure 2.6). Using this measure, we find that mice that receive a pre-test 24 hours before the LSIE protocol that exhibited escape suppression also showed significantly attenuated signals in the SNL (Figure 5.1G and H, blue *24 hrs pre vs. post, median values +/- s.e.m.: 95.1 +/- 4.8 % vs. 38.2 +/- 5.5%, p=0.002, Wilcoxon signed-rank test, n=15 trials, 5 mice*).

One possible explanation however is that these SNL responses simply attenuate during repeated presentations of the looming stimuli independent of whether or not mice had learned to suppress escape. To test this idea, we also performed photometry recordings in mice that received the pre-test immediately prior to the LSIE protocol and were thus not expected to suppress escape. While mice that received their pre-test 24hrs prior to LSIE showed a 73.3% reduction in escape probability (pre vs. post LSIE, 15/15 vs. 4/15 trials, $p<0.0001$, Fisher's exact test) those mice that received a pre-test 0.2 hours before the LSIE protocol showed no significant reduction in escape probability (pre vs. post LSIE, 12/12 vs. 11/12 trials, p=1.000, Fisher's Exact test). Furthermore, in contrast to the 24 hrs pre-test group the 0.2 hrs pre-test mice also showed no significant attenuation of their SNL response to the test stimuli (Figure 5.1G, orange; 0.2 hrs signals pre vs. post, *median values +/- s.e.m: 91.5 +/- 5.4% vs. 80.0 +/- 4.1%,* p = 0.098, Wilcoxon signed-rank test, n=12 trials, 4 mice). Additionally, we find that signals recorded during the LSIE protocol itself are distinct for each group: mice that learn to suppress escape show SNL signals that decrease with stimulus number, while SNL signals remained persistent in mice that maintained their escape behaviour following the LSIE protocol (Figure 5.1H 24 hrs vs. 0.2 hrs: p=0.023, mixed ANOVA,

post hoc tests for each bin, left to right: p=0.883, 0.750, 0.252, 0.001, 0.122, 0.0005, 0.001, 0.115, pairwise t-tests).

This difference seems to emerge during the LSIE protocol and is especially clear when comparing the first and second halves of the LSIE protocol: mice in the 24hrs group show attenuated responses second half of the LSIE protocol when compared with the first, even though stimulus contrast is higher in the latter half (Figure 5.1I low (first half) vs. high (second half) contrasts, mean +/- s.e.m.: 42.3 +/- 2.4% vs. 32.3 +/- 2.4 %, $p<0.0169$, Wilcoxon signed-rank test, n=60 trials, 5 mice), whereas mice in the 0.2 hrs group show no such difference (Figure 5.1I low (first half) vs. high (second half) contrasts, mean +/- s.e.m.: 44.3 +/- 2.5% vs. 48.9 +/- 2.6%, p=0.857, Wilcoxon signed-rank test, n=48 trials, 4 mice). Similarly, SNL responses in the 24 hrs and 0.2 hrs groups are not significantly different from each other in the first half of the protocol (mean +/- s.e.m.: 24 hrs, 42.3 +/- 2.4% vs. 0.2 hrs, 44.3 +/- 2.5%, p=0.291, Mann-Whitney U test, n=60 trials in 24 hrs group and 48 trials in the 0.2hrs group) but a difference between groups emerges in the second half that contains high contrast stimuli (mean +/- s.e.m.: 24 hrs 32.3 +/- 2.4 % vs. 48.9 +/- 2.6%, p=0.00002, Mann-Whitney U test, n=60 trials in the 24 hrs group and 48 trials in the 0.2 hrs group). We therefore find that SNL responses are attenuated specifically in those mice that learn to suppress their escape response.

5.2.2 SNL signals do not robustly indicate escape latency

The results of Figure 5.1G and H suggest that looming stimulus-evoked SNL responses are attenuated specifically in mice that learn to suppress their escape response. While this result is important in showing that stimulus salience or novelty are unlikely to account for the responses we observe in the SNL, such an attenuation of signaling is consistent with several different possible functions of the SNL. For example, the signals we observe could relate purely to a decision-making process, which might take the form of an integrator of stimulus-related input that triggers or permits escape when a

certain signal threshold is reached, similar to what has been previously proposed to explain the role of the medial SC to PAG connection in escape (Evans et al., 2018). They could be purely motor-related, relating to motor command or premotor signals received from structures such as the Cuneiform Nucleus. Alternatively, the SNL could convey a stimulus-related metric such as the perceived threat level of the stimulus or its behavioural relevance. To further complicate matters, the signal could be heterogeneous, consisting of a mixture of motor, premotor, and sensory components. We therefore next aimed to disambiguate these different cases by considering the relationship between SNL signals with escape latency and escape outcome.

If the SNL integrates stimulus-related input to trigger or permit escape when a certain signal threshold is reached, then it follows that trials with distinct escape latencies should reach similar levels of activity by escape latency reflecting such a threshold being reached. In other words, SNL activity on a given trial should be strongly and robustly predictive of escape latency and should be relatively consistent across escape trials in a given mouse. It should therefore be possible to use the signal from any given trial to predict the signal in subsequent trials, given the known escape latency. We therefore considered the variability of SNL signals within pre-LSIE trials of the same contrast (Figure 5.2A). We consider how reliably the signal on the first trial can predict the signal at escape latency in subsequent trials.

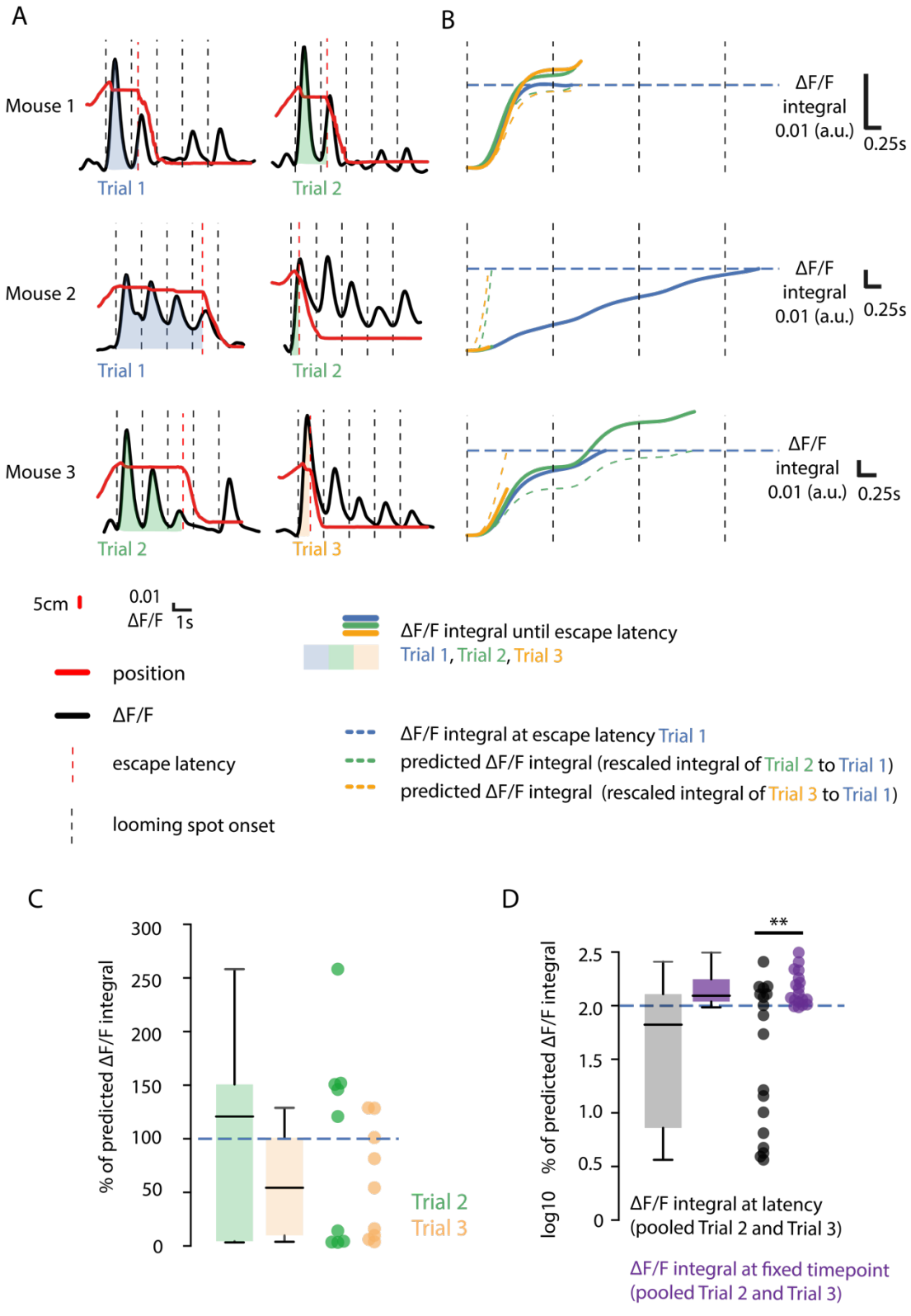

Figure 5.2: signal threshold is not a robust indicator of escape latency. *A) position tracks (red) and corresponding ΔF/F traces (black, solid line) recorded from SNL axons in the TS from two standard contrast trials, shown*

*for three naïve mice. Shaded areas indicate the ΔF/F integral of the signal until escape latency (red, dashed line). Looming spot onsets are also shown (black, dashed lines). B) observed ΔF/F integrals are shown until escape latency for trial 1 (blue), trial 2 (green) and trial 3 (orange) of the pre-test. The predicted integral at escape latency (blue, horizontal dashed line) is calculated as the value of the integral ΔF/F trace reached by escape latency in trial 1. Predicted traces for trial 2 (green, dashed line) and trial 3 (orange, dashed line) are also shown, calculated by rescaling the trace such that the ΔF/F integral at escape latency in each trial reaches the same value reached in trial 1. C) boxplots (left) and swarmplots (right) of the ΔF/F integral at escape latency for all mice in trials 2 (green) and 3 (orange) expressed as a percentage of the ΔF/F integral at escape latency of trial 1 (blue, dashed line). D) boxplots (left) and swarmplots (right) of the of the ΔF/F integral at escape latency (grey boxplot, black dots) or at a fixed timepoint 0.5 seconds after the onset of the stimulus (purple boxplot, purple dots) pooled for all for all mice in trials 2 and 3, expressed as the log_{10} percentage of the ΔF/F integral at escape latency of trial 1. ** denotes a p-value of < 0.01.*

We find that SNL signals are highly variable with respect to escape latency, illustrated by the example trials in (Figure 5.2A and B) and we find that the signal that precedes escape can be substantially different in cases where the escape latency is different (Mouse 1, Trial 2: 120.8 %, Trial 3: 128.9 % of Trial 1 signal at latency; Mouse 2, Trial 2: 4.7%, Trial 3: 4.2% of Trial 1 signal at latency; Mouse 3, Trial 2: 145.9% and Trial 3: 54.4% of Trial 1 signal at latency, Figure 5.2A and B). We find that the magnitude of the predicted signal at latency can differ from that actually observed by an order of magnitude (Figure 5.2C, median value and standard deviation for trial 2: 120.7% +/- 86.5%, n=9 trials, from 9 mice, median value and standard deviation of trial 3: 54.4% +/- 49.4% n=9 trials, from 9 mice). Furthermore, SNL signals measured at escape latency are significantly more variable than signals measured at a fixed timepoint relative to stimulus onset (Figure 5.2D, median values and standard deviations for signals measured at escape latency 1.82 +/- 0.66 and at a fixed

time point 2.09 +/- 0.15, p= 0.00898, *Wilcoxon signed-rank test,* n=18 trials, from 9 mice). Additionally, if the SNL performs the role of an integrator in the decision to escape then the signal on non-escape trials should consistently fail to reach the hypothetical signal threshold required for escape. However, we find that this is not the case: SNL signals in non-escape trials typically exceed signals of escape trials at escape latency at some point during the stimulus (Figure 5.3A-D, mean +/- s.e.m. as a percentage of the first post-test trial: 70 +/- 24.3 % for escape trials vs. 120 +/- 15.9 % for non-escape trials, p=0.0438, Mann-Whitney U test, p=0.116, permutation test of the difference of means for each group). Together this suggests that SNL signals are not a robust indicator of either escape latency or outcome.

5.2.3 SNL signals do not robustly indicate escape outcome

Another possibility is that the SNL conveys motor or premotor signals relating to escape actions. We hypothesise that if the SNL signals include such a premotor component, then the signal on trials on which an escape action is selected should be consistently larger than for trials on which no escape actions occur. To test this, we compared the signal on escape trials at escape latency with non-escapes at the same timepoint within the same mouse.

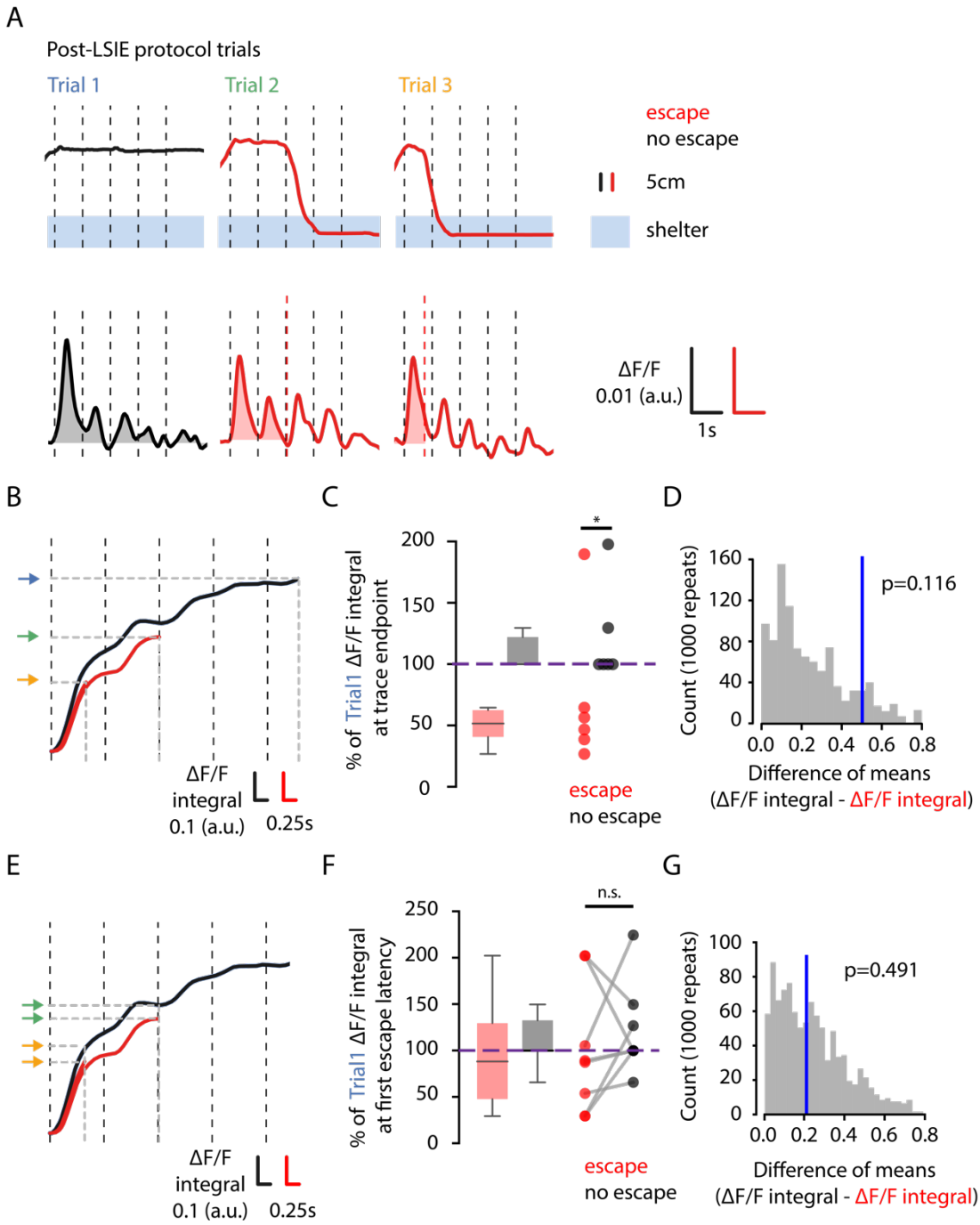

Figure 5.3: signal threshold is not a robust indicator of escape outcome. *A) position tracks (top) and corresponding ΔF/F traces (bottom) recorded from SNL axons in the TS from three trials, taken from a standard contrast post-LSIE test of a mouse that received a pre-test 0.2 hrs before the LSIE protocol and exhibits both escape (trials 2 and 3, red lines) and non-escape (trial 1, black solid line) outcomes. Shaded areas indicate the ΔF/F integral of the*

*signal until escape latency (red, dashed line) or the end of the trace when there is no escape. Looming spot onsets are also shown (black, dashed lines). B) ΔF/F integrals until escape latency (red lines) or until the end of the stimulus (black lines) for these trials in (A). Coloured arrows indicate the analysis timepoint for each trial, measured as signal until escape latency for escapes, and the maximum ΔF/F integral reached for non-escapes. C) boxplots (left) and swarmplots (right) of the signals attained using the analytical approach in B) separated by behavioural outcome. D) a permutation test performed by randomly selecting datapoints and calculating the difference of means. The histogram shows the number of calculated differences that fall in each bin and shows the proportion of permuted differences that are higher than the experimentally observed value (solid, blue line). E) ΔF/F integrals until escape latency (red lines) for this same example mouse on each escape trial (red) or until the end of the stimulus (black lines) for these trials in (A). Coloured arrows indicate the pairs of datapoints included in the analysis of (F) and (G) whereby escape latencies from escape trials are used to attain a datapoint from the comparable timepoint in non-escape trials, resulting in a single pair of datapoints per escape outcome. In this case, trial 2 and trial 3 were escapes and were used to generate two pairs of datapoints. F) boxplots (left) and point plots (right) of the pairs of signals attained using the analytical approach in (E) separated by behavioural outcome. G) a permutation test performed by randomly selecting datapoints and calculating the difference of means. The histogram shows the number of calculated differences that fall in each bin and shows the proportion of permuted differences that are higher than the experimentally observed value (solid, blue line). * denotes a p-value of < 0.05.*

As a population we do not observe a significant difference in SNL signals between escape and non-escape trials (Figure 5.3F and G, mean +/- s.e.m.: 99.9 +/- 24.4% on escape trials vs. 120.9 +/- 17.1% on non-escape trials, p=0.363, *Wilcoxon signed-rank test*, p=0.491, permutation test of the difference of means for each group, n=8 pairs of datapoints from 4 mice), indicating that there is no detectable component of these signals that can be

attributed to premotor or motor activity. In other words, within a given mouse, the signal measured on a single trial is no different for escapes than non-escapes.

Together the examples in Figure 5.2 and 5.3 suggest that the signal observed in a given trial does not robustly predict escape outcome. It also suggests that the protocol received by each mouse (pre-LSIE standard test at 0.2 hrs or 24 hrs before the LSIE protocol) may be a better indicator of signal magnitude than each trial's behavioural outcome and this would be consistent with the SNL signaling a stimulus-related metric such as the perceived threat level of the stimulus, whereby a reduced threat level might reflect a lower probability of escape while not necessarily providing a trial-by-trial readout of escape outcome.

5.2.4 Loom-evoked responses in D1 and A2a neurons in the TS

While we show in Chapter 3 that dopaminergic neurons in the SNL are required for escape, these neurons are not known to project directly to the escape circuitry. It is therefore likely that any role the SNL might play in modulating escape would have to occur through its major projection target, the TS, which we also show is required for normal escape behaviour (Figure 3.3) and is anatomically positioned to disinhibit the medial SC and/or dorsal PAG through the dorsolateral SNr. One hypothesis is that neurons in the TS that could dynamically gate escape responses are active during the presentation of looming stimuli and these responses should be greatest for stimulus contrasts that cause high probabilities of escape.

Broadly, the TS is composed of two principal cell types: medium spiny neurons that express D1 receptors and those expressing A2a receptors. These populations are known to perform distinct roles in behaviour (Kravitz et al., 2010). Furthermore, work from primates suggests that D1 and A2a populations in the TS may send opposite value signals to the SC, with each performing distinct roles in saccade target selection (Kim et al., 2017). This

raises the possibility that each population may contribute differently to escape behaviour in mice and so it is important to record from both D1 and A2a populations separately in order to understand what role, if any, each plays.

We therefore next examined the activity of D1 and A2a TS populations during escape at a variety of contrast levels (Figure 5.4) to determine how they might correlate with escape probability. To achieve this, we injected flex-GCaMP6f into the TS of Drd1-Cre (D1) or Adora2a-Cre (A2a) mice and recorded with optical fiber implants placed above the TS using fiber photometry (Figure 5.4A-C). To obtain a stimulus-response curve for D1 and A2a responses in the TS we then pseudorandomly presented looming spots at different contrast levels (Figure 2.2C).

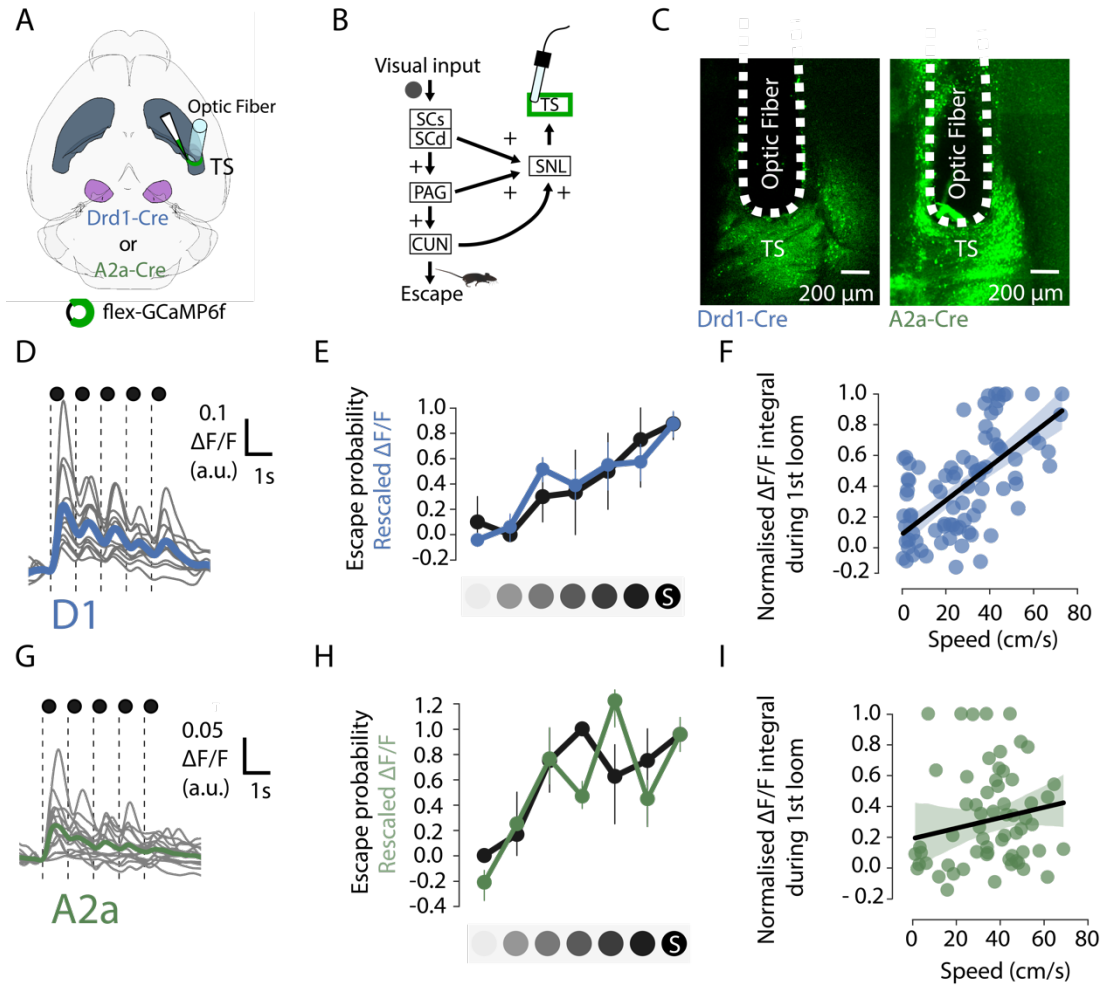

Figure 5.4: D1 and A2a neurons in TS are responsive to looming stimuli. *A) a surgical schematic, with flex-GCaMP6f injected into the TS of either Drd1-Cre or Adora2a-Cre mice to target D1 and A2a neurons respectively, and a fiber implanted in the TS. B) a simplified circuit diagram of the recording paradigm. C) examples of fiber placement and viral expression in D1 (left) and A2a (right) neurons. D) ΔF/F traces (grey lines) and average ΔF/F trace (blue line) recorded in D1 neurons for all trials at standard contrast using the contrast-response curve protocol. E) contrast-response curve (black) with the rescaled ΔF/F signal overlaid for D1 (blue line). F) ΔF/F integral during the first looming spot recorded in D1 neurons plotted against the peak speed reached towards shelter. G) ΔF/F traces (grey lines) and average ΔF/F trace (green line) recorded in A2a neurons for all trials at standard contrast using the contrast-response curve protocol. H) contrast-response curve (black) with the rescaled ΔF/F signal overlaid for A2a (green line). I) ΔF/F integral during the first looming spot recorded from A2a neurons plotted against the peak speed reached towards shelter.*

Firstly, we observe Ca^{2+} signals in both D1 and A2a neurons in response to high-contrast looming stimuli (Figure 5.4D and G). Similar to the SNL, D1 responses to looming stimuli are typically largest on the first loom in the stimulus: the peak ΔF/F signal during the first looming spot was found to be 20.2% larger than the peak ΔF/F signal observed during the second (mean normalised signal +/- s.e.m.: 93.6 +/- 3.7% vs. 73.4 +/- 5.3%, p=0.03, Wilcoxon signed-rank, n=12 trials, 4 mice), and 44.5% larger than the pooled responses from looms 3-5 (Figure 3.4C and D, 99.4 +/- 0.5% vs. 29.3 +/- 2.1%, p=0.000003, Mann-Whitney U test, n=12 trials, 4 mice).

For A2a expressing neurons, the peak ΔF/F signal during the first looming spot was found to be 11% larger than the peak ΔF/F signal observed during the second but this result was not found to be significant (mean normalised signal +/- s.e.m.: 78.5 +/- 10.3% vs. 67.2 +/- 6.1%, p=0.195, Wilcoxon signed-rank, n=12 trials, 4 mice), although responses on the first loom were 34.9% larger

than the pooled responses from looms 3-5 (Figure 3.4C and D, 78.5 +/- 10.3% vs. 43.6 +/- 6.1%, p=0.002, Mann-Whitney U test, n=12 trials, 4 mice).

We also find that while D1 responses correlate strongly with stimulus contrast (Figure 5.4E)*(ρ: 0.701, p-value: 1.8* x *10^{-14}, Spearman*'s *correlation, n=86 trials, 5 mice)* this correlation is weaker for A2a neurons (Figure 5.4H) (*ρ: 0.48, p-value: 4.67 x 10^{-05}, Spearman*'s *correlation, n=61 trials, 4 mice*). Speeds of escape were found to correlate with signal magnitude in D1 (Figure 5.2F, *ρ: 0.624, p-value: 6.39* x *10^{-11}*) but not in A2a (Figure 5.4I, *ρ: 0.176, p-value: 0.166)*. This suggests that, while both D1 and A2a populations are responsive to looming stimuli, D1 responses are more closely related to the intensity of the stimulus, and more closely related to the action taken in response to the visual threat whereas A2a neurons may play a distinct role.

5.2.5 D1 and A2a population responses are reduced following the suppression of escape

If the signals observed in the TS gate escape through disinhibition of the SC, then we would predict that they should decrease with suppression of escape. For example, reduced activity in D1 neurons of the TS is likely to reflect an increased inhibition of the SNr, a consequent increase in the inhibition that reaches the medial SC, and thus a higher threshold must be reached for escape to occur. To test whether such signals change following LSIE we used the same experimental approach as above (Figure 5.4A-C) and compared evoked responses in D1 and A2a neurons (Figure 5.5) before (Figure 5.5A and C, left) and after the LSIE protocol (Figure 5.5A and C, right).

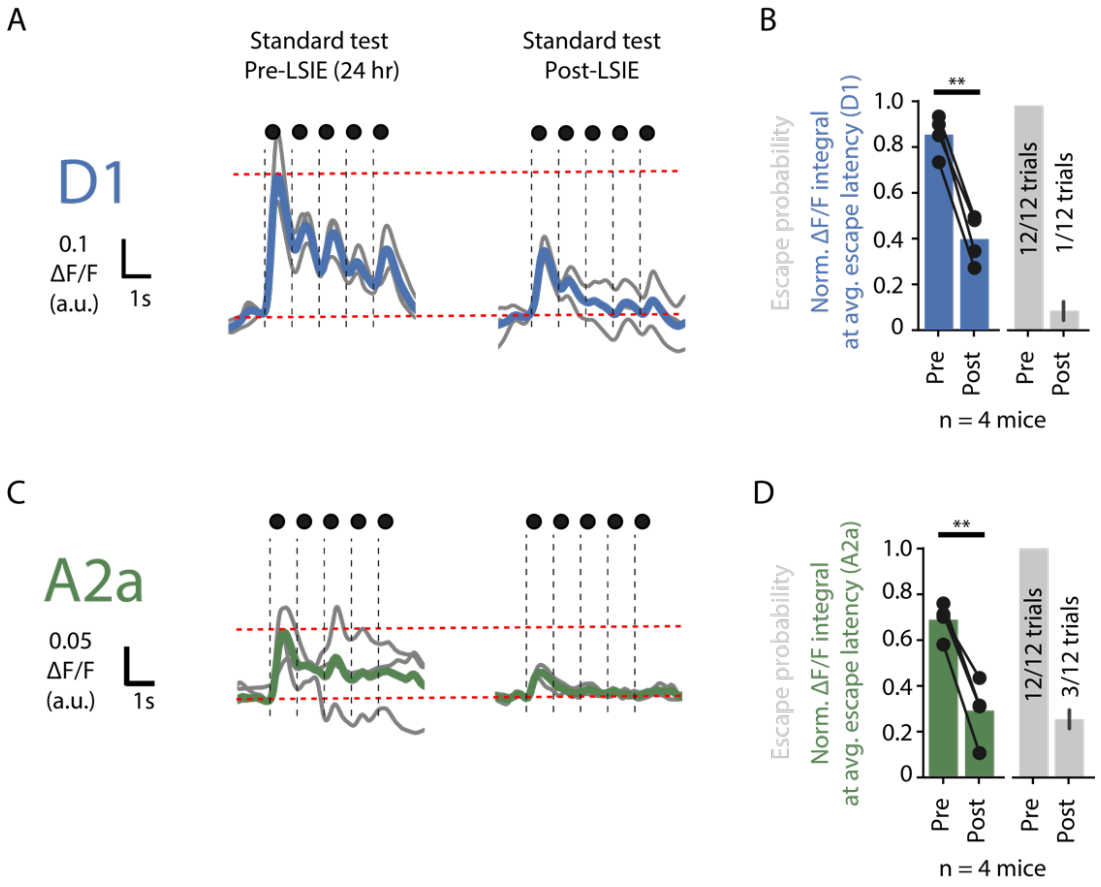

Figure 5.5: D1 and A2a signals in TS are reduced following suppression of escape. *A) ΔF/F traces (grey lines) and average ΔF/F trace (blue line) before (left) and after (right) Drd1-Cre mice underwent the LSIE protocol. The baseline and largest peak of the average of the pre-test traces (red, horizontal dashed lines) are shown for reference together with looming spot onsets (black, dashed lines) and their durations (black circles). B) the average normalised ΔF/F integral at the analysis timepoint for the pre- and post-test for D1 neurons (blue bars) together with the corresponding behavioural outcomes for these mice (grey bars). C) ΔF/F traces (grey lines) and average ΔF/F trace (green line) before (left) and after (right) Adora2a-Cre mice underwent the LSIE protocol. The baseline and largest peak of the average of the pre-test traces (red, horizontal dashed lines) are shown for reference together with looming spot onsets (black, dashed lines) and their durations (black circles). D) the average normalised ΔF/F integral at the analysis timepoint for the pre- and post-test for A2a neurons (green bars) together with the corresponding*

*behavioural outcomes for these mice (grey bars). ** denotes a p-value of < 0.01.*

We find that mice that exhibited escape suppression also showed significantly attenuated signals in D1 neurons of the TS (Figure 5.5B, *pre vs. post, median values +/- s.e.m: 88.1 +/- 4.9%* vs. 42.1 +/- 4.3 %, p=0.0025, Wilcoxon signed-rank test, n=12 trials, 4 mice) and also in A2a neurons of the TS (Figure 5.5D, *pre vs. post, median values +/- s.e.m.: 63.2 +/- 8.4%* vs. 33.1 +/- 4.7 %, p=0.0042, n=12 trials, 4 mice). This suggests that indeed the output of the TS, and presumably also the inhibitory output of the SNL-TS circuit that reaches the dorsolateral SNr is decreased as mice learn to suppress escape. This presumably leads to an overall increase in the inhibition that can reach the escape circuitry via this route during looming stimuli, after induction of LSIE.

5.2.6 Lateral visual areas, posterior Thalamus and the Amygdala project to TS

While we have thus far focused our attention on the SNL input to TS it is conceivable that other structures potentially drive the TS and impact how SNL-TS circuit influences escape decisions. Furthermore, the SNL has previously been suggested to be a reinforcer of avoidance (Watabe-Uchida & Uchida, 2019), rather than a driver of avoidance per se, which raises the possibility that some structure other than the SNL is the main driver of activity in the TS during looming stimuli. We therefore performed rabies tracing from the TS to investigate which structures, other than the SNL, could potentially drive the TS. We focus specifically on D1 neurons because the responses that we observe in D1 neurons are tightly correlated with vigour of escape (Figure 5.4I) and stimulus contrast (Figure *5.*4G) whereas we do not find the responses we observe in A2a neurons to correlate with escape vigour (Figure 5.4J*)* and they correlate more weakly with contrast (Figure 5.4 H).

To specifically trace from D1 neurons we transfected Drd1-Cre neurons with the genes for producing the TVA receptor required for rabies to gain entry to cells and the ΔG protein required for its multisynaptic spread (Wickersham et al., 2007). We then followed this with an injection of modified rabies virus into the same area (Figure 5.6A and B) resulting in labelling of neurons that monosynaptically project onto D1 neurons in the TS.

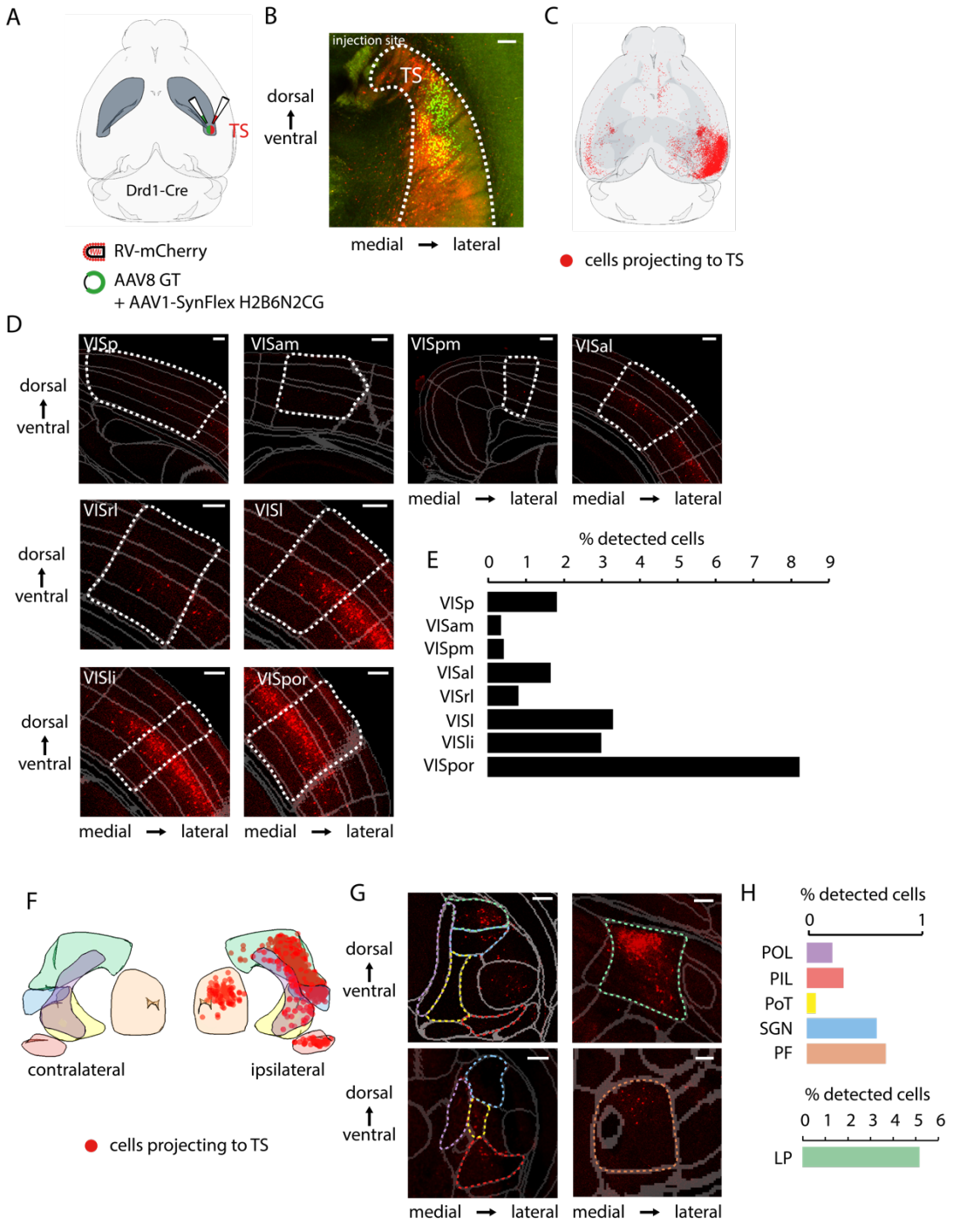

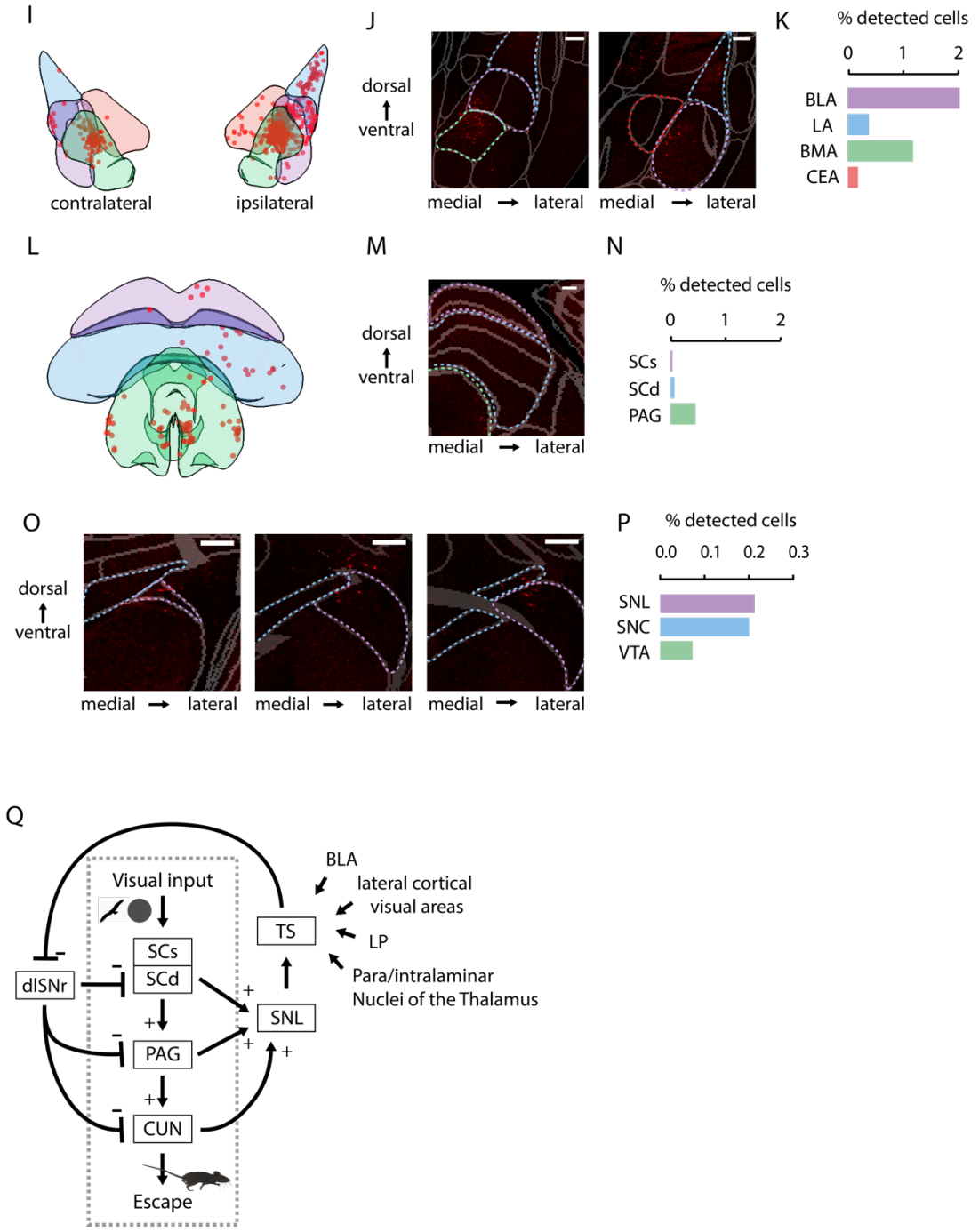

Figure 5.6: lateral visual areas, thalamic nuclei and Amygdala regions project to TS*. A) a surgical schematic in which modified RV-mCherry and flex-TVA and flex ΔG are injected into the TS of a Drd1-Cre mouse line to label monosynaptic inputs to D1 neurons in the TS. B) the injection site in the TS, with TVA expressing cells in green and rabies virus expressing cells in red. C) coordinates of detected neurons (red dots) located within Isocortex. D) example coronal sections for a variety of visual cortical areas (VISp, VISam,*

VISpm, VISal, VISrl, VISl, VISli and VISpor). White dashed line indicates the boundary of each region. E) bar plot indicating percentage of TS inputs detected in each of these regions. F) coordinates of detected cells (red dots) within visual thalamic nuclei (LP, green; SGN, blue; PoT, yellow; POL, purple; PIL, red; and PF, orange. G) example coronal sections of Thalamus with each thalamic nucleus in (F) and (H) outlined in their corresponding colour. H) bar plot indicating the percentage of TS inputs detected in each of these regions. I) coordinates of detected cells (red dots) within amygdalar nuclei (BLA, purple; LA, blue; BMA, green; and CeA, red. J) example coronal sections of Amygdala with each nucleus in (I) and (K) outlined in their corresponding colour. K) bar plot indicating the percentage of TS inputs detected in each of these regions. L) coordinates of detected cells (red dots) within superficial SC (purple), deep SC (blue) and the PAG (green). M) example coronal section of SC and PAG with each region (L) and (N) outlined in their corresponding colour. N) bar plot indicating the percentage of TS inputs detected in each of these regions. O) coronal cross section of the midbrain to show TS inputs found in the SNL (purple) and SNc (blue). P) bar plot indicating the percentage of TS inputs detected in the SNL, SNc and VTA (green). Q) a suggested circuit schematic to illustrate these inputs within the escape and SNL-TS circuitry. All scale bars indicate 200μm.

Structure	Count	% of total	Cells per mm3
Postrhinal area (VISpor)	1357	8.24	893.3
Lateral posterior nucleus of the thalamus (LP)	854	5.19	508.7
Lateral visual area (VISl)	546	3.32	359.9
Laterointermediate area (VISli)	495	3.01	807.3
Basolateral amygdalar nucleus (BLA)	337	2.05	143.5
Primary visual area (VISp)	302	1.83	36.3
Anterolateral visual area (VISal)	275	1.67	258.7
Basomedial amygdalar nucleus (BMA)	196	1.19	99.1
Rostrolateral visual area (VISrl)	135	0.82	101.0
Parafascicular nucleus (PF)	114	0.69	194.4
Supragenicular nucleus (SGN)	101	0.61	505.7
Periaqueductal gray (PAG)	75	0.46	13.6
Posteromedial visual area (VISpm)	71	0.43	61.5
Lateral amygdalar nucleus (LA)	63	0.38	72.8
Anteromedial visual area (VISam)	59	0.36	61.9
Posterior intralaminar thalamic nucleus (PIL)	53	0.32	250.9
Posterior limiting nucleus of the thalamus (POL)	37	0.22	154.8
Substantia Nigra pars Lateralis (SNL)	35	0.21	174.19
Substantia Nigra, compact part (SNc)	33	0.20	96.69
Central amygdalar nucleus (CEA)	30	0.18	17.6
Posterior triangular thalamic nucleus (PoT)	13	0.08	40.7
Superior colliculus, motor related (SCm)	12	0.07	1.7
Superior colliculus, sensory related (SCs)	6	0.04	2.1

Table 5.1: a summary of TS inputs shown in Figure 5.6 *ordered by total cell number. Percentage of total detected cells and the normalised counts per volume also shown for each structure.*

We find that the TS receives input from a variety of visual cortical areas (Figure 5.6C-E, n=1 mouse, 16470 cells detected), with particularly dense inputs arising from lateral visual areas such as Lateral Visual Area, the Laterointermediate Area and Postrhinal Area. We also observe dense inputs arising from posterior regions of the Thalamus (Figure 5.6F-H), particularly from the Lateral Posterior Nucleus of the Thalamus, the Supragenicular Nucleus, and the Posterior Intralaminar Nucleus of the Thalamus. Additionally, we observe that the Amygdala sends projections to the TS (Figure 5.I-K), with most inputs arising from the basolateral area (Figure 5.6K). Very few cells were detected in the SC and PAG (Figure 5.6L-N). Finally, we find that the TS also receives input from the SNL and SNc, with the densest innervation of the TS arising from the SNL (Figure 5.6O and P). Thus, we show that a variety of cortical, thalamic and amygdalar areas project to D1 neurons in the TS and we hypothesise that one or several of these structures may provide driving

input to the TS. These regions therefore represent promising target structures for the focus of future research.

5.3 Discussion

5.3.1 Responses in the SNL following LSIE

In this chapter we aimed to better understand the precise roles of the SNL and TS in the modulation of innate escape. We reasoned that if these regions are involved in the modulation of escape responses then there should be physiological responses in each that vary as mice progressively learn that particular threat-stimuli such as looming stimuli become non-threatening. In the SNL, given its proposed role in signaling threat-prediction error (Watabe-Uchida & Uchida, 2019), we hypothesised that this signal will attenuate as mice learn that looming stimuli are non-threatening. We find this to be the case: mice that receive a pre-test 24 hours before the LSIE protocol and suppress their escape have attenuated SNL Ca^{2+} signals in post-LSIE test trials, while mice that receive a pre-test 0.2 hours before the LSIE protocol and continue to engage escape responses do not show such attenuation. Our finding that SNL responses are attenuated following effective LSIE but not when learned suppression is occluded suggests that behavioural outcome or behavioural relevance of the stimulus better explains the signals we observe, rather than alternatives such as novelty or stimulus salience per se. If the signals conveyed novelty, for example, then one might expect the signals to decrease irrespective of behavioural outcome as the stimulus will become less novel in both groups with repeated stimulus exposure even if the escape responses remain intact. Similarly, if SNL signals convey stimulus salience per se, then one might expect signals to attenuate similarly in both groups because any reduction in salience that occurs due to stimulus repetition should be similar in both groups due to the fact that each receives the same set of stimuli. However, the signal that we measure is distinct in mice that have the same overall number of life-time exposures to looms but exhibit very different behavioural responses. This suggests that behavioural outcome, or

behavioural relevance of the stimulus, may best explain the reduction in signal that we observe following LSIE rather than alternatives such as novelty or stimulus salience.

However, we also find that SNL signals in response to looming stimuli are poor indicators of escape latency and trial-by-trial outcome. While this argues against the possibility of the SNL relaying motor signals or performing a direct role in the decision to escape per se, it is broadly consistent with the SNL conveying a learning signal and is consistent with previous literature suggesting that the SNL may signal the threat level of external stimuli.

5.3.2 The role of the TS

Additionally, in the case of the TS, which may gate behavioural responses through targeted disinhibition of the medial SC, we hypothesised that there are loom-evoked TS signals that are larger in response to stimuli that are associated with high probabilities of escape than stimuli associated with lower probabilities of escape. We find this to be broadly the case for both D1 and A2a populations, which each correlate, although to different degrees, with stimulus contrast. The responses we observe in D1 show an incrementally increasing trend with stimulus contrast (Figure 5.4G), while A2a responses are small for the lowest two contrasts tested and show little obvious relationship with contrast (Figure 5.4H). Further, only D1 responses were found to correlate with the speed of escape, which suggests they may be more directly involved in regulating escape decisions than A2a neurons. This suggests that D1 and A2a populations may play distinct roles in loom-evoked escape, but further experiments are required to establish precisely what these signals encode and how they precisely differ.

We also show that signals in both populations are significantly attenuated following learned suppression of escape. In the D1 population, such a change might reflect an increase in the inhibition that reaches the medial SC during looming stimuli once it has been learned that escape is not an appropriate

action. For A2a the nature of this decrease and its overall contribution to escape behaviour is less clear and without further experiments it is not possible to say for certain what this reduction in signal might mean in relation to escape. In contrast with the direct pathway, the indirect pathway is thought to be relayed through the GPe, which itself is made up of a genetically heterogeneous population of neurons that may play distinct roles, and so the signals we observe may be more heterogeneous than those in D1 neurons.

5.3.3 Does the SNL drive the TS?

DA acts as a neuromodulator that influences neuronal excitability (Tritsch, Sabatini 2012, Calabrese 1987, Uchimara 1989, Wilson 1992) and as a driver of long-term synaptic change through LTP and LTD. It is therefore likely that some structure other than the SNL drives activity in the TS, while the SNL takes a modulatory role, such as facilitating 'up-state' transitions or reinforcing glutamatergic pathways from other structures that project to the TS from e.g. Thalamus or Cortex. This is also further supported by our data that show mice can still escape on early trials following SNL lesion (Figure 3.3G): if the SNL were required to drive TS to permit escape then one might hypothesise that these mice should never escape (for a full discussion see Chapter6). However, given that we observe broadly similar signals in the SNL and TS during escape, and the SNL is known to contain neurons that are both dopaminergic and glutamatergic (i.e. potentially co-release glutamate (Menegas et al., 2018)) it is not possible to rule out without additional experiments that the SNL does drive the TS via glutamate-mediated excitation. It is important to follow these results with experiments in Vglut2 knockout mice to clarify the precise mechanism by which the SNL influences the TS. While we have not performed additional experiments to this effect, it has been shown by others that there is no difference in approach-avoidance behaviour between Vglut2 knockouts and their non-transgenic control littermates (Menegas et al., 2018). This suggests that glutamate release in the TS may not be necessary for escape behaviour. Additionally, there are two experiments that would help to clarify the role of the SNL as a driver or modulator. Firstly, if the SNL is a reinforcer

rather than a driver of the TS, then we expect SNL lesioned mice to still show strong Ca^{2+} responses in medium spiny neurons in the TS and these responses should correlate with behavioural outcomes (if they occur), and these should attenuate more rapidly than in controls. On the other hand, if the SNL drives the TS directly then we should not observe signals in the TS in 6-OHDA lesioned mice that lack SNL neurons. Secondly, optogenetic activation of the SNL should not change the threshold for escape on stimulated trials, and inactivation should have only a modest effect, if any, on escape probability on stimulated trials while reducing the likelihood of escape in future trials.

Although it is not clear from our results here whether the SNL acts as a direct driver of the TS or a reinforcer of other pathways projecting onto the TS, we performed tracing experiments to better understand inputs to the TS. In particular, we sought to identify brain regions other than the SNL that might be positioned to perform such a driving role. We reasoned that if structures other than the SNL drive the TS during escape, then they should also be driven directly or indirectly from the SC (i.e. should receive loom related information). Our tracing from D1 neurons in the TS reveals, similar to others (Hunnicutt et al., 2016),that a limited variety of brain regions project to D1 neurons in the TS. Interestingly, while there do not appear to be many direct projections to the TS from areas that compute escape decisions such as the SC and PAG, the most substantial inputs we observe arise from structures that are known to receive substantial input from the SC, namely the Lateral Posterior Nucleus of the Thalamus, the Paralaminar Nuclei of the Thalamus (SG, POL, PIL, PoT) and also lateral visual areas whose activity is heavily dependent on the SC such as the Postrhinal and Laterointermediate areas of Cortex (Beltramo & Scanziani, 2019). For this reason, these structures seem to be good candidates for future experiments – if they drive the TS then they might also be required for escape behaviour and we should observe that D1 responses are altered following lesions of such cell populations that project to the TS. Although there are studies on the role of the Lateral Posterior Nucleus of the Thalamus in SC driven innate threat responses(Evans et al., 2018; Shang et

al., 2018; Wei et al., 2015), these have not explicitly targeted the most posterior regions that are driven by SC (Bennett et al., 2019b).

Chapter 6: General Discussion

6.1 Summary of results

This thesis investigated the role of dopaminergic neurons in the Substantia Nigra pars Lateralis (SNL) and their major projection target, the Tail of the Striatum (TS) in the learned suppression of innate escape in mice. The main findings are as follows:

1) The SNL receives input from the core escape circuitry, from the deep layers of the SC, the PAG and the Cuneiform Nucleus.
2) The SNL and the TS are each required for normal escape behaviour.
3) Neurons in the SNL are activated by looming stimuli. The magnitude of the recorded signals scale with stimulus contrast and, therefore, also with the vigour and probability of escape.
4) The TS projects to parts of the SNr that inhibit the medial SC and/or dorsal PAG and is thus positioned to disinhibit the medial SC and/or dorsal PAG.
5) A behavioural paradigm (LSIE protocol) was developed that revealed an extremely robust form of learned suppression of innate escape.
6) LSIE is specific to visual stimuli since escape responses to auditory threats remain intact.
7) Recent (< 24 hrs) experience of loom-evoked escape significantly reduces LSIE.
8) Loom-evoked signals in the SNL are attenuated following the LSIE protocol in mice that suppress escape but remain intact in mice that undergo the LSIE protocol but maintain escape behaviour.
9) D1 and A2a expressing neurons populations in the TS are responsive to looming stimuli, and each population shows responses that corelate with stimulus contrast. These responses in D1 but not A2a neurons correlate strongly with escape vigour and both populations show attenuated signals following suppression of escape.

I will now discuss these findings within the context of what is known about the circuitry for computing escape decisions together with traditional views of Basal Ganglia function. I will also discuss the limitations of these results and, where appropriate, will discuss future experiments that could clarify or build upon the results of this thesis.

6.2 Discussion

6.2.1 The learned suppression of innate escape

One of the central aims of this thesis was to understand the flexibility of innate escape behaviour in laboratory mice. Previous studies have shown that actions that follow the decision to escape, such as the location that mice run to, are influenced by experience (Vale et al., 2017), but does previous experience influence the decision of whether or not to escape at all or does it exclusively serve the role of optimising escape actions once they have been initiated? We find that the decision of whether or not to escape from a previously threatening stimulus is indeed flexible and is heavily influenced by recent previous experience: mice can learn to completely suppress innate escape responses to looming spots, suggesting that escape decisions are modified according to an organism's experience even if that means completely overriding the innate escape response. This also suggests that, while the classification of some stimuli as threatening is innate, it may be possible to learn that such stimuli are, in fact not life-threatening. This is supported by findings from other organisms such as lizards (Cooper 2010) and crabs (Hemmi & Merkle, 2009; Hemmi & Tomsic, 2012; Tomsic et al., 2009, 2019) that show similar behaviours to be highly flexible under both ethological and laboratory settings. Our novel LSIE protocol robustly leads to suppression of the innate escape response in mice and as such it provides a basis for investigating the neural circuits that drive or facilitate flexibility in the innate escape decision.

6.2.2 The ethological relevance of the LSIE paradigm

It is important to consider the extent to which the behavioural phenomenon that we study here – the learned suppression of escape responses to looming spots – relates to decisions that might occur in nature. As I argue in Chapter 1, learning to suppress escape behaviour can be advantageous to an animal by minimising the cost of false alarm escape responses. Such false alarm responses are costly as they will reduce access to resources and the amount of time available for related behaviours such as foraging. However, such an advantage is only conferred if learned modifications last long enough to inform future action and if those modifications are contextually relevant – at least, selective to threat modality. We argue in Chapter 4 that our LSIE protocol exhibits such features: the learned suppression of escape is both long lasting and modality specific. This suggests that the mechanisms engaged during LSIE may be similar to those required for modifying escape behaviour in more ethological scenarios.

Additionally, we found that previous recent experience of loom-evoked escape significantly reduces the likelihood that a mouse will subsequently learn to suppress their escape response. One might also expect this to be the case in ethological scenarios – if a particular stimulus was perceived to be threatening in the recent past, then it is perhaps advantageous to adapt less readily even if it is later learned that such a stimulus no longer leads to negative outcomes. We therefore find that innate escape behaviour can be robustly induced by a simple protocol and find evidence suggesting that this may resemble flexibility of innate behaviour that occurs in ethological scenarios.

6.2.3 The SNL-TS circuit are crucial parts of the escape circuitry

The second central aim of this thesis was to use this LSIE paradigm to identify and characterise circuits that might mediate the learned control of innate escape behaviour. We focused on a Basal Ganglia sub-circuit comprised of the SNL and TS because the Basal Ganglia are thought to play a crucial role

in action selection (Mink, 1996) and because it has been suggested that this circuit computes threat prediction error (Watabe-Uchida & Uchida, 2019). We find that activity in the SNL and TS is correlated with escape probability and escape vigour and that lesion of either the SNL or TS leads to deficits of escape behaviour suggesting that the SNL-TS circuit may be a fundamental and previously unappreciated part of the escape circuitry.

These data, and the finding that the SNL receives substantial input from the deep layers of the SC suggest that looming stimulus-related information must pass through the SNL or TS to permit escape. Additionally, as the inhibitory output of the TS exclusively innervates the dorsolateral parts of the SNr, which tonically inhibit the medial SC, it is likely that activity within the SNL-TS circuit leads to disinhibition of the escape circuitry (Figure 6.1).

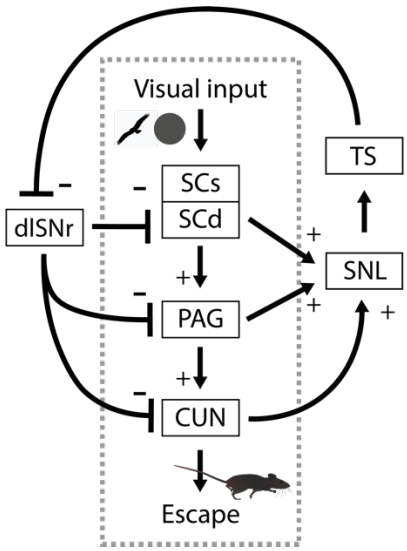

Figure 6.1: a proposed circuit schematic of the SNL-TS-SNr circuit in relation to the known escape circuitry*. "+" indicates known or presumed excitatory connections, while "-" indicates known inhibitory connections.*

Such a mechanism would perhaps be surprising given the presumed need to enact innate escape decisions rapidly. One might expect such decisions to be computed over a minimal number of synapses (Peek & Card, 2016) and the

requirement for Basal Ganglia control would add at least four synapses (e.g. SC to SNL, SNL to TS, TS to SNr, SNr to SC). This layer of complexity potentially slows down escape decisions but may be a necessary price to pay for flexibility.

6.2.4 SNL-TS responses are suitable for a role in modulating escape

It is not possible from the data in this thesis alone to determine whether the SNL or TS actively modulate the escape circuitry. This would require transient manipulations of the SNL or TS through e.g. optogenetic experiments and we have performed no experiments to determine the sufficiency of the SNL or TS for driving such modulation of escape. However, the activity we recorded in the SNL-TS circuit is consistent with such a role: SNL responses correlate with escape metrics and stimulus intensity, and these responses are attenuated specifically as mice learn to suppress escape. Furthermore, responses in the TS are also attenuated following learned suppression of escape. While these results are correlative, activity in the SNL and TS change in the way that one might expect from structures that modulate escape. Together with the finding that these structures are required for normal escape behaviour, this does suggest that this activity may be causally involved in the modulation of escape behaviour, but it remains to be definitively shown.

6.2.5 Mechanisms by which the SNL-TS circuit might influence escape.

If the SNL-TS circuit is causally involved in the learned control of escape, then what is the nature of its function? By what mechanism could the SNL-TS circuit modulate behavioural responses to looming stimuli? In the following section, I will suggest possible mechanisms by which the SNL-TS circuit might interact with the known escape circuitry, drawing from the results of this thesis, and also from literature on the function of the Basal Ganglia and the mechanisms by which they are thought to influence action selection in general.

6.2.6 The SNL-TS circuit may influence the flow of information from superficial to deep SC

As outlined in Chapter 1, the SC is a layered structure that can be broadly separated into superficial and deep layers. Neurons in the superficial layers of SC tend to respond similarly to a wide range of stimuli whereas neurons in the deep SC are more likely to respond in a highly selective manner to particular stimuli such as high contrast looming spots. For example, neurons in the superficial layers of SC respond to high contrast looming spots, inverse looming spots, overhead passing spots, spots of increasing contrast, white looming spots and flickering checkerboard stimuli (Lee et al., 2020). On the other hand, neurons in deep SC show a strong preference for high-contrast looming spots that are known to elicit escape rather than the other stimuli. Additionally, activity within the deep SC attenuates with repeated exposure in a stimulus and location specific manner while responses of neurons in the superficial layers attenuate to a much lesser extent suggesting that familiar stimuli are more likely to trigger responses in the superficial than the deep SC. These data have led some to suggest that the SC filters information along its superficial-deep axis, whereby the deep layers respond only to stimuli that are found to be “behaviourally relevant” in that they are novel and/or require an action be taken (Lee et al., 2020). How such a physiological change arises is an open question, but it could plausibly involve a reduction of excitability in the deep SC, local modification of the strength of specific connections from superficial to deep SC, or it may require another structure, such as the Striatum, to process a range of contextual and learned information and use this to gate responses to specific stimuli that have been learned to be non-relevant.

Within such a hypothesised circuit, the Basal Ganglia and in particular the SNL-TS circuit could play an important role. We show that parts of the SNr that receive input from the TS send a dense inhibitory projection to the intermediate and deep SC. Thus, the SNL-TS-SNr circuit is well positioned to

influence information flow from superficial to deep layers of SC or to gate deep SC responses (Figure 6.1). As looming stimuli become more familiar through experience, the SNr to SC projection could weaken the responses of deep SC neurons to reduce the likelihood of looming stimuli overcoming the threshold required to drive the PAG and consequent escape. As suggested in Chapter 3, lesioning the SNL or TS disinhibits the SNr, which itself inhibits the SC, thereby preventing escape. Additionally, given that it has been shown that the SNL/SNr projects to the Cuneiform Nucleus (Caggiano et al., 2018) this circuit could also directly regulate downstream motor nuclei to prevent inappropriate actions from being executed. Our observation that D1 and A2a signals in the TS are attenuated following the learned suppression of escape is also consistent with such a model: once mice have learned to suppress escape responses, looming stimuli drive less activity in the TS, and consequently there is likely to be greater SNr-mediated tonic inhibition of the SC.

6.2.7 The SNL may drive the TS directly or reinforce thalamo- and cortico- striatal pathways

While the SNL receives substantial inputs relating to visual threat-stimuli and densely projects to the TS, it is unclear whether activity in the SNL acts as a driving signal or a modulatory one. Broadly speaking, dopamine has two modes of action in the Striatum: either as a driver of long-term synaptic changes on cortico- or thalamo- striatal projections through LTP and LTD (Surmeier et al., 2011) or as a neuromodulator that influences neuronal excitability (Calabresi et al., 1987; Tritsch & Sabatini, 2012; Uchimura & North, 1989; Wickens & Wilson, 1998). The medium spiny neurons of the Striatum are hyperpolarised at rest due to the dominance of an inward rectifying K+ current (Surmeier et al., 2011, Wilson 1993), which is difficult to overcome without substantial synchronous glutamatergic input classically thought to arise from cortico- or thalamo-striatal projections. Dopaminergic input does not drive these striatal neurons to fire per se, but rather facilitates or attenuates the glutamate driven transition to an “up state” or modifies the firing rate once

in this “up state” (Lahiri & Bevan, 2020; Planert et al., 2013). It has also been shown that coincident activity of both glutamatergic and dopaminergic neurons is required for long-term changes in outputs of the Striatum through LTP and LTD (Surmeier et al., 2011) and dopamine is therefore also highly likely to be required for the reinforcement of synapses within the TS. However, the SNL also expresses Vglut and may therefore co-release glutamate in the TS, raising the possibility that the SNL could also drive the TS glutamatergically.

Whether the SNL is a driver or modulator of activity in the TS has important implications in the escape circuitry. If the SNL is a driving influence, then its activity would directly increase the inhibitory output of the TS and lead to a transient reduction of the inhibitory output of the SNr that reaches the SC, facilitating the occurrence of escape. Thus, SNL activity would directly influence the threshold for escape in the deep SC, possibly on a trial-wise basis. However, we find that this is unlikely to be the case for several reasons. Firstly, if the SNL is a robust driver of escape one might expect its activity to be highly predictive of escape latency, but we find that this is not the case (Figure 5.2). Additionally, one might predict that SNL signals on non-escape trials should not reach levels of activity that are found to be “sufficient” for escape on different trials within the same mouse. However, we find that SNL signals on non-escape trials often exceed those on escape trials at escape latency (Figure 5.3). This suggests that if the SNL drives the TS, then its contribution does not robustly lead to escape. Further, this is consistent with our SNL lesion data (Figure 3.3G) showing that even though escape is impaired, some mice are still able to escape on early trials. If the SNL were required to drive the TS then one would expect mice with SNL lesions to never escape at all.

What role, then, could the SNL play within the SNL-TS-SNr circuit? If the SNL is purely modulatory, then an external driver would be required (e.g. from Thalamus/Cortex) to drive TS neurons, thereby gating SNr-mediated inhibition of SC. The SNL could then possibly perform the role of a modulator by

reinforcing or reducing these cortico- or thalamo-striatal connections that drive the TS. As such, the likelihood of a looming stimulus driving the TS to disinhibit deep SC could be increased or decreased by the SNL based on previous experience by modifying the strength of cortico- or thalamo-striatal connections. This would be consistent with lesions of the SNL, which result in a mixture of outcomes: although escape behaviour was strongly impaired, we found that some mice still escaped on early but not late trials possibly reflecting a more rapid suppression of escape in lesioned mice than in controls (Figure 3.3).

We have proposed that the SNL-TS-SNr circuit acts as an inhibitory gate on the deep SC. However, it may be advantageous for mice to err on the side of caution in the first encounter with a potential threat. Therefore, we would expect any inhibitory gate to be off before the first encounter with a potential threat. In other words, we would expect the escape threshold to be low and escape to be very likely on the first trial. This scenario might also help explain our behavioural results showing that mice forget that a stimulus was previously threatening in just 24 hours while they remember that a stimulus was non-threatening for up to two weeks. If the gate is off, or close to this theoretical minimum, on the first encounter with a threat then further reinforcement of escape would simply maintain the status quo rather than materially increasing the probability or vigour of escape in the longer term. As discussed in Chapter 4, it might be advantageous to "forget" recently experienced visual threats somewhat quickly. This would mean that each day, all contexts are by default treated equally and a high level of vigilance maintained across all environments allowing escape behaviour to be dynamically adjusted to suit the changing external circumstances. Another advantage of rapid decay of escape memory is that there is little opportunity for "accumulation effects" over the lifetime of the organism potentially profoundly inhibiting it from exploration for resources and mates.

If the TS is not driven by the SNL but is instead driven by glutamatergic cortico- or thalamo-striatal projections, then those projections should also be required for normal escape behaviour. It is also likely that structures required for normal escape should themselves receive substantial inputs from the SC. We have identified several candidate structures: the Lateral Posterior Nucleus of the Thalamus receives much of its input from the superficial SC, and it presumably also passes this to the Postrhinal Area whose activity derives from SC (Beltramo & Scanziani, 2019); the Posterior Paralaminar Nuclei of the Thalamus (SG, POL, PIL, PoT) receive input from the deeper layers of the SC and it has recently been suggested that their activity opposes the habituation of stopping behaviour that is induced by optogenetic stimulation of SC NTSR+ neurons (Sans-Dublanc et al., 2020b). Interestingly the Posterior Intralaminar Nucleus of the Paralaminar Nuclei sends a dense and specific projection to the ventral parts of the TS. Future experiments should test the role of each of these TS-projecting and presumably glutamatergic inputs through targeted lesions of TS-projecting neurons in each region, and through transient optogenetic manipulations to understand their contribution, if any, to the modulation of innate escape.

6.2.8 Comparison with reinforcement learning

Our results suggest that learning to override the innate escape response may involve a mechanism that differs fundamentally from reinforcement learning. In reinforcement learning it is thought that cortico- or thalamo-striatal connections that are initially weak are gradually strengthened with experience if their activity coincides with phasic dopaminergic activity that signals reward. However, as outlined in Chapter 1, innate behaviours such as escape are useful precisely because they do not require previous experience to be enacted. This raises the possibility that innate behaviours might be regulated differently to other learned behaviours. Escape is the default response to looming spots in naïve mice. As such, the SC must be disinhibited on the first encounter with a potential threat to permit escape. This means that if the SNL-TS-SNr circuit acts as an inhibitory gate on the deep layers of SC as we

propose here, then this gate needs to be “off” on the first encounter with a potential threat to permit or facilitate activity in the deep layers of SC that drive escape. Furthermore, if the TS is primarily driven by e.g. thalamo-striatal projections, then these projections need to be initially strong: sufficiently strong to drive the TS, whose inhibition of the SNr needs to reduce the tonic inhibition that the SC receives from the SNr. I therefore hypothesise that initially strong thalamo-striatal connections drive the TS to permit escape and are gradually weakened as evidence mounts that stimuli that are innately perceived to be threatening actually pose no threat. The absence of dopaminergic input from the SNL when stimuli are non-threatening would lead to a gradual reduction in the potency of the glutamatergic inputs to the TS and this, in turn, would lead to a reduced disinhibition of the deep layers of SC. This would be consistent with our observations that, following LSIE, signals in the SNL and TS are reduced (Figure 5.1 and 5.5), and would also help to explain why SNL lesioned mice appear to rapidly reduce their escape response to the test stimulus (Figure 3.3G).

6.2.9 The SNL receives inputs that could relate to both stimulus relevance and behavioural outcome

One issue raised in Chapter 3 is that the SNL receives significant inputs from premotor nuclei. This suggests that, in addition to signals from the deep SC, which are driven by behaviourally relevant visual stimuli such as looming spots, the SNL may also receive information relating to the motor consequences of escape decisions. For example, structures such as the Cuneiform Nucleus and Pedunculopontine Nucleus could provide information about whether escape actions were selected or not. This is consistent with ideas put forward in reinforcement learning, that reinforcement can occur through the law of effect – that previous outcomes e.g. rewards and punishments can influence future action, but also through the law of exercise – whereby previous actions are reinforced simply because they were previously selected in response to a given stimulus. Learning to suppress

escape may require both of these forms of learning – to learn that a particular stimulus does not lead to aversive outcomes but also that the actions selected in previous threat-encounters were the appropriate ones. The range of inputs to the SNL that we observe in our anatomical tracing (Fig 3.1) would enable the SNL to achieve the desired learning outcome in both cases.

6.3 Limitations

6.3.1 6-OHDA lesions

To show that the SNL is important for normal escape behaviour we injected 6-OHDA into the TS where it is selectively taken up by the dopaminergic neurons that project there (see Methods, section 2.5.2). This method has some noteworthy caveats. Firstly, although the majority of TS projecting dopaminergic neurons arises from the SNL some dopaminergic neurons in the lateral parts of the SNc also project to the TS and their function would also be expected to be compromised in our lesion experiment. However, these neurons lie at the SNL/SNc border (Figure 5.6O) and may in fact be part of the same population of neurons. These studies would therefore benefit from follow-up experiments using lesions that are based on the genetic targetability of the SNL population, which is known to contain both dopaminergic and Vglut expressing neurons. Additionally, it is unclear whether our observed effects of lesioning on escape probability and vigour comes about due to the acute loss of dopaminergic input to the TS or due to the long-term effects of dopamine depletion in the TS, which has been shown to cause decreased arborisation of D1 (and to lesser extent A2a) neurons and reduced synapses (Parent & Parent, 2016).

It has also been shown that dopaminergic neurons in the SNc also release dopamine onto the SNr to directly regulate their output and it is likely that this is also the case for the SNL. This would provide a means by which dopaminergic neurons could affect escape outcomes while bypassing the TS. However, given that lesions of the TS with NMDA also impair escape it is

unlikely to be a significant issue for the interpretation of our 6-OHDA lesion results.

6.3.2 NMDA lesions

NMDA induces excitotoxic cell death at the site of injection, but it may also lead to off target changes such as cell death in locations other than the site of injection. Given that the TS and SNL are interconnected, it is difficult to attribute the precise role of each structure based on lesions alone. This result would need to be followed with approaches that only transiently inactivate the TS, for example either opto- or chemo- genetically.

6.3.3 Photometry

Fiber photometry is a useful method for recording from distinct neural populations based on genetic markers that enable the expression of e.g. fluorescent Ca^{2+} indicators such as GCaMP6f. In the case of dopaminergic neurons in the SNL, where we assume the signal to be relatively synchronous and coherent, it allows the identification and characterisation of the function of a specific population. However, in the case of D1- and A2a-receptor-expressing populations, which are potentially more heterogeneous in their function and occupy distinct territories in the TS (Miyamoto et al., 2019), the limitations of the method as a measure of bulk signal, and the variability due to e.g. fiber placement, or baseline fluctuations, become more important. Implicit in the interpretation of our D1/A2a LSIE recordings is an assumption that the recorded population mostly contributes to controlling a single action or type of action, but the TS consists of distinct territories each of which comprises different proportions of D1 and A2a neurons (Miyamoto et al., 2019). This makes interpretation of these results challenging and future experiments should employ methods that are less ambiguous (i.e. with single cell resolution), with higher spatial and temporal resolution, such as high-density electrophysiological recordings together with opto-tagging to identify D1/A2a populations. This would allow a more detailed understanding of

distinct populations of neurons along the entire DV axis without pooling the responses in the ML and AP axes as is the case with fibre photometry. Alternatively, more detailed post-hoc analysis of fiber placement while defining such functional territories may also be of interest.

Additionally, because the Drd1-Cre mouse line, used for photometry recordings in D1-receptor-expressing neurons of the TS, also expresses Cre widely in cortical Layer 6b, there is some off-target expression in some mice in this experiment. This is a potential caveat as it means that some proportion of the signals that we record from the TS may be contributed to by cortico-striatal projection neurons whereas this is not the case for A2a neurons.

6.3.4 Anatomical tracing

One limitation in this thesis regarding the anatomy is the low sample size, as we show experiments from single mice. This means that we do not comprehensively trace from, or label, all subregions of the TS in these experiments. We therefore cannot state definitively based on these results alone whether additional structures, other than those shown, project to the TS or whether other parts of the TS, that are not labelled here (i.e. ventral parts of the TS), project to distinctive regions in the SNr. However, our results are consistent with the recently published findings of others which I will briefly outline here. Firstly, it has been previously shown that the TS receives a distinct set of inputs when compared with the rest of the Striatum (Hunnicutt et al., 2016). This work used anterograde tracing of different cortical and thalamic regions and reveals areas projecting to the TS that are consistent with our rabies mediated tracing results, such as the posterior visual areas, Lateral Posterior Nucleus of the Thalamus and Basolateral Amygdala. Additionally, a recent publication that considers the anatomical topography of the SNr confirms our finding here showing that the TS distinctly labels the dorsolateral SNr but not the other areas in the SNr (Foster 2020). It therefore seems likely that we can rely on the anatomical data that we present here, as it is broadly consistent with the observations of others.

6.4 Summary

As animals become familiar with their environment, external stimuli that are innately perceived as threatening can become learned as non-threatening. This form of learning can significantly impact individual fitness by potentially increasing foraging time and access to mates. The evolutionary importance of learned suppression of innate escape behaviour provided the general motivation for this thesis.

In the lab, mice show robust escape responses to overhead, high-contrast visual looming stimuli making them an ideal mammalian genetic model to dissect the mechanisms of such learned control of escape behaviour. It is also believed that mammalian dopaminergic neurons in the SNL which project to the TS signal threat prediction error and could thus potentially mediate adaptive control of innate behaviours. Also, the SNL and the TS are densely interconnected with structures that mediate escape behaviour and our lesion experiments show that they are necessary for escape.

In this thesis I show that the TS provides adaptive control of escape behaviour using a novel behavioural protocol that results in LSIE to previously threatening visual stimuli. Escape suppression lasted for over two weeks and was specific to visual threat since it did not reduce the probability of escape to threatening auditory stimuli. Photometry experiments in the TS showed large, reliable, calcium signals in dopaminergic inputs in response to looming stimuli that correlated with stimulus saliency and escape probability. These dopamine signals in the TS were significantly attenuated during and following the LSIE protocol only when mice exhibited escape suppression. Similarly, both D1- and A2a-receptor-expressing TS neurons showed reduced responses following LSIE indicating that these dopaminergic responses to looming stimuli undergo experience-dependent modulation. I conclude that dopaminergic TS

activity is involved in the modulation of escape behaviour and that these signals may be adjusted according to prior experience and threat prediction.

Bibliography

Ache, J. M., Namiki, S., Lee, A., Branson, K., & Card, G. M. (2019). State-dependent decoupling of sensory and motor circuits underlies behavioral flexibility in Drosophila. *Nature Neuroscience*, *22*(7), 1132–1139. https://doi.org/10.1038/s41593-019-0413-4

Bandler, R., & Shipley, M. T. (1994). Columnar organization in the midbrain periaqueductal gray: modules for emotional expression? In *Trends in Neurosciences*. https://doi.org/10.1016/0166-2236(94)90047-7

Beltramo, R., & Scanziani, M. (2019). A collicular visual cortex: Neocortical space for an ancient midbrain visual structure. *Science*, *363*(6422), 64–69. https://doi.org/10.1126/science.aau7052

Bennett, C., Gale, S. D., Garrett, M. E., Newton, M. L., Callaway, E. M., Murphy, G. J., & Olsen, S. R. (2019a). Higher-Order Thalamic Circuits Channel Parallel Streams of Visual Information in Mice. *Neuron*, *102*(2), 477-492.e5. https://doi.org/10.1016/j.neuron.2019.02.010

Bennett, C., Gale, S. D., Garrett, M. E., Newton, M. L., Callaway, E. M., Murphy, G. J., & Olsen, S. R. (2019b). Higher-Order Thalamic Circuits Channel Parallel Streams of Visual Information in Mice. *Neuron*, *102*(2), 477-492.e5. https://doi.org/10.1016/j.neuron.2019.02.010

Blanchard, R. J., Hebert, M. A., Ferrari, P., Palanza, P., Figueira, R., Blanchard, D. C., & Parmigiani, S. (1998). Defensive behaviors in wild and laboratory (Swiss) mice: The mouse defense test battery. *Physiology and Behavior*, *65*(2), 201–209. https://doi.org/10.1016/S0031-9384(98)00012-2

Bryan Jones, R., & Waddington, D. (1992). Modification of fear in domestic chicks, Gallus gallus domesticus, via regular handling and early environmental enrichment. *Animal Behaviour*, *43*(6), 1021–1033. https://doi.org/10.1016/S0003-3472(06)80015-1

Caggiano, V., Leiras, R., Goñi-Erro, H., Masini, D., Bellardita, C., Bouvier, J., Caldeira, V., Fisone, G., & Kiehn, O. (2018). Midbrain circuits that set locomotor speed and gait selection. *Nature*. https://doi.org/10.1038/nature25448

Calabresi, P., Mercuri, N., Stanzione, P., Stefani, A., & Bernardi, G. (1987). Intracellular studies on the dopamine-induced firing inhibition of neostriatal neurons in vitro: Evidence for D1 receptor involvement. *Neuroscience*, *20*(3), 757–771. https://doi.org/10.1016/0306-4522(87)90239-9

Chon, U., Vanselow, D. J., Cheng, K. C., & Kim, Y. (2019). Enhanced and unified anatomical labeling for a common mouse brain atlas. *Nature Communications*, *10*(1). https://doi.org/10.1038/s41467-019-13057-w

Chou, X. L., Wang, X., Zhang, Z. G., Shen, L., Zingg, B., Huang, J., Zhong, W., Mesik, L., Zhang, L. I., & Tao, H. W. (2018). Inhibitory gain modulation of defense behaviors by zona incerta. *Nature Communications*, *9*(1). https://doi.org/10.1038/s41467-018-03581-6

Claudi, F, Tyson, A. L., Petrucco, L., Margrie, T. W., Portugues, R., & Branco, T. (2020). *Brainrender : a python-based software for visualizing anatomically registered data*.

Claudi, Federico, Petrucco, L., Tyson, A., Branco, T., Margrie, T., & Portugues, R. (2020). BrainGlobe Atlas API: a common interface for neuroanatomical atlases. *Journal of Open Source Software*, *5*(54), 2668. https://doi.org/10.21105/joss.02668

Cooper, W. E. (2004). *lizard (Podarcis lilfordi)*. *May 2014*. https://doi.org/10.1655/04-20

Cooper, W. E., Hawlena, D., & Pérez-Mellado, V. (2010). Influence of Risk on Hiding Time by Balearic Lizards (Podarcis lilfordi): Predator Approach Speed, Directness, Persistence, and Proximity. *Herpetologica*. https://doi.org/10.1655/08-084r.1

Cui, H., & Malpeli, J. G. (2003). Activity in the parabigeminal nucleus during eye movements directed at moving and stationary targets. *Journal of Neurophysiology*, *89*(6), 3128–3142.

https://doi.org/10.1152/jn.01067.2002

De Franceschi, G., Vivattanasarn, T., Saleem, A. B., & Solomon, S. G. (2016). Vision Guides Selection of Freeze or Flight Defense Strategies in Mice. *Current Biology*, *26*(16), 2150–2154. https://doi.org/10.1016/j.cub.2016.06.006

Dean, P., Redgrave, P., & Westby, G. W. M. (1989). Event or emergency? Two response systems in the mammalian superior colliculus. *Trends in Neurosciences*, *12*(4), 137–147. https://doi.org/10.1016/0166-2236(89)90052-0

Drager, U. C., & Hubel, D. H. (1975). Responses to visual stimulation and relationship between visual, auditory, and somatosensory inputs in mouse superior colliculus. *Journal of Neurophysiology*. https://doi.org/10.1152/jn.1975.38.3.690

Drager, U. C., & Hubel, D. H. (1976). Topography of visual and somatosensory projections to mouse superior colliculus. *Journal of Neurophysiology*. https://doi.org/10.1152/jn.1976.39.1.91

Evans, D. A., Stempel, A. V., Vale, R., & Branco, T. (2019). Cognitive Control of Escape Behaviour. In *Trends in Cognitive Sciences* (Vol. 23, Issue 4, pp. 334–348). https://doi.org/10.1016/j.tics.2019.01.012

Evans, D. A., Stempel, A. V., Vale, R., Ruehle, S., Lefler, Y., & Branco, T. (2018). A synaptic threshold mechanism for computing escape decisions. *Nature*, *558*(7711), 590–594. https://doi.org/10.1038/s41586-018-0244-6

Foster, N. N. (2020). *The mouse cortico-basal ganglia-thalamic network*.

Gale, S. D., & Murphy, G. J. (2018a). Distinct cell types in the superficial superior colliculus project to the dorsal lateral geniculate and lateral posterior thalamic nuclei. *Journal of Neurophysiology*. https://doi.org/10.1152/jn.00248.2018

Gale, S. D., & Murphy, G. J. (2018b). Distinct cell types in the superficial superior colliculus project to the dorsal lateral geniculate and lateral posterior thalamic nuclei. *Journal of Neurophysiology*, *120*(3), 1286–1292. https://doi.org/10.1152/jn.00248.2018

Gandhi, N. J., & Katnani, H. A. (2011). Motor functions of the superior colliculus. *Annual Review of Neuroscience*, *34*, 205–231. https://doi.org/10.1146/annurev-neuro-061010-113728

Griggs, W. S., Kim, H. F., Ghazizadeh, A., Costello, M. G., Wall, K. M., & Hikosaka, O. (2017). Flexible and stable value coding areas in caudate head and tail receive anatomically distinct cortical and subcortical inputs. *Frontiers in Neuroanatomy*, *11*. https://doi.org/10.3389/fnana.2017.00106

Gross, C. T., & Canteras, N. S. (2012). The many paths to fear. *Nature Reviews Neuroscience*, *13*(9), 651–658. https://doi.org/10.1038/nrn3301

Hemmi, J. M. (2005). Predator avoidance in fiddler crabs: 1. Escape decisions in relation to the risk of predation. *Animal Behaviour*, *69*(3), 603–614. https://doi.org/10.1016/j.anbehav.2004.06.018

Hemmi, J. M., & Merkle, T. (2009). High stimulus specificity characterizes anti-predator habituation under natural conditions. *Proceedings of the Royal Society B: Biological Sciences*. https://doi.org/10.1098/rspb.2009.1452

Hemmi, J. M., & Tomsic, D. (2012). The neuroethology of escape in crabs: From sensory ecology to neurons and back. In *Current Opinion in Neurobiology* (Vol. 22, Issue 2, pp. 194–200). https://doi.org/10.1016/j.conb.2011.11.012

Howe, M. W., & Dombeck, D. A. (2016). Rapid signalling in distinct dopaminergic axons during locomotion and reward. *Nature*, *535*(7613), 505–510. https://doi.org/10.1038/nature18942

Hoy, J. L., Bishop, H. I., & Niell, C. M. (2019). Defined Cell Types in Superior Colliculus Make Distinct Contributions to Prey Capture Behavior in the Mouse. *Current Biology*. https://doi.org/10.1016/j.cub.2019.10.017

Hughes, R. N., Watson, G. D. R., Petter, E. A., Kim, N., Bakhurin, K. I., & Yin, H. H. (2019). Precise Coordination of Three-Dimensional Rotational Kinematics by Ventral Tegmental Area GABAergic Neurons. *Current Biology*. https://doi.org/10.1016/j.cub.2019.08.022

Hunnicutt, B. J., Jongbloets, B. C., Birdsong, W. T., Gertz, K. J., Zhong, H., &

Mao, T. (2016). A comprehensive excitatory input map of the striatum reveals novel functional organization. *ELife*, *5*(November2016). https://doi.org/10.7554/eLife.19103

Illing, R. B., & Graybiel, A. M. (1986). Complementary and non-matching afferent compartments in the cat's superior colliculus: Innervation of the acetylcholinesterase-poor domain of the intermediate gray layer. *Neuroscience*, *18*(2), 373–394. https://doi.org/10.1016/0306-4522(86)90160-0

Jiang, H., & Kim, H. F. (2018). Anatomical inputs from the sensory and value structures to the tail of the rat striatum. *Frontiers in Neuroanatomy*, *12*. https://doi.org/10.3389/fnana.2018.00030

Kim, H. F., Amita, H., & Hikosaka, O. (2017). Indirect Pathway of Caudal Basal Ganglia for Rejection of Valueless Visual Objects. *Neuron*, *94*(4), 920-930.e3. https://doi.org/10.1016/j.neuron.2017.04.033

Kravitz, A. V., Freeze, B. S., Parker, P. R. L., Kay, K., Thwin, M. T., Deisseroth, K., & Kreitzer, A. C. (2010). Regulation of parkinsonian motor behaviours by optogenetic control of basal ganglia circuitry. *Nature*, *466*(7306), 622–626. https://doi.org/10.1038/nature09159

Lahiri, A. K., & Bevan, M. D. (2020). Dopaminergic Transmission Rapidly and Persistently Enhances Excitability of D1 Receptor-Expressing Striatal Projection Neurons. *Neuron*, *106*(2), 277-290.e6. https://doi.org/10.1016/j.neuron.2020.01.028

Lee, K. H., Tran, A., Turan, Z., & Meister, M. (2020). The sifting of visual information in the superior colliculus. *ELife*, *9*, 1–23. https://doi.org/10.7554/eLife.50678

Lerner, T. N., Shilyansky, C., Davidson, T. J., Evans, K. E., Beier, K. T., Zalocusky, K. A., Crow, A. K., Malenka, R. C., Luo, L., Tomer, R., & Deisseroth, K. (2015). Intact-Brain Analyses Reveal Distinct Information Carried by SNc Dopamine Subcircuits. *Cell*, *162*(3), 635–647. https://doi.org/10.1016/j.cell.2015.07.014

Magani, F., Luppi, T., Nuñez, J., & Tomsic, D. (2016). Predation risk modifies behaviour by shaping the response of identified brain neurons. *Journal*

of Experimental Biology. https://doi.org/10.1242/jeb.136903

Matsumoto, M., & Hikosaka, O. (2009). Two types of dopamine neuron distinctly convey positive and negative motivational signals. *Nature*, *459*(7248), 837–841. https://doi.org/10.1038/nature08028

May, P. J. (2005). The mammalian superior colliculus: Laminar structure and connections. *Progress in Brain Research*, *151*, 321–378. https://doi.org/10.1016/S0079-6123(05)51011-2

Mayerich, D., Abbott, L., & McCormick, B. (2008). Knife-edge scanning microscopy for imaging and reconstruction of three-dimensional anatomical structures of the mouse brain. *Journal of Microscopy*, *231*(1), 134–143. https://doi.org/10.1111/j.1365-2818.2008.02024.x

McHaffie, J. G., Stanford, T. R., Stein, B. E., Coizet, V., & Redgrave, P. (2005). Subcortical loops through the basal ganglia. *Trends in Neurosciences*. https://doi.org/10.1016/j.tins.2005.06.006

Menegas, W., Akiti, K., Amo, R., Uchida, N., & Watabe-Uchida, M. (2018). Dopamine neurons projecting to the posterior striatum reinforce avoidance of threatening stimuli. *Nature Neuroscience*, *21*(10), 1421–1430. https://doi.org/10.1038/s41593-018-0222-1

Menegas, W., Babayan, B. M., Uchida, N., & Watabe-Uchida, M. (2017). Opposite initialization to novel cues in dopamine signaling in ventral and posterior striatum in mice. *ELife*, *6*. https://doi.org/10.7554/eLife.21886

Menegas, W., Bergan, J. F., Ogawa, S. K., Isogai, Y., Venkataraju, K. U., Osten, P., Uchida, N., & Watabe-Uchida, M. (2015). Dopamine neurons projecting to the posterior striatum form an anatomically distinct subclass. *ELife*, *4*(AUGUST2015). https://doi.org/10.7554/eLife.10032

Mink, J. W. (1996). The Basal Ganglia: focused selection and inhibition of competing motor programs. *Pergamorr Progress in Neurobiology*, *50*, 26. https://learn.bu.edu/bbcswebdav/pid-6634749-dt-content-rid-25380329_1/courses/19sprgcasps504_a1/Mink_1996.pdf

Miyamoto, Y., Nagayoshi, I., Nishi, A., & Fukuda, T. (2019). Three divisions of the mouse caudal striatum differ in the proportions of dopamine D1 and D2 receptor-expressing cells, distribution of dopaminergic axons,

and composition of cholinergic and GABAergic interneurons. *Brain Structure and Function*, *224*(8), 2703–2716. https://doi.org/10.1007/s00429-019-01928-3

Niedworok, C. J., Brown, A. P. Y., Jorge Cardoso, M., Osten, P., Ourselin, S., Modat, M., & Margrie, T. W. (2016). AMAP is a validated pipeline for registration and segmentation of high-resolution mouse brain data. *Nature Communications*, *7*(May), 1–9. https://doi.org/10.1038/ncomms11879

Peek, M. Y., & Card, G. M. (2016). Comparative approaches to escape. In *Current Opinion in Neurobiology* (Vol. 41, pp. 167–173). https://doi.org/10.1016/j.conb.2016.09.012

Pereyra, P., De La Iglesia, H. O., & Maldonado, H. (1996). Training-to-testing intervals different from 24 h impair habituation in the crab Chasmagnathus. *Physiology and Behavior*. https://doi.org/10.1016/0031-9384(95)02013-6

Planert, H., Berger, T. K., & Silberberg, G. (2013). Membrane Properties of Striatal Direct and Indirect Pathway Neurons in Mouse and Rat Slices and Their Modulation by Dopamine. *PLoS ONE*, *8*(3), 1–14. https://doi.org/10.1371/journal.pone.0057054

Poulin, J. F., Gaertner, Z., Moreno-Ramos, O. A., & Awatramani, R. (2020). Classification of Midbrain Dopamine Neurons Using Single-Cell Gene Expression Profiling Approaches. *Trends in Neurosciences*, *43*(3), 155–169. https://doi.org/10.1016/j.tins.2020.01.004

Ragan, T., Kadiri, L. R., Venkataraju, K. U., Bahlmann, K., Sutin, J., Taranda, J., Arganda-Carreras, I., Kim, Y., Seung, H. S., & Osten, P. (2012). Serial two-photon tomography for automated ex vivo mouse brain imaging. *Nature Methods*, *9*(3), 255–258. https://doi.org/10.1038/nmeth.1854

Randlett, O., Haesemeyer, M., Forkin, G., Shoenhard, H., Schier, A. F., Engert, F., & Granato, M. (2019). Distributed Plasticity Drives Visual Habituation Learning in Larval Zebrafish. *Current Biology*. https://doi.org/10.1016/j.cub.2019.02.039

Redgrave, P., Prescott, T. J., & Gurney, K. (1999). The basal ganglia: A vertebrate solution to the selection problem? In *Neuroscience* (Vol. 89, Issue 4, pp. 1009–1023). https://doi.org/10.1016/S0306-4522(98)00319-4

Sahibzada, N., Dean, P., & Redgrave, P. (1986). Movements resembling orientation or avoidance elicited by electrical stimulation of the superior colliculus in rats. *Journal of Neuroscience*. https://doi.org/10.1523/jneurosci.06-03-00723.1986

Sans-Dublanc, A., Chrzanowska, A., Reinhard, K., Lemmon, D., Montaldo, G., Urban, A., & Farrow, K. (2020a). Brain-wide mapping of neural activity mediating collicular-dependent behaviors 1 2. *BioRxiv*, 2020.08.09.242875. https://doi.org/10.1101/2020.08.09.242875

Sans-Dublanc, A., Chrzanowska, A., Reinhard, K., Lemmon, D., Montaldo, G., Urban, A., & Farrow, K. (2020b). Brain-wide mapping of neural activity mediating collicular-dependent behaviors 1 2. *BioRxiv*.

Sargeant, A. B., & Eberhardt, L. E. (1975). Death Feigning by Ducks in Response to Predation by Red Foxes (Vulpes fulva). *American Midland Naturalist*. https://doi.org/10.2307/2424542

Seabrook, T. A., Burbridge, T. J., Crair, M. C., & Huberman, A. D. (2017). Architecture, Function, and Assembly of the Mouse Visual System. *Annual Review of Neuroscience*, *40*, 499–538. https://doi.org/10.1146/annurev-neuro-071714-033842

Shang, C., Chen, Z., Liu, A., Li, Y., Zhang, J., Qu, B., Yan, F., Zhang, Y., Liu, W., Liu, Z., Guo, X., Li, D., Wang, Y., & Cao, P. (2018). Divergent midbrain circuits orchestrate escape and freezing responses to looming stimuli in mice. *Nature Communications*, *9*(1). https://doi.org/10.1038/s41467-018-03580-7

Shang, C., Liu, Z., Chen, Z., Shi, Y., Wang, Q., Liu, S., Li, D., & Cao, P. (2015). A parvalbumin-positive excitatory visual pathway to trigger fear responses in mice. *Science*. https://doi.org/10.1126/science.aaa8694

Su, C. Y., & Wang, J. W. (2014). Modulation of neural circuits: How stimulus context shapes innate behavior in Drosophila. *Current Opinion in*

Neurobiology, *29*, 9–16. https://doi.org/10.1016/j.conb.2014.04.008

Surmeier, D. J., Carrillo-Reid, L., & Bargas, J. (2011). Dopaminergic modulation of striatal neurons, circuits, and assemblies. *Neuroscience*, *198*, 3–18. https://doi.org/10.1016/j.neuroscience.2011.08.051

Sztarker, J., & Tomsic, D. (2008). Neuronal correlates of the visually elicited escape response of the crab Chasmagnathus upon seasonal variations, stimuli changes and perceptual alterations. *Journal of Comparative Physiology A: Neuroethology, Sensory, Neural, and Behavioral Physiology*. https://doi.org/10.1007/s00359-008-0333-3

Tafreshiha, A., van den Burg, S., Smits, K., Blömer, L., & Heimel, J. A. (2020). *Visual stimulus-specific habituation of innate defensive behaviour in mice*. https://doi.org/10.1101/2020.05.11.087825

Tan, K. R., Yvon, C., Turiault, M., Mirzabekov, J. J., Doehner, J., Labouèbe, G., Deisseroth, K., Tye, K. M., & Lüscher, C. (2012). GABA Neurons of the VTA Drive Conditioned Place Aversion. *Neuron*, *73*(6), 1173–1183. https://doi.org/10.1016/j.neuron.2012.02.015

Thiele, S. L., Warre, R., & Nash, J. E. (2012). Development of a unilaterally-lesioned 6-OHDA mouse model of Parkinson's disease. *Journal of Visualized Experiments*, *60*. https://doi.org/10.3791/3234

Thorndike, E. L. (1911). *The animal behavior series. Animal intelligence: experimental studies*. 1–328. http://www.biodiversitylibrary.org/bibliography/55072

Tinbergen, N. (1989). *The Study of Instinct*. Clarendon Press. https://books.google.co.uk/books?id=d8aotwEACAAJ

Tinbergen, N., & Perdeck, A. C. (2008). On the Stimulus Situation Releasing the Begging Response in the Newly Hatched Herring Gull Chick (Larus Argentatus Argentatus Pont.). *Behaviour*. https://doi.org/10.1163/156853951x00197

Tomsic, D., de Astrada, M. B., Sztarker, J., & Maldonado, H. (2009). Behavioral and neuronal attributes of short- and long-term habituation in the crab Chasmagnathus. *Neurobiology of Learning and Memory*. https://doi.org/10.1016/j.nlm.2009.01.004

Tomsic, D., Sztarker, J., Tomsic, D., & Sztarker, J. (2019). Crustacean Visual Circuits Underlying Behavior. In *Oxford Research Encyclopedia of Neuroscience*. https://doi.org/10.1093/acrefore/9780190264086.013.210

Tovote, P., Esposito, M. S., Botta, P., Chaudun, F., Fadok, J. P., Markovic, M., Wolff, S. B. E., Ramakrishnan, C., Fenno, L., Deisseroth, K., Herry, C., Arber, S., & Lüthi, A. (2016). Midbrain circuits for defensive behaviour. *Nature*. https://doi.org/10.1038/nature17996

Tritsch, N. X., & Sabatini, B. L. (2012). Dopaminergic Modulation of Synaptic Transmission in Cortex and Striatum. *Neuron*, *76*(1), 33–50. https://doi.org/10.1016/j.neuron.2012.09.023

Tyson, A. L., Rousseau, C. V, Niedworok, C. J., Keshavarzi, S., Tsitoura, C., & Margrie, T. W. (2020). A deep learning algorithm for 3D cell detection in whole mouse brain image datasets. *BioRxiv*, 1–9.

Uchimura, N., & North, R. A. (1989). *in Rat Nucleus Accumbens Neurons*. *62*(6), 1280–1286.

Vale, R., Evans, D. A., & Branco, T. (2017). Rapid Spatial Learning Controls Instinctive Defensive Behavior in Mice. *Current Biology*, *27*(9), 1342–1349. https://doi.org/10.1016/j.cub.2017.03.031

Vale, R., Evans, D., & Branco, T. (2018). A behavioral assay for investigating the role of spatial memory during instinctive defense in mice. *Journal of Visualized Experiments*, *2018*(137), 3–10. https://doi.org/10.3791/56988

Vander Weele, C. M., Siciliano, C. A., Matthews, G. A., Namburi, P., Izadmehr, E. M., Espinel, I. C., Nieh, E. H., Schut, E. H. S., Padilla-Coreano, N., Burgos-Robles, A., Chang, C. J., Kimchi, E. Y., Beyeler, A., Wichmann, R., Wildes, C. P., & Tye, K. M. (2018). Dopamine enhances signal-to-noise ratio in cortical-brainstem encoding of aversive stimuli. In *Nature*. https://doi.org/10.1038/s41586-018-0682-1

Wallace, M. T., Meredith, M. A., & Stein, B. E. (1998). Multisensory integration in the superior colliculus of the alert cat. *Journal of Neurophysiology*, *80*(2), 1006–1010. https://doi.org/10.1152/jn.1998.80.2.1006

Wang, Q., & Burkhalter, A. (2013). Stream-related preferences of inputs to

the superior colliculus from areas of dorsal and ventral streams of mouse visual cortex. *Journal of Neuroscience*. https://doi.org/10.1523/JNEUROSCI.3067-12.2013

Wang, Q., Ding, S. L., Li, Y., Royall, J., Feng, D., Lesnar, P., Graddis, N., Naeemi, M., Facer, B., Ho, A., Dolbeare, T., Blanchard, B., Dee, N., Wakeman, W., Hirokawa, K. E., Szafer, A., Sunkin, S. M., Oh, S. W., Bernard, A., … Ng, L. (2020). The Allen Mouse Brain Common Coordinate Framework: A 3D Reference Atlas. *Cell*, *181*(4), 936-953.e20. https://doi.org/10.1016/j.cell.2020.04.007

Watabe-Uchida, M., & Uchida, N. (2019). Multiple Dopamine Systems: Weal and Woe of Dopamine. *Cold Spring Harbor Symposia on Quantitative Biology*, 037648. https://doi.org/10.1101/sqb.2018.83.037648

Watabe-Uchida, M., Zhu, L., Ogawa, S. K., Vamanrao, A., & Uchida, N. (2012). Whole-Brain Mapping of Direct Inputs to Midbrain Dopamine Neurons. *Neuron*, *74*(5), 858–873. https://doi.org/10.1016/j.neuron.2012.03.017

Wei, P., Liu, N., Zhang, Z., Liu, X., Tang, Y., He, X., Wu, B., Zhou, Z., Liu, Y., Li, J., Zhang, Y., Zhou, X., Xu, L., Chen, L., Bi, G., Hu, X., Xu, F., & Wang, L. (2015). Processing of visually evoked innate fear by a non-canonical thalamic pathway. *Nature Communications*. https://doi.org/10.1038/ncomms7756

Wickens, J. R., & Wilson, C. J. (1998). Regulation of action-potential firing in spiny neurons of the rat neostriatum in vivo. *Journal of Neurophysiology*, *79*(5), 2358–2364. https://doi.org/10.1152/jn.1998.79.5.2358

Wickersham, I. R., Finke, S., Conzelmann, K.-K., & Callaway, E. M. (2007). Retrograde neuronal tracing with a deletion-mutant rabies virus. *Nature Methods*, *4*(1), 47–49. https://doi.org/10.1038/nmeth999

Yilmaz, M., & Meister, M. (2013). Rapid innate defensive responses of mice to looming visual stimuli. *Current Biology*, *23*(20), 2011–2015. https://doi.org/10.1016/j.cub.2013.08.015

Zhang, S. P., Bandler, R., & Carrive, P. (1990). Flight and immobility evoked by excitatory amino acid microinjection within distinct parts of the

subtentorial midbrain periaqueductal gray of the cat. *Brain Research*, *520*(1–2), 73–82. https://doi.org/10.1016/0006-8993(90)91692-A

Zhou, Z., Liu, X., Chen, S., Zhang, Z., Liu, Y., Montardy, Q., Tang, Y., Wei, P., Liu, N., Li, L., Song, R., Lai, J., He, X., Chen, C., Bi, G., Feng, G., Xu, F., & Wang, L. (2019). A VTA GABAergic Neural Circuit Mediates Visually Evoked Innate Defensive Responses. *Neuron*, *103*(3), 473-488.e6. https://doi.org/10.1016/j.neuron.2019.05.027

Zhou, Zheng, Liu, X., Chen, S., Zhang, Z., Liu, Y., Montardy, Q., Tang, Y., Wei, P., Liu, N., Li, L., Song, R., Lai, J., He, X., Chen, C., Bi, G., Feng, G., Xu, F., & Wang, L. (2019). A VTA GABAergic Neural Circuit Mediates Visually Evoked Innate Defensive Responses. *Neuron*, *103*(3), 473-488.e6. https://doi.org/10.1016/j.neuron.2019.05.027